

PERFORMANCE OF A LINE COMMUTATED INVERTER FED INDUCTION MOTOR DRIVE

A DISSERTATION

Submitted in partial fulfilment of the
requirements for the award of the degree

of

MASTER OF ENGINEERING

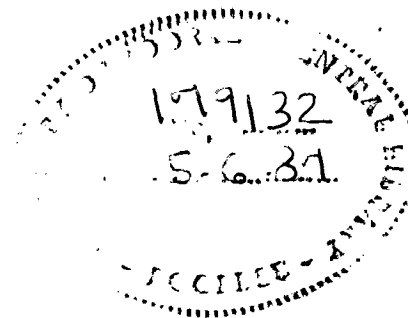
in

ELECTRICAL ENGINEERING
(Power Apparatus and Electric Drives)

By

ALOK KUMAR GOEL

179132
5-6-87



DEPARTMENT OF ELECTRICAL ENGINEERING
UNIVERSITY OF ROORKEE
ROORKEE-247 667 (INDIA)

January, 1987

DEDICATED

TO

MY PARENTS

C A N D I D A T E ' s D E C L A R A T I O N

I hereby certify that the work which is being presented in dissertation entitled, " PERFORMANCE OF A LINE COMMUTATED INVERTER FED INDUCTION MOTOR DRIVE", in partial fulfilment of the requirements for the degree of MASTER OF ENGINEERING IN ELECTRICAL ENGINEERING of specialization Power Apparatus and Electric Drives submitted in the Deptt. of Electrical Engineering, University of Roorkee, Roorkee, is an authentic record of my own work carried out during a period of nine months commencing from July 1985 to March 1986, under the supervision of Dr. K.B.Naik, Professor and Head Electrical Engineering Department , Kamla Nehru Institute of Technology, Sultanpur (Ex-Reader, Department of Electrical Engineering, University of Roorkee, Roorkee) and Dr. Bhim Singh, Lecturer Department of Electrical Engineering, University of Roorkee, Roorkee.

The matter embodied in this dissertation has not been submitted elsewhere for the award of any other degree or diploma.

Goel ---

(ALOK KUMAR GOEL)

This is to certify that the above statement made by the candidate is correct to the best of my knowledge.

Naik

(Dr.K.B.Naik)
Professor & Head
Electrical Engineering Deptt.
K.N.Institute of Technology
SULTANPUR

Bhim Singh
16.1.87

(Dr.Bhim Singh)
Lecturer
Deptt.of Electrical Engineering
University of Roorkee
ROORKEE

Dated: Jan. 16, 1987.

ACKNOWLEDGEMENTS

It is my pleasure to take this opportunity to express my sincere gratitude to Dr. K.B.Naik, Professor and Head, Electrical Engineering Department, Kamla Nehru Institute of Technology, Sultanpur (Ex-Reader, Department of Electrical Engineering, University of Roorkee, Roorkee) and Dr. Bhim Singh, Lecturer, Department of Electrical Engineering, University of Roorkee, Roorkee for their valuable guidance and discussion throughout the phase of this investigation which led to the successful completion of this venture.

I am thankful to Dr. P.Mukhopadhyay, Professor and Head, Electrical Engineering Department, University of Roorkee, Roorkee, for providing computer and laboratory facilities. I am very thankful to faculty members Dr. D.R.Kohli, Dr. V.K.Verma, Sri S.P.Gupta and Sri Y.P.Singh, Electrical Engineering Department, University of Roorkee, Roorkee, for their valuable suggestions given by them time to time.

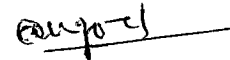
I am very grateful to Sri Pramod Agrawal, Lecturer, Electrical Engineering Department, University of Roorkee, Roorkee for his affection, useful suggestions and readiness to help during the every stage of this work.

(iii)

Thanks are also very much due to Mr. Om Hari Pande, my friend who inspired me at various stages during the work.

I duly acknowledge the help received from the staff members of laboratory and work-shop during the experimental work.

I am obliged to my parents, elder brother Praveen and sister Ila for the help and encouragement I received all along the course of this study.



(ALOK KUMAR GOEL)

ABSTRACT

The dissertation deals ^{with} the design, analysis and experimental studies of a line commutated inverter fed induction motor drive. In this scheme, a three phase a.c. supply is converted into a variable d.c. supply using a combination of three phase uncontrolled bridge converter and an auto transformer. The commutation of thyristors of line commutated inverter is achieved using three phase capacitor bank which are charged by the back e.m.f. of motor.

The whole work of dissertation broadly has been categorized as literature survey, design and fabrication of firing and power circuits, theoretical prediction of steady state performance of induction motor and experimental studies. The literature survey at the beginning of dissertation reveals the progress made in the field of line commutated inverter for variable frequency output and solid state converters fed variable frequency operation of cage I.M. In chapter-II the details of experimental setup in which system description and design of power and firing circuits are discussed.

The starting methods and detailed experimental investigations to study the feasibility of the system as well as to obtain performance of motor under varied operating conditions are given in chapter-III. In

chapter-IV steady state analysis and performance of the system has been predicted analytically using equivalent circuit approach as well as digital simulation along with experimental results to establish the validity of predicted results.

The feasibility of the line commutated inverter fed induction motor system to operate as a variable frequency source and as a group drive are described in chapter-V and VI, respectively. Lastly the main conclusions and suggestions for further work are given.

NOMENCLATURE

The detailed list of the symbols used in the present work is given below:

C	: capacitance
E_m	: peak value of phase voltage
F	: p.u. frequency
I_2	: rotor current referred to stator
I_d	: d.c. link current
I_m, I_I	: motor and inverter current respectively
P	: number of poles
P_{fm}, P_{fI}	: power factors of motor and inverter respectively
P_o, P_I	: motor and inverter outputs respectively
P_L, P_{DC}	: input power to static load and d.c. link power respectively
R	: total resistance of motor per phase referred to stator
R_2	: rotor resistance per phase referred to stator equivalent to load on motor
R_m	: p.u. core loss resistance
s	: slip
T	: motor torque
T_L	: load torque
T_R	: turn ratio of transformer
V	: a.c. side inverter voltage
V_C	: control voltage
V_d	: d.c. link voltage

(vii)

- W_0 : base synchronous speed of motor
- X : total leakage reactance of motor per phase referred to stator
- X_c : p.u. reactance of capacitor at rated frequency
- X_m : p.u. magnetising reactance
- α : firing angle
- β : inverter angle of advance
- η_s : overall system efficiency
- η_m : motor efficiency

ABBREVIATIONS

a.c.	:	alternating current
CSI	:	current source inverter
d.c.	:	direct current
e.m.f.	:	electromotive force
F H.P.	:	<u>fraction</u> horse power
H.P.	:	horse power
Hz	:	hertz
I.M.	:	induction motor
KVA	:	kilo volt ampere
L.C.I.	::	line commutated inverter
p.f.	:	power factor
PIV	:	peak inverse voltage
PWM	:	pulse width modulation
SCI	:	self commutated inverter
SCR	:	silicon controlled rectifier
suffix	:	direct and quadrature axis quantities d,q

CONTENTS

	PAGE
Candidate's Declaration	(i)
Acknowledgements	(ii)
Abstract	(iv)
Nomenclature	(vi)
CHAPTER I INTRODUCTION	1
1.1 General	1
1.2 Literature Review	6
1.3 Scope of Present Work	8
CHAPTER II DETAILS OF EXPERIMENTAL SETUP	11
2.1 General	11
2.2 Description of Experimental Setup	12
2.3 Requirements of a Trigger Scheme	14
2.4 Proposed Trigger Scheme	16
2.5 Results and Discussions	18
2.6 Conclusions	19
CHAPTER III EXPERIMENTAL INVESTIGATIONS ON STEADY STATE PERFORMANCE OF THE SYSTEM	20
3.1 General	20
3.2 Starting Methods	20
3.3 Results and Discussions	23
3.4 Conclusions	27
CHAPTER IV ANALYSIS AND PERFORMANCE OF A LINE COMMUTATED INVERTER FED INDUCTION MOTOR	28
4.1 General	28
4.2 Analysis	29
4.3 Digital Simulation	35
4.4 Discussions of Results	36
4.5 Conclusions	38

CHAPTER V	EXPERIMENTAL INVESTIGATIONS ON SYSTEM AS A VARIABLE FREQUENCY SOURCE	39
5.1	General	39
5.2	Experimental Setup and Procedure	40
5.3	Discussions of Results	42
5.4	Conclusions	46
CHAPTER VI	EXPERIMENTAL INVESTIGATIONS ON SYSTEM AS A GROUP DRIVE	48
6.1	General	48
6.2	Experimental Setup and Procedure	49
6.3	Discussions of Results	51
6.4	Conclusions	54
CHAPTER VII	CONCLUSIONS AND SUGGESTIONS FOR FURTHER WORK	56
7.1	General	56
7.2	Main Conclusions	56
7.3	Suggestions for Further Work	58
	BIBLIOGRAPHY	60
	APPENDICES	
	Appendix A : Pin Details and Connection Diagrams of Different I.C. Chips	65
	Appendix B : Details and Parameters of Machines Used	66
	Appendix C : Listing of Computer Programs	67

CHAPTER - I

INTRODUCTION

1.1 General

Presently, the d.c. motor and d.c. controller combination is the dominant electric vehicle drive system configuration, with only a few vehicles using an a.c. system. However, recent studies comparing various electric vehicle propulsion system approaches have concluded that most promising drive system for electric vehicle use is the a.c. induction motor drive [1,2].

The modern trend in industries is towards the replacement of d.c. drives by a.c. drives in many applications because of comparative advantages of a.c. motors in general and induction motor in particular [3]. The squirrel cage induction motor are known to have higher power to weight ratio, robust physical structure, lesser maintenance requirements and above all, the lower cost. The d.c. machine has the following drawbacks:

- (i) increased cost per KVA and decreased power per weight ratio as compared to their a.c. counterpart due to commutator, ?
- (ii) accentuated sparking at high currents and speeds,
- (iii) limited armature voltage rating,
- (iv) limited armature current rating due to commutation problem
- (v) unsuitable to operate in dusty and explosive environment and require frequent maintenance.

The above deficiencies obviously can not be tolerated in many industrial applications. A suggested alternative is to use a cage I.M., operating at variable frequency supplied from a static frequency converter. The use of a cage I.M. has the following advantages:

- (i) Its construction is simple and robust,
- (ii) comparatively less cost per KVA as compared to d.c. counterpart.
- (iii) the power perweight ratio is about twice that of d.c. motor.

Although the cage I.M. has the above advantages, the cost of control equipment is considerably higher and the control techniques are very complex. The research and development efforts in a.c. drives technology have been focused recently on solving the above problems. As a result of availability of improved voltage and current rating SCRs and the trend of their prices to come down day by day in the recent years, people have shown considerable interest in variable speed I.M. drives and in the recent years, many new techniques, suitable for speed control of I.M. have been developed.

Mainly phase control and static frequency converters are used for the speed control of three phase squirrel cage I.M. phase control [3,4] usually is limited to small capacity of motors particularly to those loads where load increases with speed as in case of fans drives.

Induction motors used in the static variable frequency drive systems have the operating characteristics and features which meet the requirements of modern variable speed drive systems. Some of these are, the capability of operation at very high and low speeds, at high torque and overloads in a constant power or torque mode, and in the negative torque region for dynamic braking.

The variable frequency operation of an induction motor is obtained by the use of frequency converter. A frequency converter is a device that can convert the input supply of fixed voltage and frequency to an a.c. supply of variable frequency and variable voltage. The rotating type of frequency converters were used previously but now they are replaced by the solid state frequency converters.

The static frequency converters are divided into two categories:

- (i) cyclo converters
- (ii) d.c. link converters

A cycloconverter [5] converts a.c. supply of fixed frequency to a lower output frequency through a one step conversion process. The output frequency range is limited to one third of the supply frequency and therefore the drives employing cycloconverters are suitable only for operation at low frequency. The output voltage of cycloconverter contains complex harmonic patterns. However, one advantage of cyclo-

converter drives is that regeneration is simple and the system can be easily designed for four quadrant operation of cage I.M. The cyclo-converter drives are normally used in very ^{large} power applications. The cost and complexity of power and control circuits make them uncompetitive with other classes of drives in general applications.

A d.c. link converter is a two stage conversion drives in which power from the a.c. network is first rectified to d.c. and then inverted to obtain a.c. voltage at variable frequency. This type of inverter can operate over a large frequency range and is suitable for wide range speed control of a.c. drives. The voltage source inverters [6,7] use either a controlled rectifier or a d.c. chopper to have a variable voltage d.c. link. Which is fed to a three phase forced commutated bridge inverter and v/f control is used to maintain maximum value of torque constant in wide range of speed control. In these circuits, the commutating capacitor is usually charged by the d.c. link voltage and hence the commutation capability deteriorates under the low speed operation when d.c. link voltage decreases. Moreover, these inverters generate a three phase square wave voltage with high values of low order harmonics. These drawbacks can be minimized upto certain extent by using pulse-width modulated inverters [8]. The harmonic losses of the machine are reduced significantly in P.W.M. inverters, but the inverter efficiency is reduced because of the higher rate of the commutation. In addition to this, the P.W.M. circuits

require sophisticated trigger control schemes to achieve the desired level of performance. A current source inverter [9,10] unlike the voltage source inverter, works with a stiff d.c. current source. Though the CSI has merits, it suffers from certain limitations also. The frequency range of the CSI is low. It cannot operate on no load as a certain minimum value of the load current is necessary for entering the satisfactory commutation of the inverter. The response of the drive fed from the CSI is sluggish and tends to give stability problem while running at lower speeds with light loads. The CSI have a limited scope in the multimotor drive applications.

A.Nabae et al [11] have proposed a method of flux control technique of I.M. for its variable frequency operation. Which is capable of controlling with quick field weakening and superior response and stability. This method is to control the stator current as a vector quantity on the basis of slip frequency control. More specifically, it is designed to calculate the commanded stator current of the induction motor by corresponding to flux and torque commands on the basis of motor constants and use the calculated commands to control the stator current. However, the control/converting technique are complicated in nature and cost of system is also higher.

It is possible to overcome some of the difficulties associated with cyclo-converter and forced commutated

inverter circuits by using the line commutated inverter [12]. The absence of the forced commutation circuits makes the operation of the LCI simple, reliable and more effi-cient. The converter grade SCRs can be used for the LCI and its use results in saving in cost. The trigger circuit requirements of this scheme are simple as compared to cyclo-converter or forced commutated inverter circuits. Another novel features of this scheme is that the voltage and current wave shapes are sinusoidal as the LCI operates from the mains. A need is, therefore, felt to make use of the advantages of line commutation in the development of the alternative variable frequency source from which a simple I.M. or a group of induction motors can be fed. With this view, an attempt has been made in this investigation to design and develop a d.c. link line commutated inverter for an I.M. drive. How?

1.2 Literature Review

In the recent past, numerous attempts have been made for using LCI synchronous machine system in the commutator less d.c. motor mode. Tadakuma, Tamura and Tanaka [13] have described the driving characteristics of commutator less motor controlled by induced voltage detector. Rosa [14] has described the utilization and rating of machine commutated inverter synchronous motor drives. In which he analyzed a d.c. link type variable frequency inverter synchronous motor drive, the relationship between the

operation of the machine commutated thyristor inverter and the characteristics of the synchronous motor.

Brockhurst [15] published his work on performance equation for d.c. commutatorless motor using salient pole type synchronous machines. In which, the development of design oriented algebraic expression of machine performance measures in terms of machine inductance is described.

Tokeda, Morimoto and Hirasa [16] have discussed the generalised analysis for steady state characteristics of d.c. commutatorless motors. The variation of commutation angle, shift angle and demagnetisation due to armature reaction, safety margin angle, average torque and speed with mean input current are examined quantitatively for windings and saliency.

Rangandhachari et al [17,18] proposed the synchronous machine alongwith such inverter as a commutatorless shunt motor and variable frequency source to feed I.M. This scheme has the disadvantage of using an extra synchronous machine which not only affects the systems efficiency and cost but also demands a separate d.c. source for its excitation. However, Tasuchiya et al [19] and Ajay Kumar et al [20] have reported that the LCI alongwith synchronous machine may give the performance like d.c. series motor and is called as series d.c. commutatorless motor. But the scheme suffers from the disadvantage of commutation failure due to increase in overlap angle of

Basis 71

LCI and/or armature reaction of synchronous motor specially at higher loads.

Very recently an attempt [21,22] has been made on the LCI for the variable speed operation of only a fraction horse power I.M. and it was limited to the feasibility of the system. H²:

1.3 Scope of Present Work:

The exhaustive literature survey reveals that little research work has been reported on the performance of a LCI fed I.M. Therefore, a need is felt to investigate the variable speed operation as well as the analysis and performance of integral horse power rating cage motor using LCI.

An attempt has been made in the investigation to study the steady state performance of a 3-phase I.M. fed from an LCI. In this scheme a three-phase a.c. supply of fixed frequency and voltage is converted into a variable voltage d.c. supply to feed LCI using a combination of three phase uncontrolled bridge converter and an auto transformer. The commutation of thyristors of LCI is achieved using three-phase capacitor bank which are charged by the back e.m.f. of motor.

The objectives of the proposed work were the followings:

1. To develop a simple firing scheme for operating

- the LCI alongwith the power circuit of the drive.
2. To develop a general equivalent circuit of the overall scheme being applicable to loaded as well as unloaded conditions.
 3. To simulate the whole system on a digital computer and to predict the performance using suitable numerical technique. This is to be used to see the validity of the proposed equivalent circuit approach.
 4. To study the feasibility of the system as a variable frequency source and as a group drive.

The whole scheme has been fabricated in ^{the} a laboratory and the performance of the motor is obtained practically to verify the results analytically predicted. The feasibility of LCI I.M. system as a variable frequency source to feed different types of load and as a group drive is also studied.

Outline of Chapters

In chapter II, the details of experimental setup has been described. Starting methods and detailed experimental investigations to study the feasibility of the system are discussed in chapter III. Analysis and performance of LCI fed I.M. is described in chapter IV. The variable frequency source and as a group drive of the system is described in chapter V and chapter VI respectively. In the last chapter

the main conclusions and suggestions for further work are enlisted. The details of machines used and the listing of developed computer program for analysis are given in the Appendices.

CHAPTER - II

DETAILS OF EXPERIMENTAL SETUP

2.1 General

In this investigation the LCI is used to achieve wide speed control of three phase I.M. To obtain the variable frequency operation of such inverter, a suitable firing circuit capable to operate over a wide range of frequency should be developed. A large number of firing circuits have been reported in the literature [23-26] based on fixed frequency supply. A variable frequency firing scheme [27] though uses minimum number of components, it introduces complicated delay scheme to produce the pulses. The firing scheme described in [28] uses large number of components and also the tachogenerator signal is used as a reference voltage and therefore needs an extra device.

In the present chapter details of power circuit and a simple firing scheme suitable for variable frequency operation of a three phase thyristor bridge inverter are described. The proposed firing circuit is suitable to operate at the frequencies much higher from the main frequency to as low as few Hertz. The trigger scheme uses cosine wave crossing technique to generate firing pulses and many of the drawbacks mentioned above are eliminated.

2.2 Description of Experimental Setup

Fig. 2.1 shows the block diagram of the system used in this work. The system consists of three phase auto transformer uncontrolled bridge rectifier, d.c. link filter choke, line commutating inverter, step up transformer, capacitor bank and a three phase squirrel cage I.M.

The three phase auto transformer alongwith uncontrolled rectifier provides a variable voltage d.c. source. The d.c. link inductor smoothes out the link current ripples and keeps the current continuous in the circuit. The LCI supplies the active power from the d.c. link to the I.M. The flow of power to the motor can be controlled by adjusting the d.c. link voltage and the inverter firing angle. The step up transformer serves the purpose of isolation and stepping up the inverter voltage. The lagging reactive power needed for inverter, transformer and I.M. is provided by capacitor bank connected at the motor terminals. The terminal voltage of the motor is decided by the d.c. link voltage and inverter firing angle. The speed of motor or output frequency of the inverter can be varied by controlling the d.c. link voltage, the value of terminal capacitor bank and the inverter firing angle. The magnetic circuit of the motor and the transformer due to saturation provides an approximately constant voltage to frequency ratio or output flux thus resulting full utilization of motor capacity.

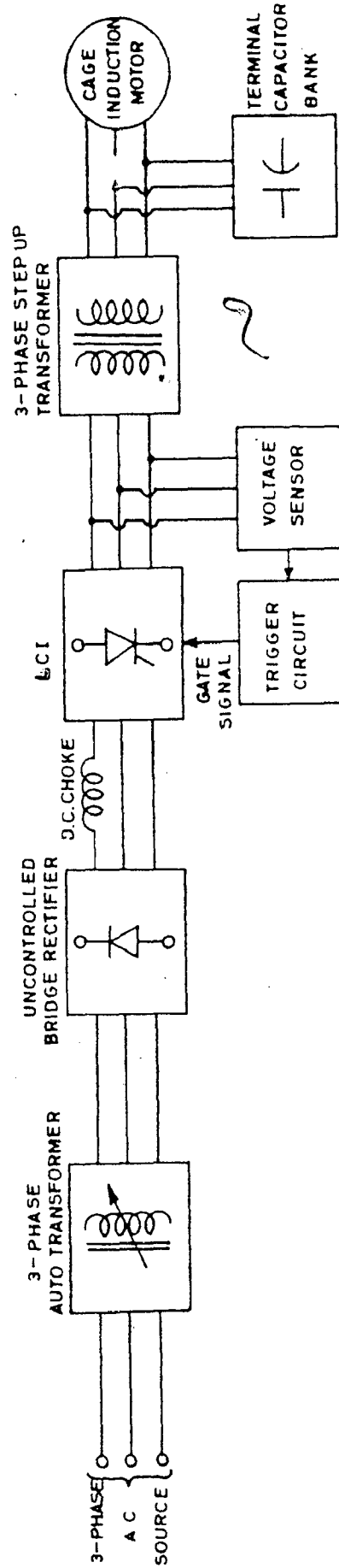


FIG.2.1 BLOCK DIAGRAM FOR LCI FED INDUCTION MOTOR SYSTEM

In the proposed power circuit the following two blocks have been designed and fabricated.

(i) Uncontrolled Six Pulse Bridge Rectifier.

For selecting the diodes for uncontrolled six pulse bridge rectifier, the supply voltage input to the uncontrolled bridge rectifier is 400 volts, 50 Hz line to line a.c., therefore, the peak inverse voltage (PIV) across each arm of the bridge will be given by,

$$\text{PIV} = \frac{\pi}{3} V_{d_o}$$

where $V_{d_o} = \frac{3\sqrt{2}}{\pi} V_{L-L}$

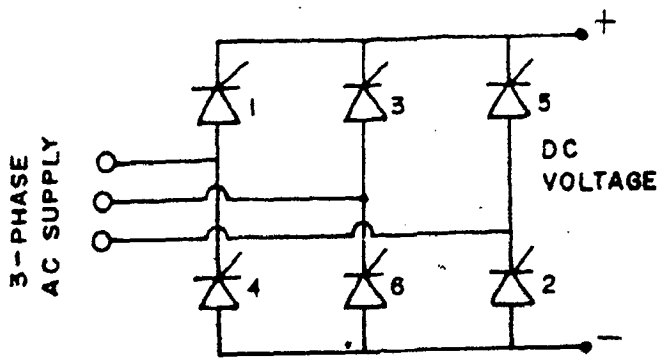
$$V_{d_o} = \frac{3\sqrt{2}}{\pi} \times 400 = 540.2 \text{ Volts}$$

$$\text{Therefore PIV} = \frac{\pi}{3} \times 540.2 = 566 \text{ Volts}$$

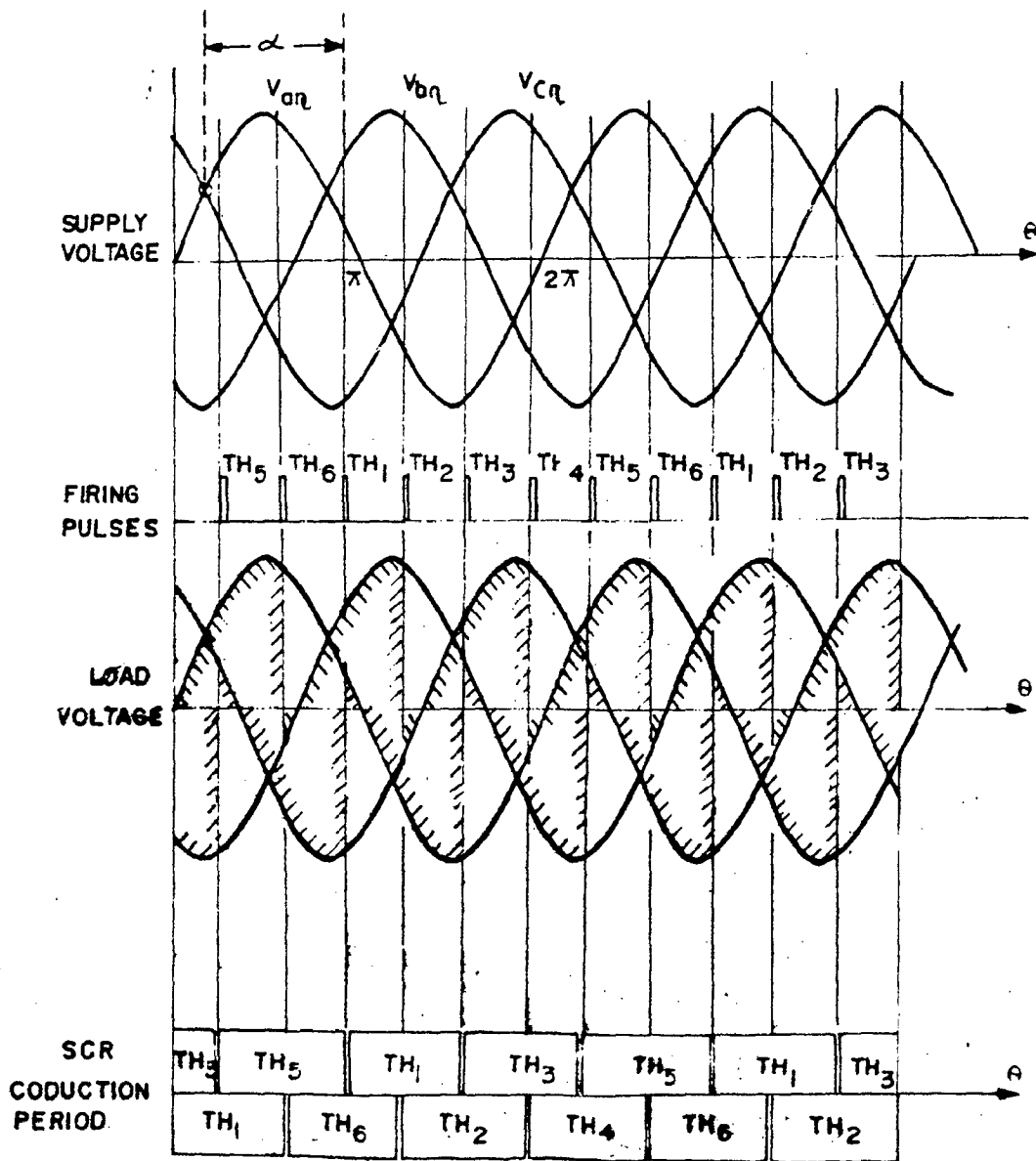
Allowing a safety factor of about 2.0, so that the diode can easily take a reasonable transient over voltage, diode with 1200 volts PIV rating are used. Therefore, the diodes selected for uncontrolled bridge rectifier are of 16 amperes and 1200 volts.

(ii) Three Phase Bridge Inverter

Fig. 2.2 shows the diagram of a three phase fully controlled SCR bridge alongwith voltage waveforms and firing sequence of thyristors [5]. The bridge can be operated as a converter or inverter depending upon the delay angle being less than or above 90° . One SCR each in upper and lower portions



(a)



(b)

FIG 2.2. THREE PHASE FULLY CONTROLLED BRIDGE CONVERTER
(a) SCHEMATIC DIAGRAM (b) WAVE FORMS

of the bridge conducts at a time for 120° duration and is turned OFF only when the next SCR of the same portion in sequence is gated. SCRs are switched ON in sequence at every 60° angle thus the gate pulses should have a frequency six times than the source frequency.

The voltage rating of the SCRs is decided by the maximum voltage developed across the device. For the present work, since the maximum output a.c. voltage of LCI is 240 volt rms line to line so the SCR of 800 volts rating can be used after taking a safety factor of 2.0. As the thyristors of bridge inverter are commutated by the stator induced e.m.f. of the motor a sufficient time is available for the commutation of thyristors even at high values of super synchronous speed of the motor. Therefore converter grade thyristors may be used. The current rating of SCR is to be decided on the basis of d.c. link current. In the present LCI the d.c. link current is expected to have a maximum value of 15A. Therefore the thyristor of 800 PIV, 16A converter grades are used for LCI with the proper protection for all elements of circuit.

2.3 Requirements of a Trigger Scheme

As described earlier in section 2.2, that in the bridge inverter, SCRs are switched ON in sequence at every 60° angle, thus the frequency of gate pulse needed is six times the frequency of the motor operation. Moreover to

keep each SCR ON for 120° duration either each gate pulse should be of more than 60° duration or each SCR should be gated twice at the interval of 60° by short gate pulses. The large duration of pulse not only increases gate circuit losses but also needs carrier frequency ANDING to reduce saturation in pulse transformers still the size of pulse transformer is to be larger. In the proposed scheme later technique is used.

For the proper operation of system, it is desirable that the power amplifier should exhibit a linear output input characteristics. In a three phase fully controlled bridge, the terminal voltage is expressed in the following way, [29, 30].

$$V_d = \frac{3\sqrt{3} E_m}{\pi} \cos \alpha \quad (2.1)$$

If the firing angle bears linear relation with control voltage, V_c , the power amplifier processes a non-linear characteristics.

On the other hand, if cosine wave crossing technique is used, the control voltage is related with delay angle in the following manner,

$$KV_c = \cos \alpha \quad (2.2)$$

The equation (2.1) now can be written in the following way,

$$V_d = \frac{3\sqrt{3} K E_m}{\pi} V_c \quad (2.3)$$

Equation (2.3) results in a linear characteristic. The proposed scheme uses same cosine wave crossing technique to make the power circuit suitable for open loop as well as closed loop operation.

2.4 Proposed Trigger Scheme

The block diagram of the scheme is shown in Fig. 2.3(a) The relevant wave forms at different points of firing circuit are shown in Fig. 2.3(b). The scheme consists of step down transformer, comparator, differentiator, monostable multivibrator, OR gate and power amplifier blocks. A stage by stage description alongwith design features is given below. The detailed wiring diagram is shown in Fig. 2.4.

Step Down Transformer

Three single phase transformer with centre tapped secondary winding have been used. The primary windings being arranged in delta are connected a.c. side of thyristor bridge while secondary windings are arranged to have six phase configuration to produce six channels. Each channel generates a firing pulse to trigger a SCR.

Comparator

The secondary voltage of the transformer is compared with a d.c. reference signal using a 741 Op.Amp. Comparator to produce alternating rectangular waveform of variable

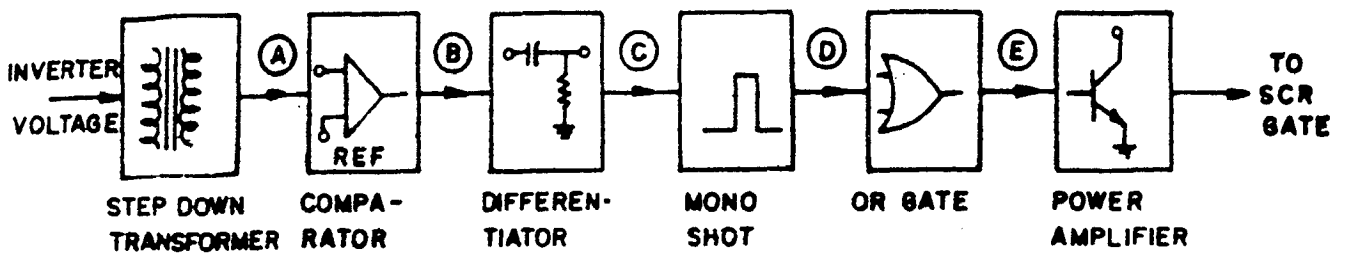


FIG.2.3(a) BLOCK DIAGRAM OF FIRING CIRCUIT

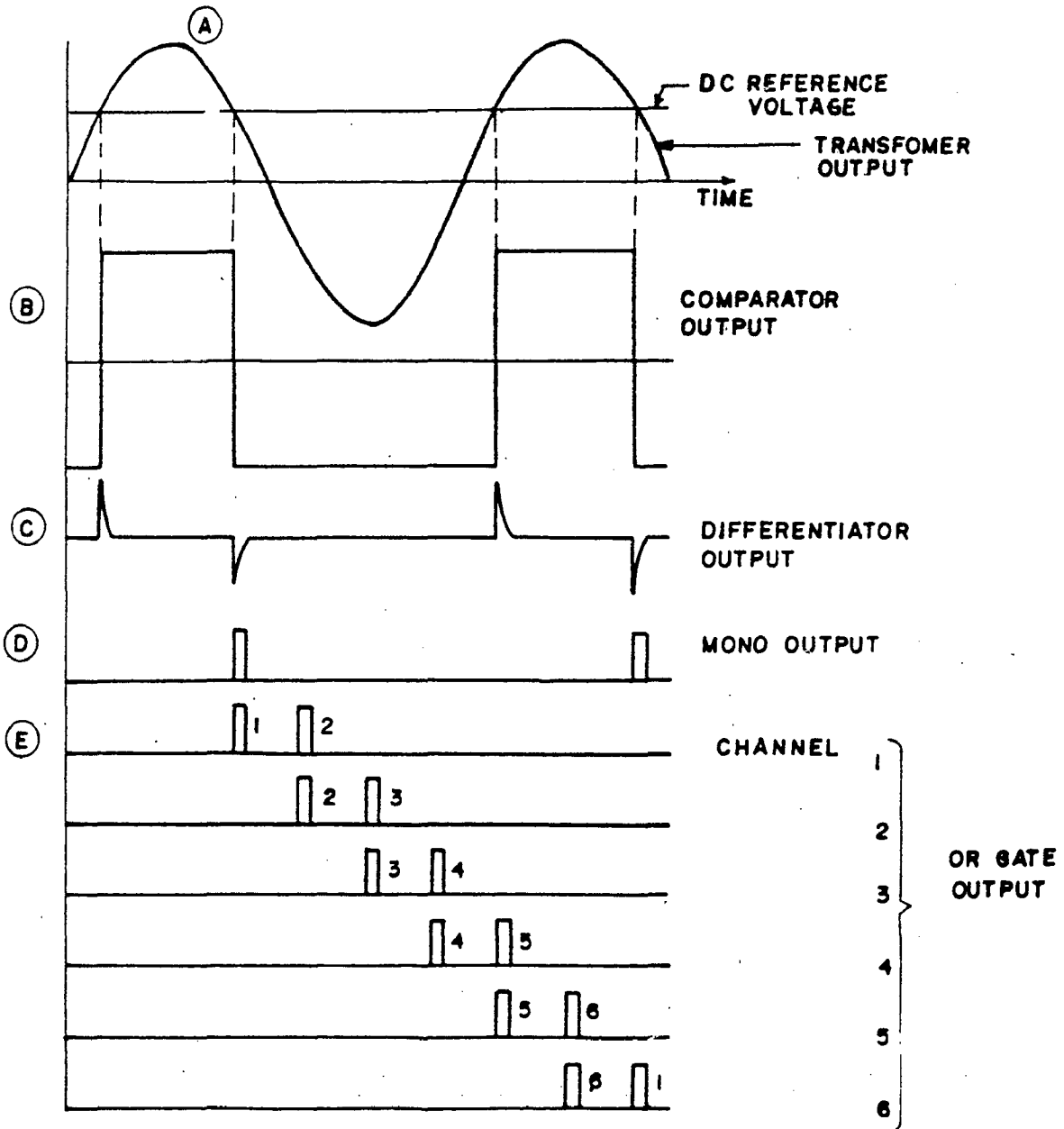


FIG.2.3(b) WAVEFORMS AT DIFFERENT POINTS OF FIRING CIRCUIT.

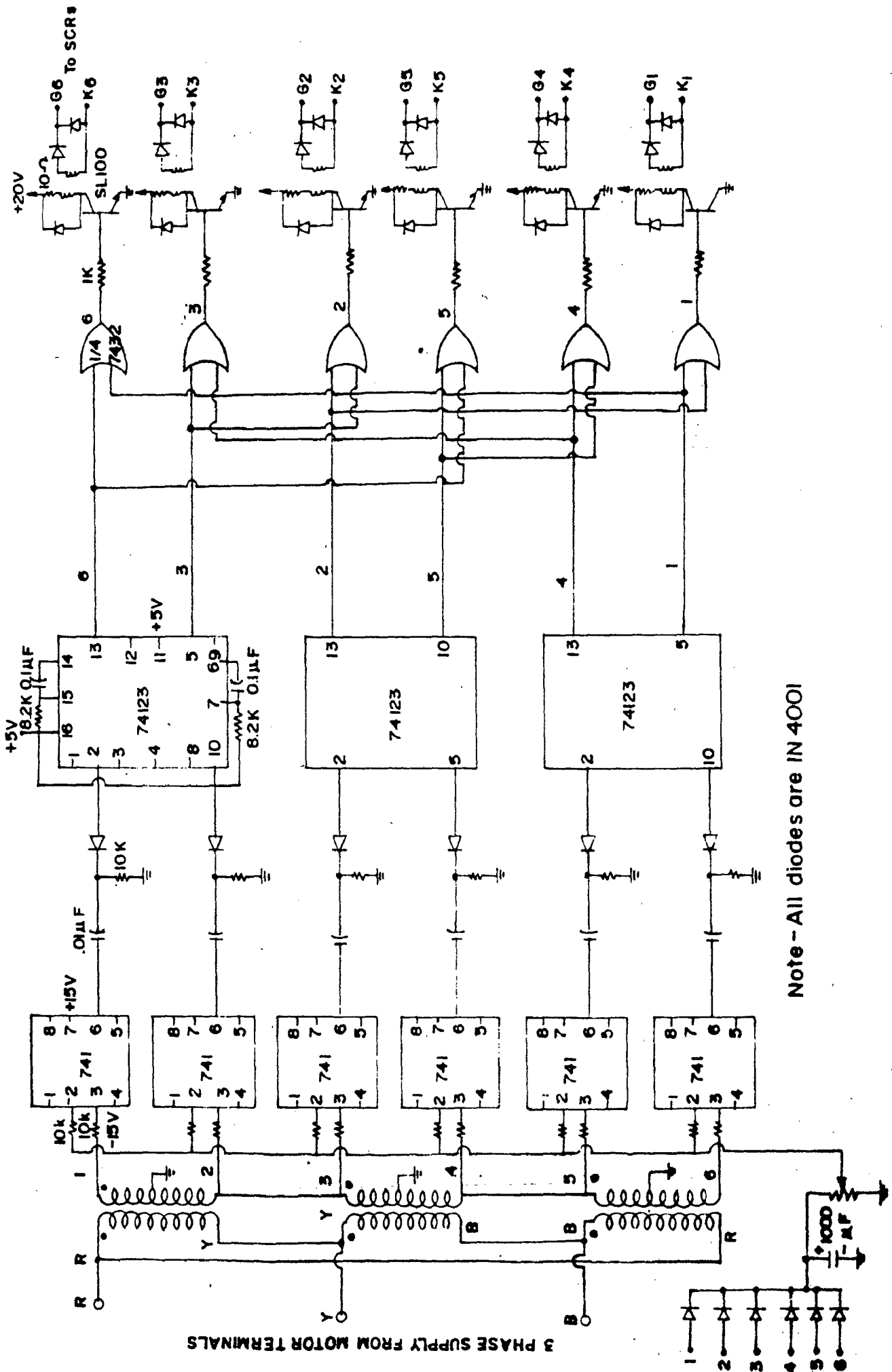


FIG. 2.4 DETAILED FIRING CIRCUIT OF A 3 PHASE FULLY CONTROLLED BRIDGE INVERTER.

pulse width. To avoid the possibility of varying the delay angle due to change in inverter output terminal voltage, the d.c. reference voltage is generated by rectifying the secondary voltages of transformers and using a capacitance filter. This also eliminates the possibility of collapsing the generation of firing pulses as d.c. reference voltage can never be greater than the peak value of the secondary voltage.

Differentiator

A simple R - C differentiator is used to differentiate the rectangular voltage waveform. As it is planned to operate system from 5 Hz to 100 Hz, the values of elements R and C are decided to have proper differentiation in the whole range. For proper differentiation $RC \ll 1$.

The elements R and C are selected as 10 K ohm and 0.01 μ F respectively.

Monoshot

Monoshot block produces an output pulse of 0.5 m sec. using negative edge triggering to produce delay angle between 90° and 180° suitable for inverter operation. A higher pulse width is chosen due to highly inductive nature of induction machine at light load. The positive spike of differentiator is blocked by a reverse connected diode. A 74123 dual mono-stable multivibrator is used for this purpose. The elements R and C of the pulse forming circuit

are selected as 8.2 K ohms and 0.1 μ F respectively.

OR Gate

As operation of bridge inverter requires conduction of each SCR for two consecutive modes of 60° duration, the scheme uses gating of each SCR twice at the interval of 60° . This avoids the possibility of failure of inverter operation in the presence of discontinuous conduction. This is achieved using OR operation of two required pulses. A quad 7432 OR Gate IC has been used for this purpose.

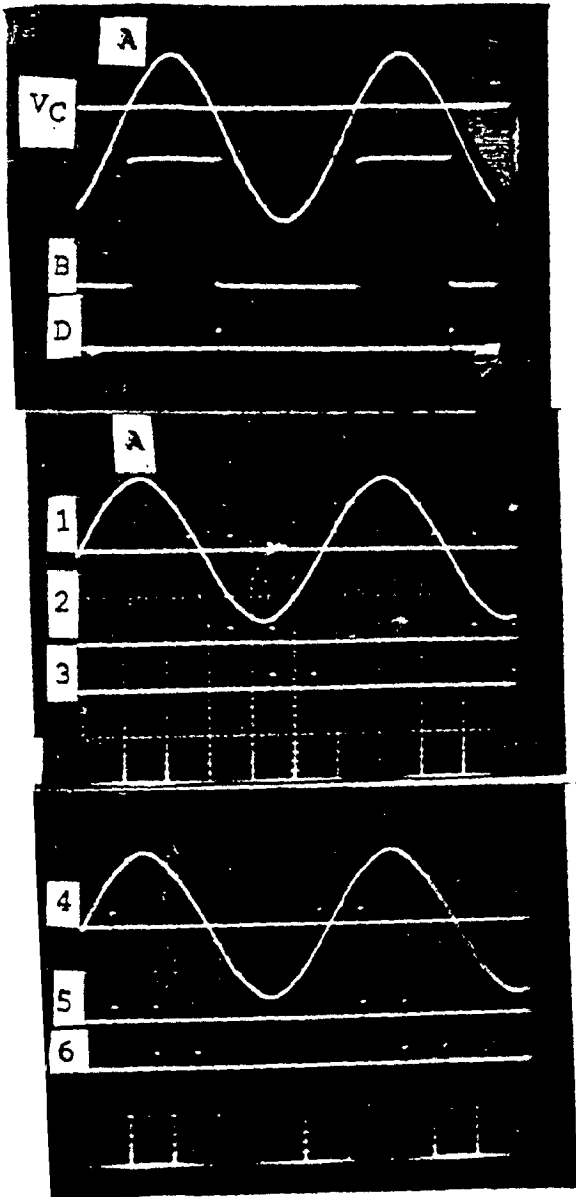
Power Amplifier

The required strength to the pulse is given by the power amplifier to trigger a SCR SL 100 is used as a medium power switch and the isolation of firing circuit to the power circuit is achieved using pulse transformer.

The detail pin diagrams of different integrated circuits used are given in Appendix - A.

2.5 Results and Discussions

The proposed power circuit and trigger circuit were fabricated and tested for LCI induction motor system over a large frequency range. The waveforms at the different points of firing circuit are recorded using storage CRO and shown in Fig. 2.5(a). The waveform are identical to the theoretical waveforms. The operation of the scheme has been found to be highly stable when control voltage and



G.2.5(a) Experimental waveforms at different points of firing circuit.

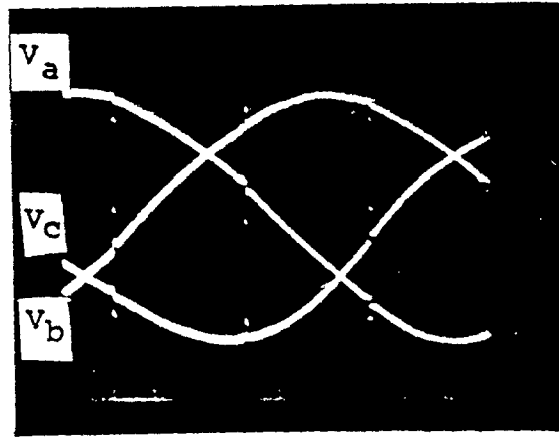


FIG. 2.5(b) Experimental waveform of inverter output voltages

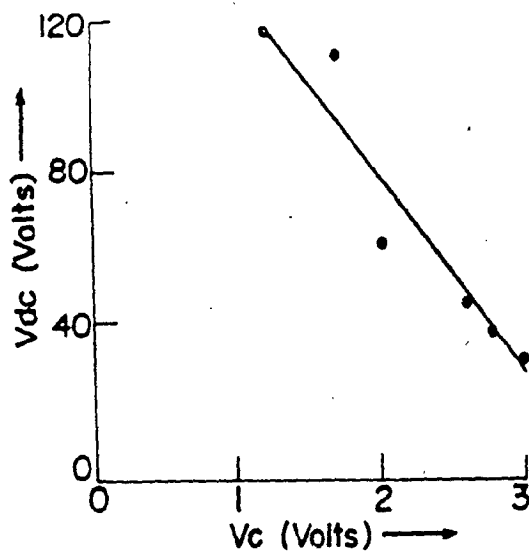


FIG. 2.6 Direct voltage versus control voltage characteristic.

operating frequency were varied simultaneously. The voltage waveforms at the output of a LCI are shown in Fig. 2.5(b). The notches shown on the voltage waveforms indicate the commutation overlap and also show the triggering of SCR of that mode. The d.c. link voltage versus control voltage characteristic to achieve inverter operation is obtained experimentally and is shown in Fig. 2.6. This characteristic is observed almost linear.

2.6 Conclusions

The complete design details of power circuit and firing circuit for LCI system are described. Based on these the power module and control scheme are fabricated and tested. For the firing circuit a cosine wave crossing method is used to generate firing pulses to result LCI as linear power amplifier. The developed scheme is found to be suitable for speed control of polyphase induction motors using d.c. link LCI. The scheme may also be used for closed loop operation of I.M.. The triggering of thyristors using pulses of short width reduces gate circuit losses and also reduces the size of pulse transformers.

CHAPTER - III

EXPERIMENTAL INVESTIGATIONS ON STEADY STATE PERFORMANCE OF THE SYSTEM

3.1 General

An exhaustive survey of published literature given in chapter-I reveals that a large work has been reported on the performance of the LCI fed synchronous machines covering wide aspects of its operation. On the other hand a little investigation has been carried out to study the performance of LCI fed I.M. [21,22]. No work has so far been done on this aspect for the motors of integral horse power ratings which are widely used in the industries. A need is therefore felt to investigate the feasibility of LCI fed induction motor for its variable speed operation. In this work, the steady state performance of the LCI fed three phase cage induction motor is obtained experimentally at no load as well as loaded conditions. The effects of d.c. link voltage and terminal capacitor have been studied to vary the speed of motor. The speed versus torque characteristics and performance in terms of the efficiency, power factor and currents of motor and inverter have been obtained for various combinations of d.c. link voltage and terminal capacitor values. Various tests have been carried out on a 4 H.P. semi squirrel cage I.M.

3.2 Starting Methods

As described in section 2.2 the system consists of three

phase auto transformer, uncontrolled bridge rectifier, smoothing inductor, line commutated bridge inverter, three phase step up transformer, a set of three phase capacitor banks and a three phase squirrel cage I.M. A three phase supply alongwith a three phase auto transformer and three phase uncontrolled rectifier provides a variable d.c. voltage input to the bridge inverter. Since source is variable d.c. voltage, it cannot supply lagging reactive power needed for the magnetization of magnetic circuit of the I.M. Therefore, the I.M. cannot be started directly by this source. The capacitor banks connected at the terminals of motor are charged due to induced e.m.f. of I.M. and hence supplies the required lagging reactive power. This shows that if the I.M. is brought to some speed by any means enough to provide magnetization as well as to commutate thyristors of the bridge inverter, the system will start working and draw active power from d.c. source while reactive power from capacitor banks.

Following two methods can be used to start the I.M.

3.2.1 Starting by a coupled d.c. motor

Fig. 3.1 shows the detailed circuit diagram of the system. In this method, the I.M. is brought at the proper speed by a coupled d.c. machine operating as a motor and the terminal capacitor bank is connected which results self excitation in the induction machine. The trigger signals for the inverter circuit are derived from the induced e.m.f. of the

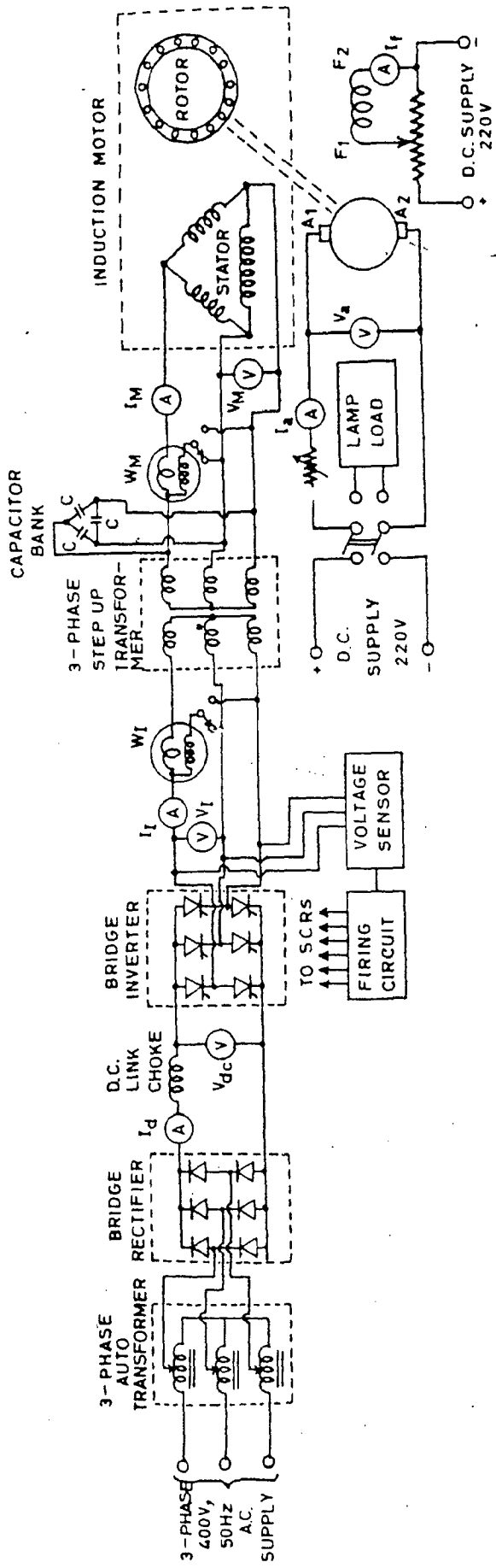


FIG.3.1 DETAILED CIRCUIT DIAGRAM OF THE LCI FED INDUCTION MOTOR SYSTEM FOR FIRST STARTING METHOD

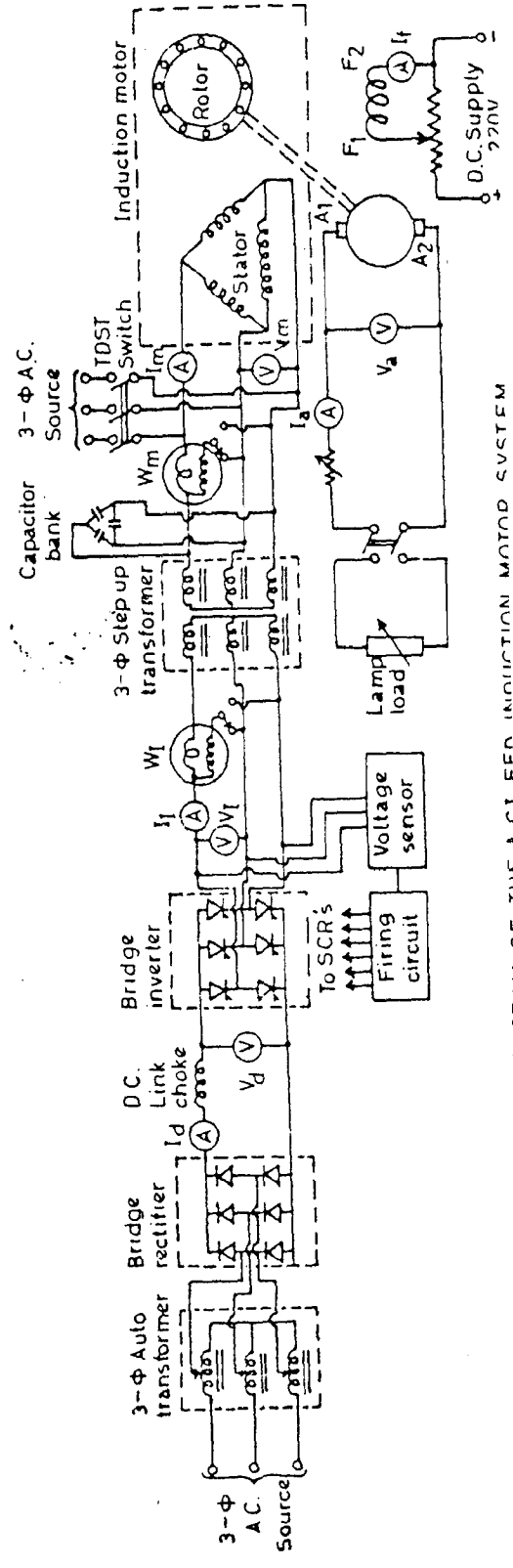


FIG.3.2 DETAILED CIRCUIT DIAGRAM OF THE LCI FED INDUCTION MOTOR SYSTEM FOR FIRST STARTING METHOD

stator of I.M. by the voltage sensor. Using fully controlled bridge, the inverter operation is achieved when firing angle exceeds 90° . If a d.c. source of proper polarity and magnitude is connected on the d.c. side of the inverter, the active power flows from the d.c. source to the motor. The power fed by d.c. machine is reduced slowly while d.c. link power is increased by adjusting d.c. link voltage and the induction machine changes its mode of operation gradually from generating to motoring at a frequency which is set itself. When power supplied by d.c. machine becomes negligible it may be switched off.

The main objective of this experimental investigation is to study the stability of the system, that is, to see whether induction machine will run as a motor stably if the d.c. machine is switched off. Surprisingly, it is observed that the machine run quite stably when driving machine is switched off. It is due to the fact that at the instant of switching off, the induction motor was operating at no load and the required losses were supplied by d.c. link and the driving machine. As soon as the d.c. machine is switched off, the speed of the induction motor falls slightly due to insufficient active power available. This reduces the motor induced e.m.f. The d.c. link voltage becomes greater than the reflected d.c. voltage of the inverter thus permits more current and power flow to the motor. As fall in speed is associated with more input of active power to the motor, the stable motoring operation is achieved. During stable

operation, the motor draws active power from d.c. link and the lagging reactive power requirement of the motor, the transformer and the inverter is supplied by terminal capacitor bank. This method can only be used for starting of the I.M. at no load.

3.2.2 Starting by a three phase supply

Fig. 3.2 shows a circuit diagram if starting of the I.M. is to be achieved by a normal three phase supply. To start the operation of the system, first of all the motor is initially connected to a three phase supply and is brought up to no load speed. The suitable value of capacitors is connected at the motor terminals and with the help of variable d.c. link voltage, the power flow through inverter is established. It is observed that, with the increase in d.c. link power output, the power drawn from the 3-phase supply decreases. When active power fed from the 3-phase source become negligible, it is switched off. The cage machine is continued to run taking its no load losses from d.c. link through inverter and its terminal voltage and frequency are decided by the d.c. link voltage, the value of terminal capacitor and the firing angle of inverter.

3.3 Results and Discussions

To obtain the experimental performance of the I.M. at varied loading conditions, the motor is loaded with the help of coupled d.c. machine running as separately excited d.c.

generator. The details of motor generator set are given in Appendix-B. Various experimental data were obtained by instruments located at appropriate points in the circuit as shown in Fig. 3.1. The test curves pertaining to the performance of the I.M. at no load and loaded conditions are shown in Fig. 3.3 to Fig. 3.5. The oscillogrames of the inverter output voltage and current, motor terminal voltage and current are recorded on a storage oscilloscope at no load and loaded conditions and are shown in Fig. 3.6.

The following salient features may be observed from the experimental results.

1. It can be observed from Fig. 3.3(a) that the speed of the I.M. reduces at no load with the increase in the value of terminal capacitors because of decrease in frequency. Similarly, it is observed from the experiments that by removal of terminal capacitors, the speed rises resulting increase in frequency. The speed of the motor is seen to be highly sensitive with the variation of capacitor in the higher speed range.
2. Fig. 3.3(b) shows the effect of d.c. link voltage on the no load speed of the motor for fixed value of terminal capacitors. The speed of the motor rises almost linearly with the increase in d.c. link voltage. With the proper selection of terminal capacitors and d.c. link voltage, a wide range of speed control can be achieved. On the selected machine, the range of speed control is observed from 30% to

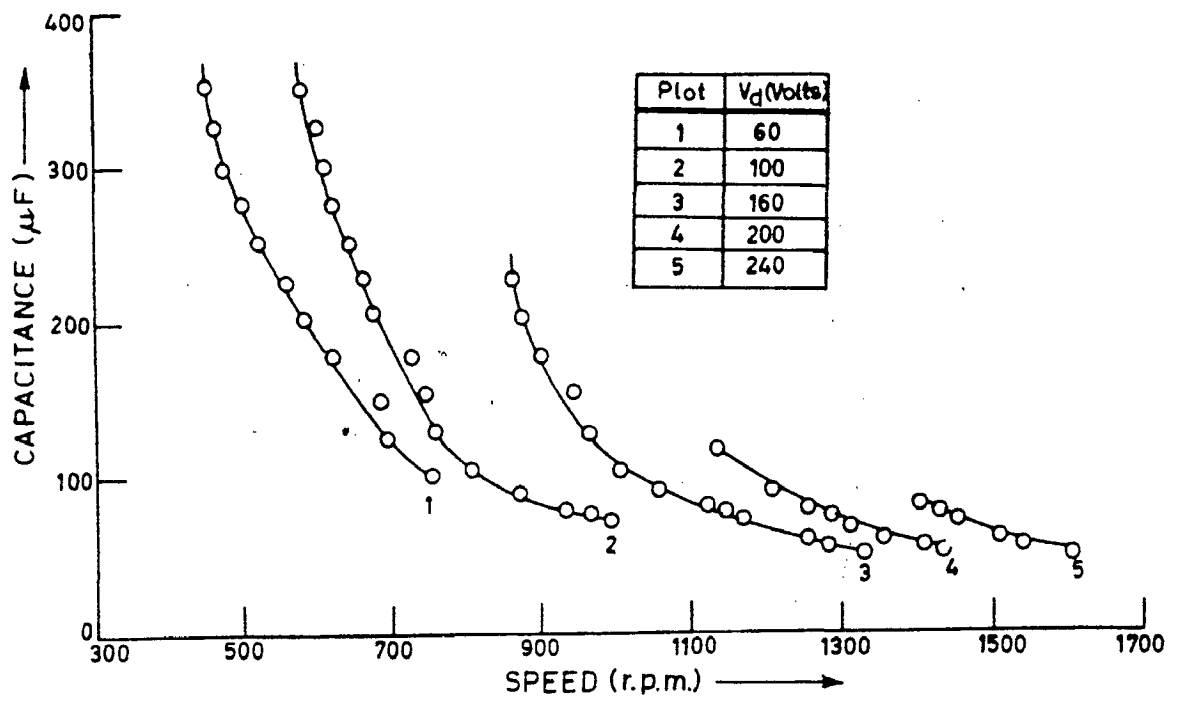


FIG. 3.3 (a) VARIATION OF CAPACITANCE WITH SPEED AT NO LOAD.

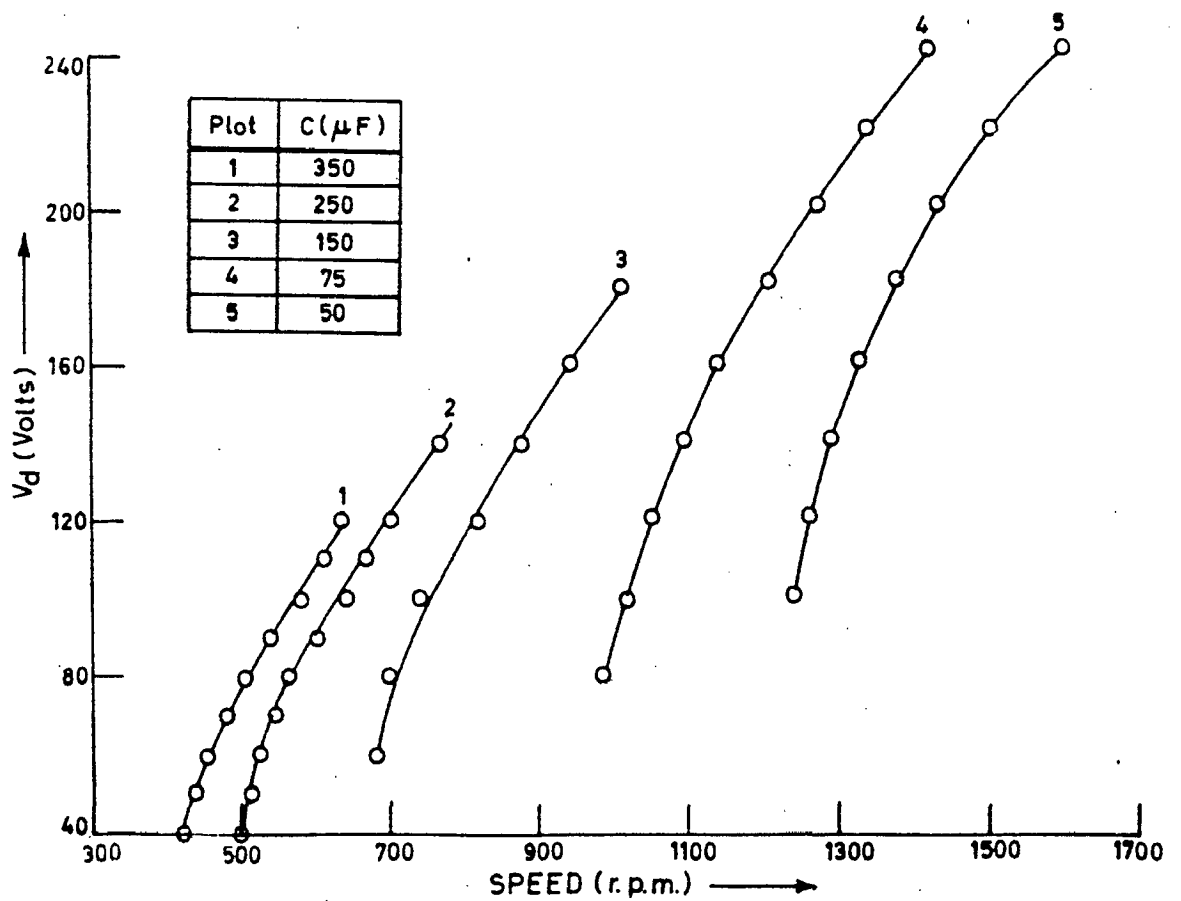


FIG. 3.3 (b) VARIATION OF V_d WITH SPEED AT NO LOAD.

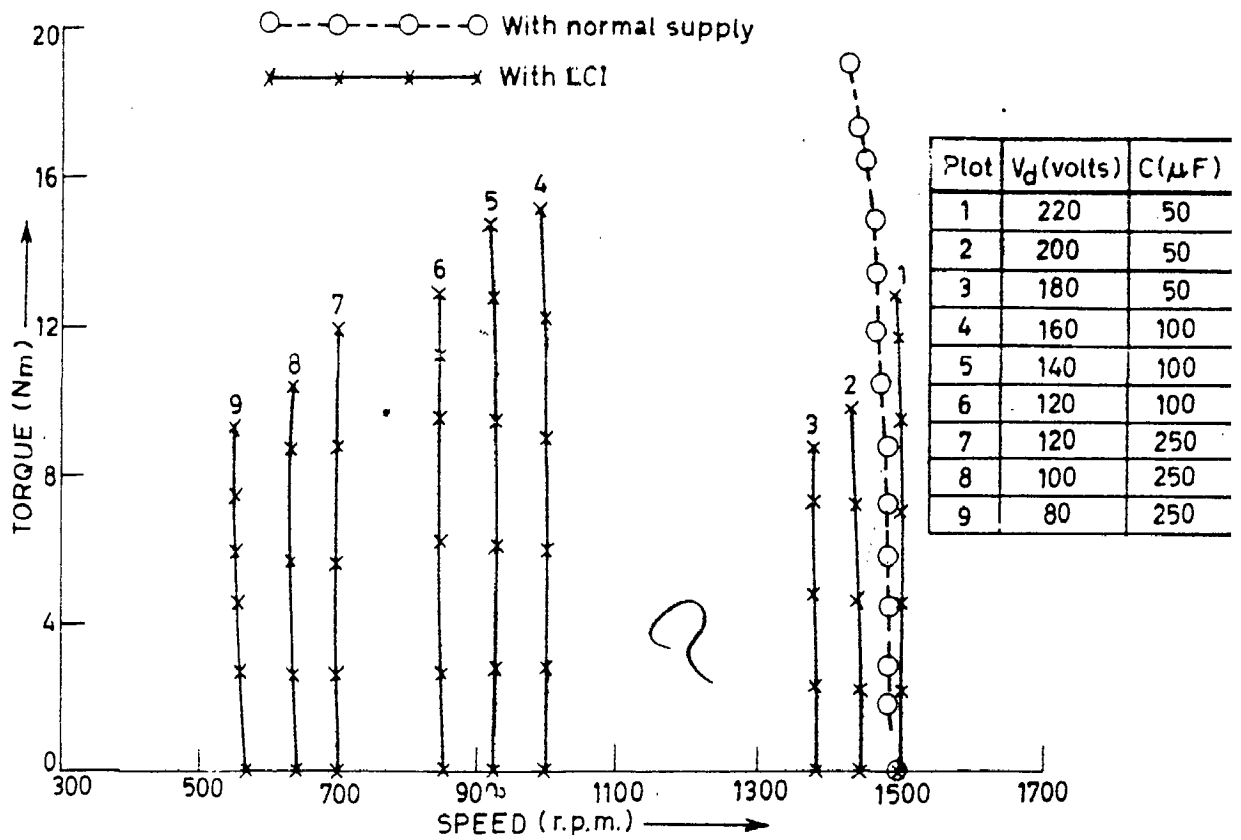


FIG. 3.4(a) Torque - speed characteristics of a LCI fed induction motor .

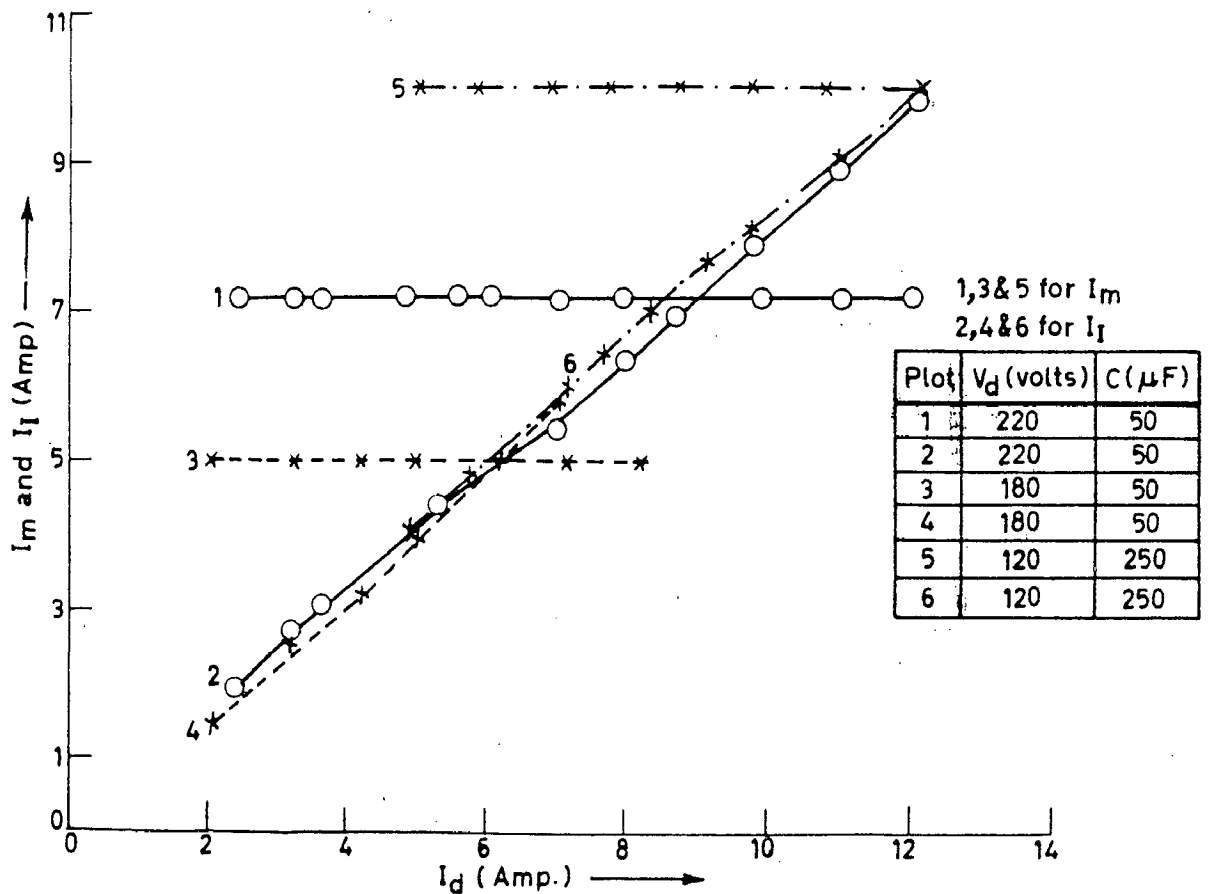


FIG. 3.4(b) Variation of motor (I_m) and inverter (I_i) currents with d.c. link current (I_d).

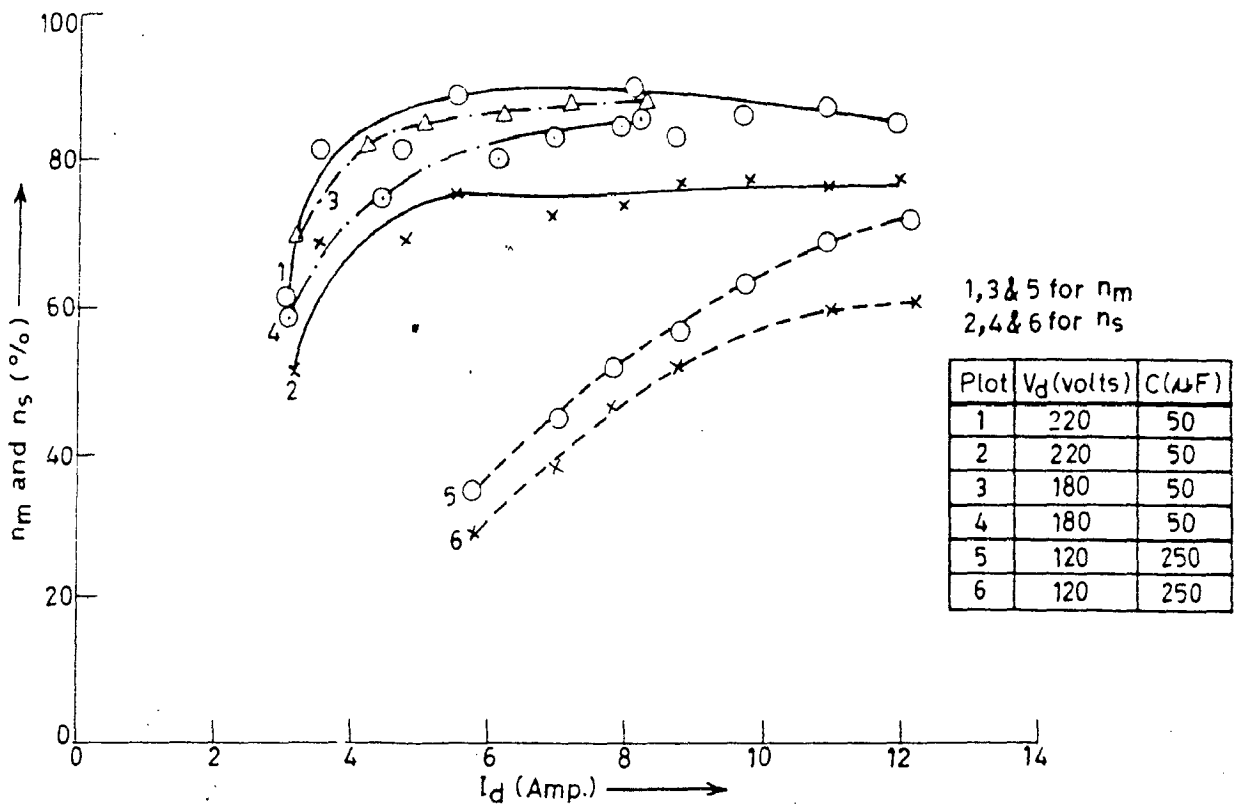


Fig. 3.4(c) Variation of motor (n_m) and system (n_s) efficiencies with d.c. link current (I_d).

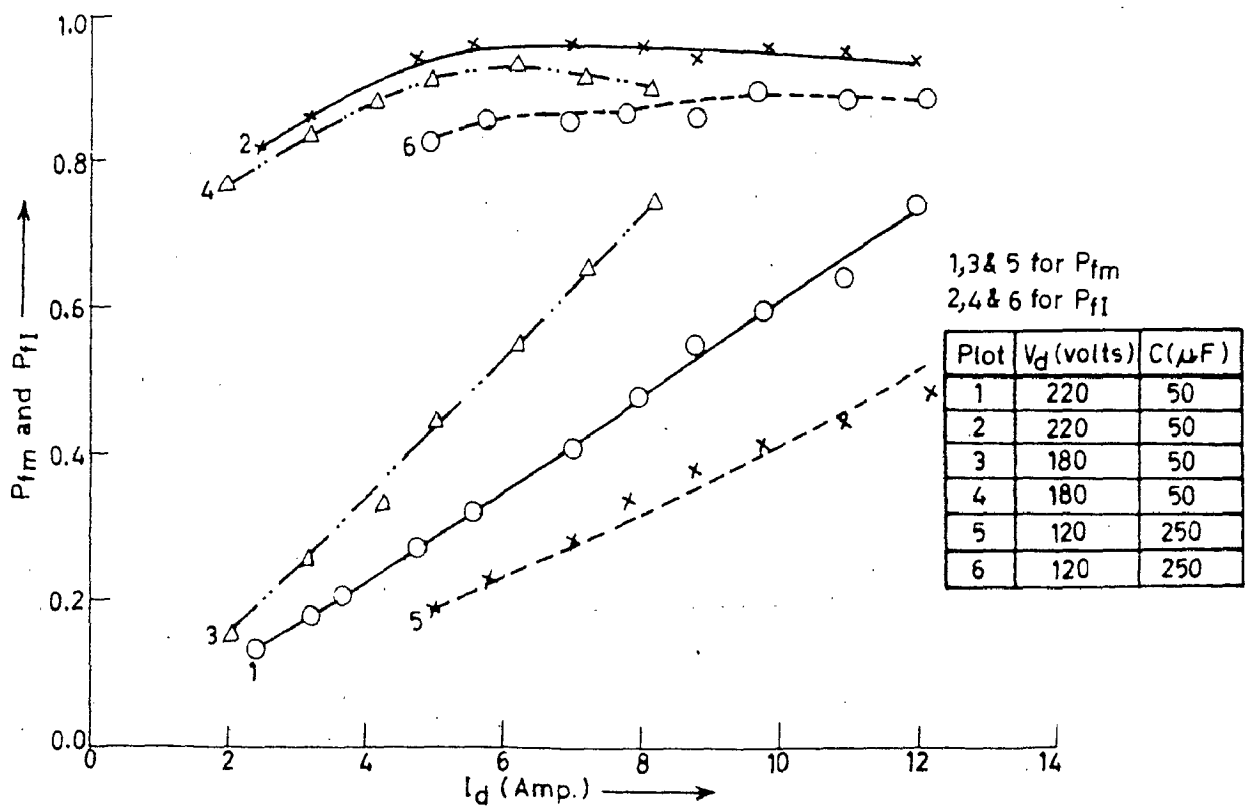


Fig 3.4 (d) Variation of motor (P_{fm}) and inverter (P_{fi}) with d.c. link current (I_d).

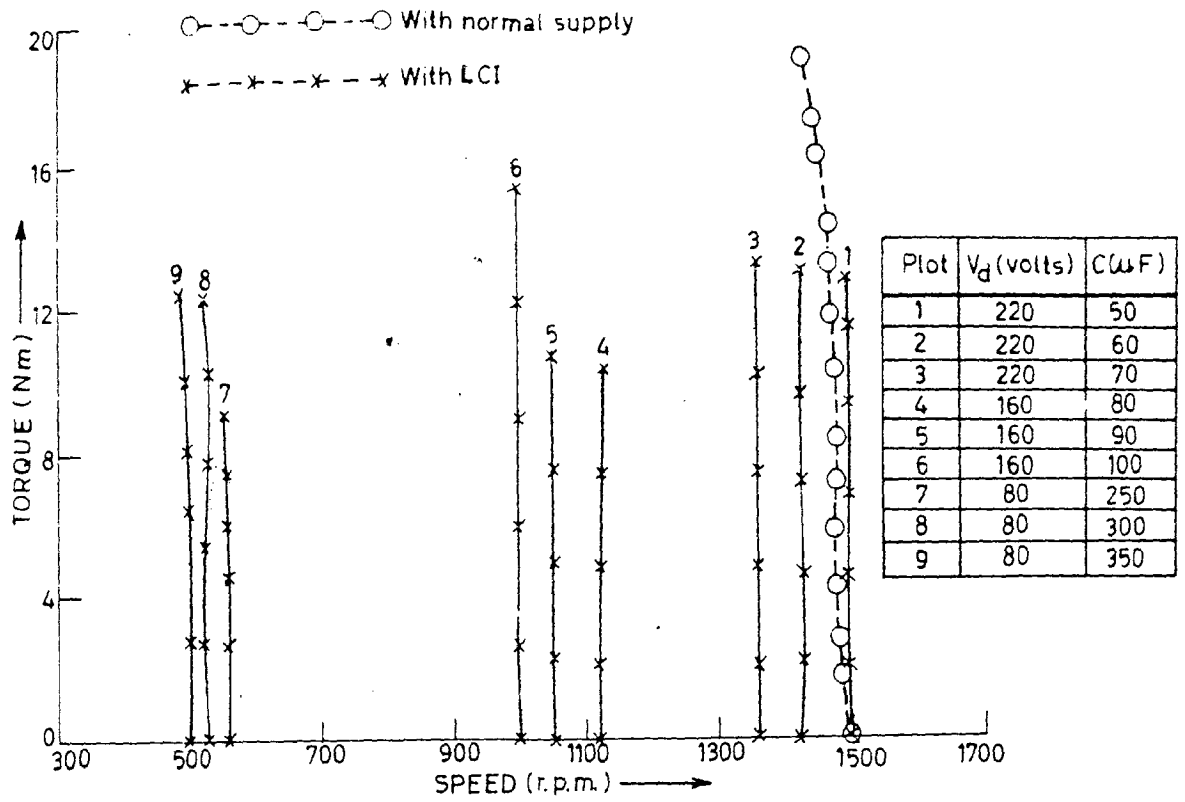


Fig. 3.5(a) Torque-speed characteristics of a LCI fed induction motor.

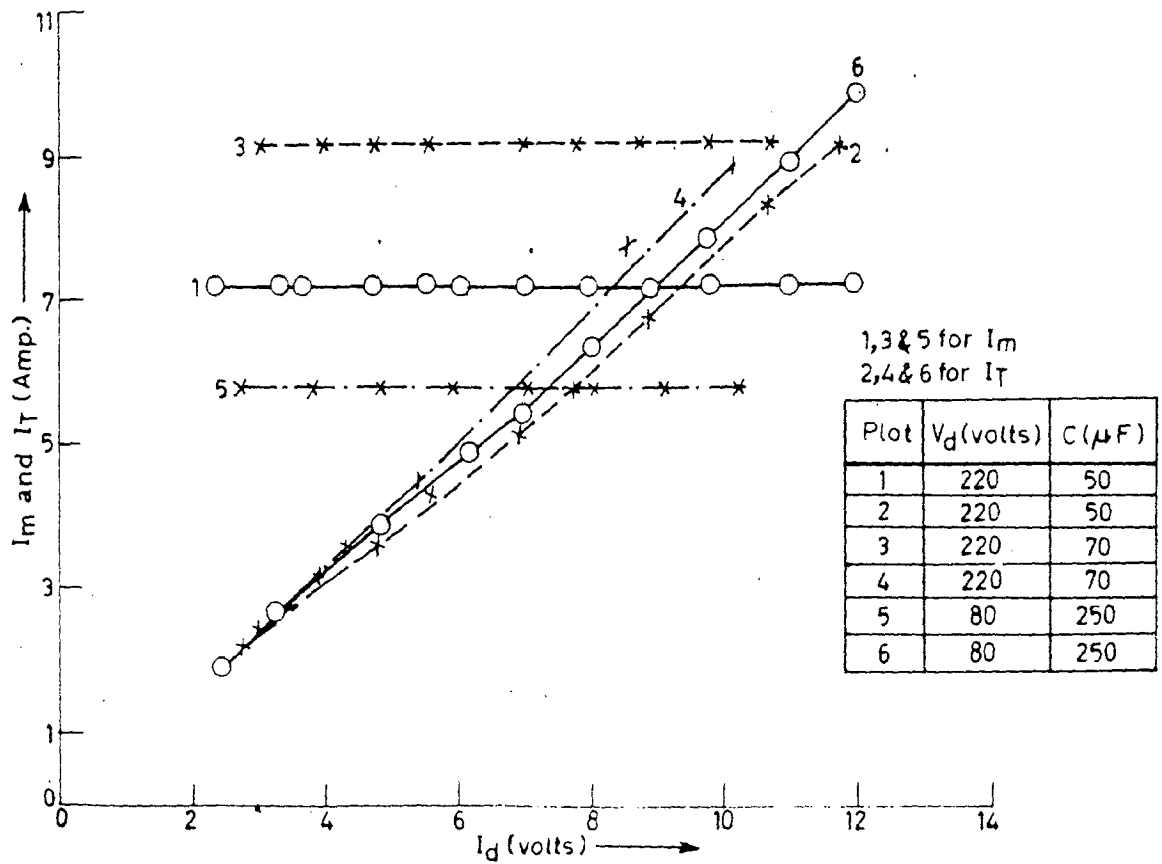


Fig. 3.5(b) Variation of motor (I_m) and inverter (I_i) currents with d.c. link current (I_d).

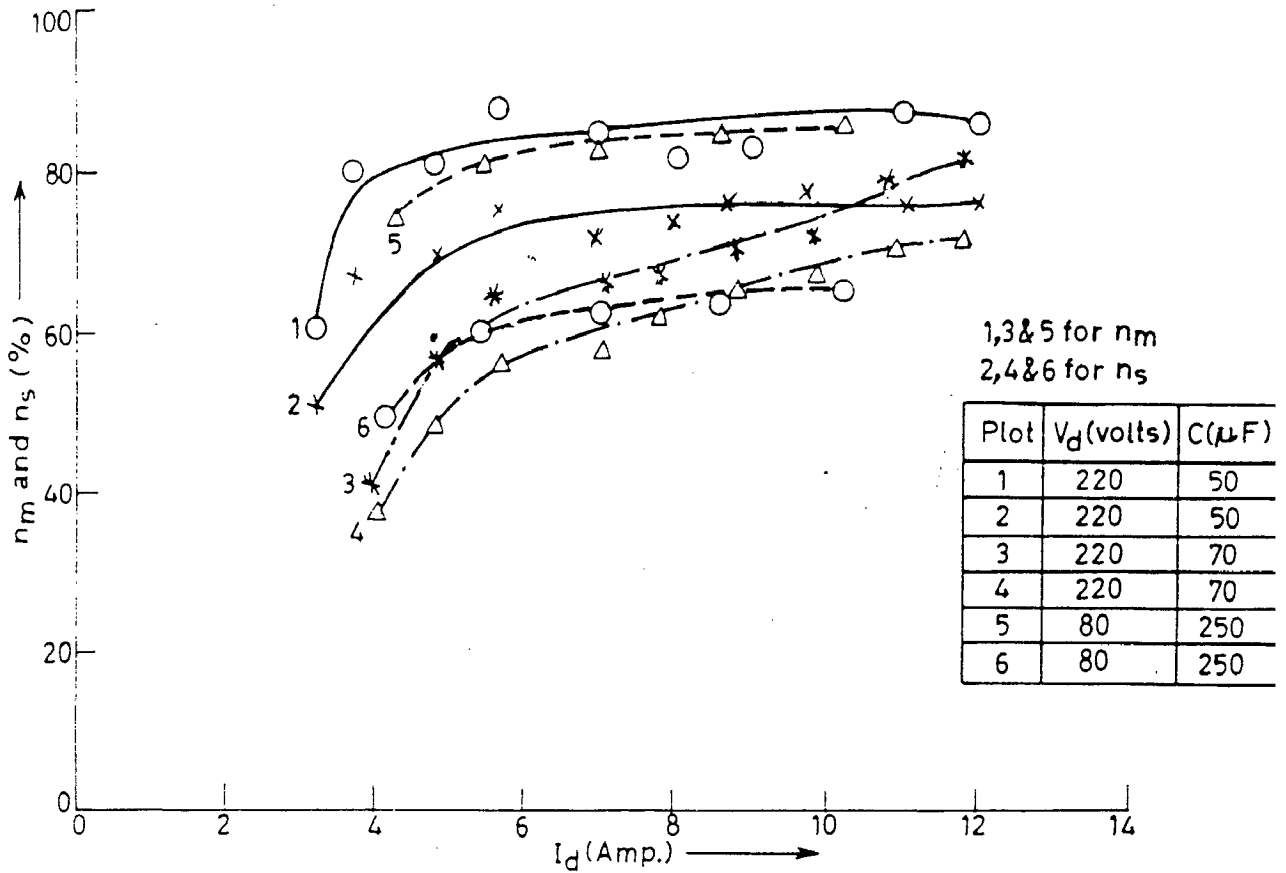


Fig. 3.5(c) Variation of motor (n_m) and system (n_s) efficiencies with d.c. link current (I_D).

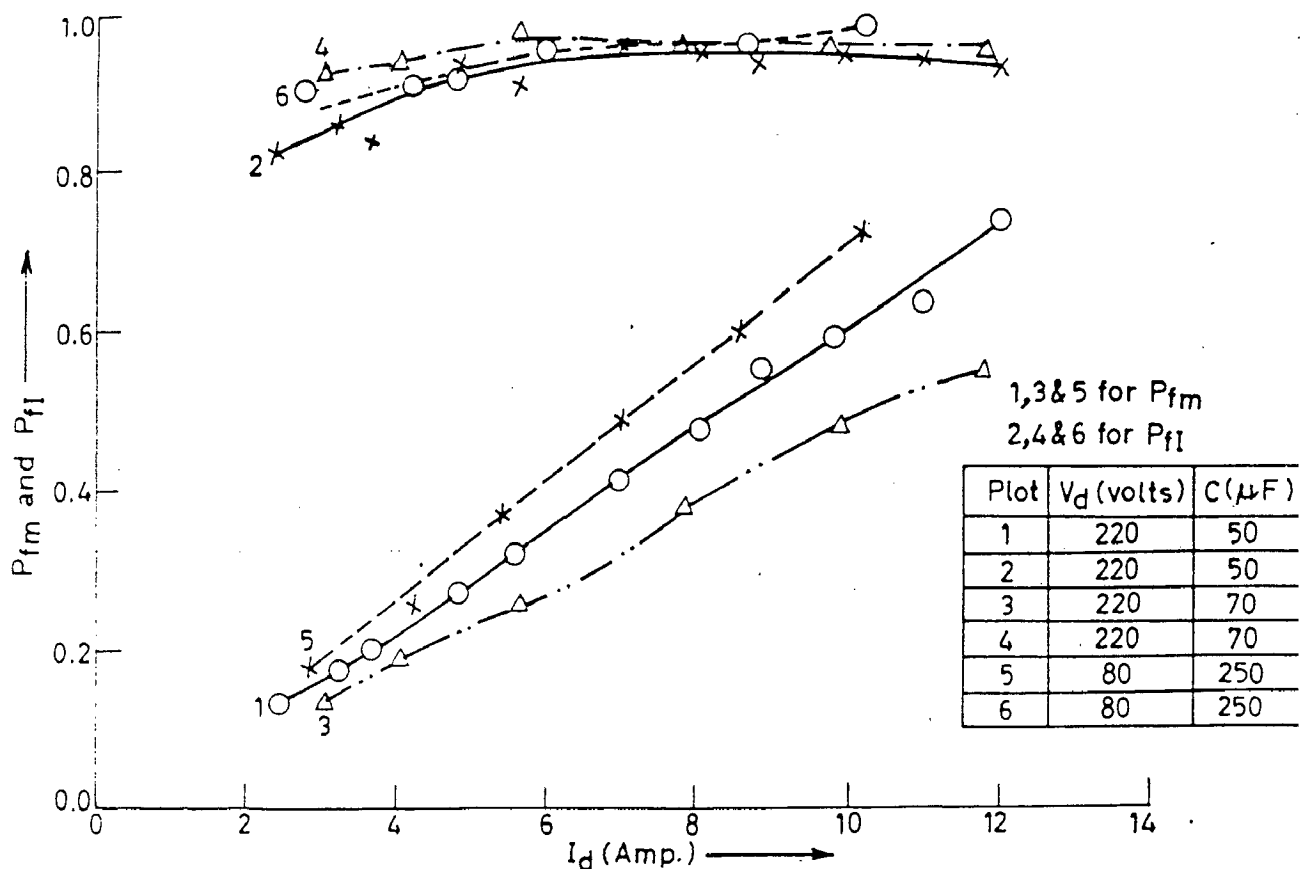


Fig. 3.5(d) Variation of motor (P_{fm}) and inverter (P_{fI}) with d.c. link current (I_D).

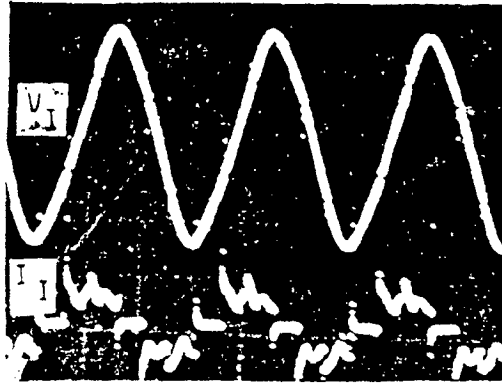


Fig. 3.6 a (i)

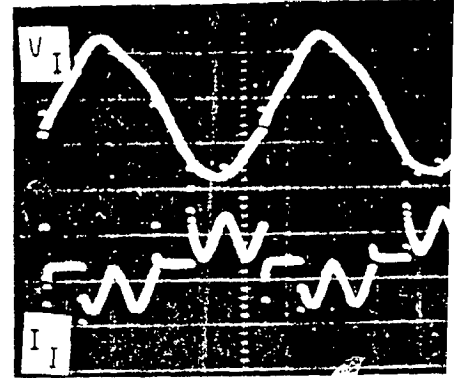


Fig. 3.6 a (ii)

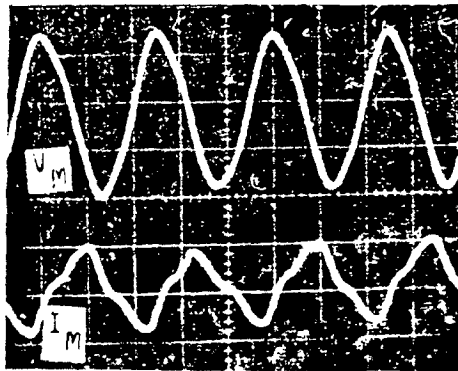


Fig. 3.6 b (i)

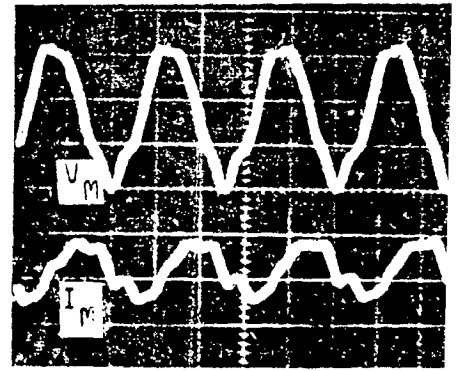


Fig. 3.6 b (ii)

Fig. 3.6 VOLTAGE (V) AND CURRENT (I) WAVEFORMS OF (a) INVERT (i) AT NO LOAD (ii) AT LOAD, (b) MOTOR (i) AT NO LOA (ii) AT LOAD.

110%.

It may be suggested here that during high speed region, the speed control should be obtained by varying value of terminal capacitor. While d.c. link voltage should be selected on the basis of loading of the motor. At low speeds, it would be preferable to vary d.c. link voltage while keeping terminal capacitor fixed.

3. It can be seen from experimental data under loaded condition of motor shown in Fig. 3.4(a) that there is a little fall in the speed of the motor with the load and is much lesser than that of the case when motor is fed by normal three phase supply. This is due to the fact that the system frequency increases with the increase of load. It might be due to extra lagging reactive power requirement with the increase in load which can only be met if terminal voltage or frequency of the motor is increased. It is observed experimentally that the frequency of the system increases slightly as the load is increased on the motor. For most of the purpose, the LCI fed induction motor can be treated as constant speed drive.

4. From Figs. 3.4(a) and 3.5(a), it can be observed that motor current is almost constant with load. It is due to the power factor of motor which is very poor at no load and rises with load as evident from Figs. 3.4(d) and 3.5(d). However, the inverter current increases with load as shown in Fig. 3.4(b) and 3.5(b). It is due to that the power

factor of inverter is almost constant as again shown in Fig. 3.4(d) and 3.5(d). This constancy in inverter power factor is also due to that inverter was operating at a firing angle very near to 180° causing very small requirement of reactive power by inverter.

5. Fig. 3.4(c) and 3.5(c) shows the variation of efficiency of motor as well as of system. It is observed from these figs. that motor efficiency rises with load. It is due to constant losses of induction motor from no load to loaded condition caused by constant stator current and constant flux in the machine. However, the overall efficiency of the system is also rises but with reduced rate. It is because of increased losses in transformer (step-up) and inverter with increased current in those elements under loaded conditions. The motor and system efficiencies decreases at increased d.c. link voltage at constant value of capacitor due to rise of motor current which is constant at different loads.

6. Fig. 3.6 shows the waveforms of inverter output voltage and current alongwith motor voltage and current at no load as well as loaded conditions. It is observed that the voltage waveforms are almost sinusoidal and free from harmonics. However, the small notches related to overlap during commutation process may be observed in inverter voltage waveforms. The current waveforms are rich in harmonics at no load.

3.4 Conclusions

The various starting methods of the system are discussed in detail which may be adopted for satisfactory starting of motor under no load as well as loaded conditions. The performance of motor under no load as well as loaded condition fed from LCI for its variable frequency operation is studied in detail. Under loaded condition an interesting features of the system is observed that the speed of motor remains constant irrespective of load. However, the speed may be increased by increasing the d.c. link voltage or by decreasing the value of capacitance. It is concluded that at the higher speed range the system is very sensitive to the capacitance, therefore the speed control at higher speeds may be obtained by varying the capacitance and at lower speed range it may be controlled by varying the d.c. link voltage.

CHAPTER - IV

ANALYSIS AND PERFORMANCE OF A LINE COMMUTATED INVERTER FED INDUCTION MOTOR

4.1 General

The L.C.I. is widely used for the speed control of synchronous motor. Watson [21,22] has also attempted to use this inverter for the speed control of three phase I.M. of F.H.P. rating. An approximate equivalent circuit was used to predict the performance of the motor at no load. No attempt has been made so far, to analyse the performance of the motor at loaded conditions.

In this chapter, an attempt has been made to present the steady state analysis of an integral horse power rating squirrel cage I.M. using L.C.I. The analytical models for no load as well as loaded conditions of the motor are developed using equivalent circuit approach and are simulated on a digital computer to obtain the steady state performance in terms of torque speed characteristics, efficiency, power factor, motor and inverter currents with respect to d.c. link current. The effects of terminal capacitor and d.c. link voltage are studied to obtain wide range of speed control. The corresponding test results on a 4 H.P. induction motor (details are given in Appendix- B) are presented alongwith computed results to justify the validity of developed model.

4.2 Analysis

The analysis is carried out separately for no load and loaded conditions of the motor. The following simplifying assumptions are considered.

- (i) The forward drop of thyristors and their circuit losses are neglected.
- (ii) The overlap angle is neglected as it was also observed very small for the system.
- (iii) The effects of space and time harmonics are ignored.
- (iv) Leakage inductances and winding resistances of motor and transformer are assumed constant.
- (v) The transformer and motor parameters are lumped together.
- (vi) The losses in capacitor banks are assumed negligible.

Fig. 4.1 shows the approximate equivalent circuit of the system at any per unit operating frequency 'F' and slip 'S'. The no load branch parameters R_m and X_m are p.u. core loss resistance and magnetising reactance and include the corresponding quantities for both induction motor and transformer. R and X are p.u. total resistance (excluding rotor resistance R_2 of motor referred to stator side) and leakage reactances of transformer windings and stator of motor. All parameters are normalised on the base of motor rated per phase quantities.

4.2.1 Analytical Model

For a given d.c. link voltage (V_d) and inverter firing angle (α), the a.c. side inverter voltage (v) per phase may be calculated and is referred to the motor stator side by turn ratio of transformer and is as follows:

$$V = \frac{\sqrt{3} V_d T_R}{(3 \sqrt{2} \cos \beta)} \quad \text{--- (4.1)}$$

Where T_R = Turn ratio of transformer

and $\beta = (180^\circ - \alpha)$

Where β is known as inverter angle of advance.

In this circuit for a given capacitance 'C' (X_c with p.u. reactance at rated frequency), the p.u. frequency 'F' is the unknown variable to be determined. The no load parameters (R_m, X_m) depend on voltage to frequency ratio (V/F). To obtain these parameters, the no load test on the combination of transformer and motor is carried out at rated frequency (i.e. $F = 1$) and at various values of supply voltage. The variation of R_m and X_m with (V/F) is obtained using these experimental data and is shown in Fig. 4.2. To simplify the analysis, these characteristics are linearized in the following way

$$X_m = K_1 - K_2 (V/F) \quad \text{--- (4.2a)}$$

$$R_m = K_3 + K_4 (V/F) \quad \text{--- (4.2b)}$$

To obtain an expression being function of frequency, the active and reactive power balance of the whole system

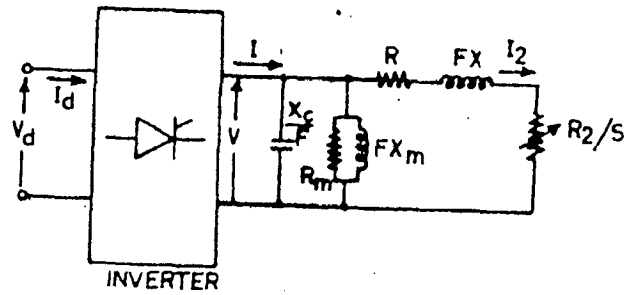


FIG. 4.1 EQUIVALENT CIRCUIT OF LCI-FED INDUCTION MOTOR-SYSTEM.

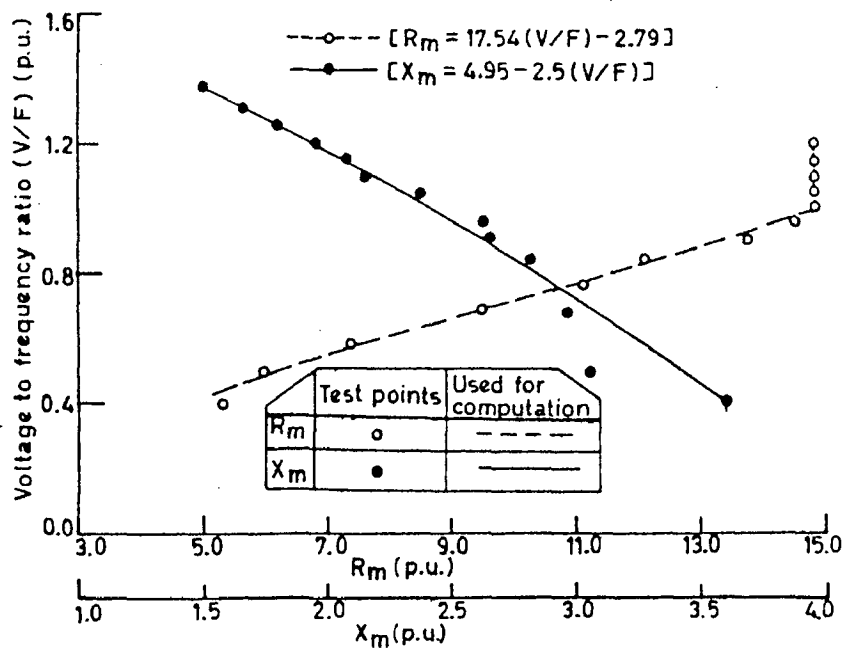


FIG. 4.2 VARIATION OF CORELOSS RESISTANCE (R_m) AND MAGNETISING REACTANCE (X_m) WITH VOLTAGE TO FREQUENCY RATIO (V/F).

is carried out.

(i) Active Power Balance

$$\text{Power supplied by inverter } P_I = V_I \cos \beta \quad \text{--- (4.3)}$$

Power required by the combination of motor and transformer to meet their no load losses,

$$P_{mT} = \frac{V^2}{R_m} \quad \text{--- (4.4)}$$

$$\text{Power fed to the load, } P_L = VI_2 \cos \phi_2 \quad \text{--- (4.5)}$$

$$\text{Where, } I_2 = V / [(R + \frac{R_2}{S})^2 + (FX)^2]^{1/2} \quad \text{--- (4.6)}$$

and $\cos \phi_2 = (R + R_2/S) / [(R + R_2/S)^2 + (FX)^2]^{1/2} \quad \text{--- (4.7)}$

Equating active power supplied to the consumed value,

$$VI \cos \beta = \frac{V^2}{R_m} + VI_2 \cos \phi_2 \quad \text{--- (4.8)}$$

(ii) Reactive Power Balance

Reactive power needed by inverter for its operation,

$$Q_I = VI \sin \beta \quad \text{--- (4.9)}$$

Reactive power required by motor and transformer,

$$Q_{mT} = V^2 / (FX_m) \quad \text{--- (4.10)}$$

$$\text{Reactive power required to load, } Q_L = VI_2 \sin \phi_2 \quad \text{--- (4.11)}$$

$$\text{Reactive power supplied by capacitor, } Q_C = V^2 F / X_C \quad \text{--- (4.12)}$$

The reactive power balance equation is

$$(V^2 F / X_C) = (V^2 / FX_m) + VI \sin \beta + VI_2 \sin \phi_2 \quad \text{--- (4.13)}$$

To obtain a generalized formulation suitable to no load and loaded conditions a binary variable N is introduced in equation (4.8) and (4.13) which assumes value either 0 or 1 to decide, the state of operation. As the rotor current I_2 is negligible at no load and increases with load, the multiplication of N with I_2 will provide information regarding the state of operation. A '0' indicates no load operation while '1' stands for loaded condition. The equation (4.8) and (4.13) are rewritten in the following way,

$$VI \cos \phi = (V^2/R_m) + N V I_2 \cos \phi_2 \quad \dots (4.14)$$

$$(V^2F/X_c) = (V^2/FX_m) + VI \sin \phi + N VI_2 \sin \phi_2 \quad \dots (4.15)$$

Eliminating I in equations (4.14) and (4.15), one may get,

$$V^2F/X_c = V^2/(FX_m) + (V^2 \tan \phi / R_m) + N V I_2 (\tan \phi \cos \phi_2 + \sin \phi_2) \quad \dots (4.16)$$

Using equation (4.2), (4.6) and (4.7), the equation (4.16) gets simplified in the following way,

$$(A_1 F^3 + A_2 F^2 + A_3 F + A_4) = \frac{N X X_c}{[(R_1 + R_2/S)^2 + (FX)^2]} \cdot (B_1 F^2 + B_2 F + B_3) \quad \dots (4.17)$$

Where,

$$A_1 = K_1 K_3$$

$$A_2 = (K_1 K_4 - K_2 K_3) V - X_c K_1 \tan \phi$$

$$A_3 = K_2 X_c \tan \phi V - K_2 K_4 V^2 - X_c K_3$$

$$A_4 = - X_c K_4 V$$

$$\begin{aligned} B_1 &= A_1(R_1+R_2/S) \tan\beta - (K_2K_4 - K_1K_3) VX \\ B_2 &= - (K_2K_4 - K_1K_3) (R_1+R_2/S)V \tan\beta - K_2K_4V^2 X \\ B_3 &= - (R_1+R_2/S) K_2K_4V^2 \tan\beta \end{aligned}$$

At no load, $N = 0$, hence equation (4.17) is reduced to a polynomial

$$g_0(F) = A_1F^3 + A_2F^2 + A_3F + A_4 = 0 \quad \text{--- (4.18)}$$

During loading conditions, $N = 1$ and equation (4.17) is simplified in the following way,

$$g_1(F) = D_1F^5 + D_2F^4 + D_3F^3 + D_4F^2 + D_5F + D_6 = 0 \quad \text{--- (4.19)}$$

where,

$$\begin{aligned} D_1 &= A_1X^2; D_2 = A_2X^2; D_3 = A_3X^2 + (R_1 + \frac{R_2}{S})^2 A_1 \\ D_4 &= (R_1 + \frac{R_2}{S})^2 A_2 + A_4X^2 - XX_c B_1 \\ D_5 &= (R_1 + \frac{R_2}{S})^2 A_3 - XX_c B_2 \\ D_6 &= (R_1 + \frac{R_2}{S})^2 A_4 - XX_c B_3 \end{aligned}$$

The equations (4.18) and (4.19) are nonlinear algebraic equations and a suitable numerical technique is to be used to compute the value of 'F' (p.u. frequency) for the given values of d.c. link voltage (Vd), inverter firing angle (β), capacitor bank (X_c) and 'S' during loading conditions. In this investigation, 'Newton Raphson' method [31] has been found suitable for obtaining one real root of equation (4.18) and (4.19). This method requires an

initial guess of the unknown variable, say, F_0 . Since at the instant of disconnection of the motor from normal supply, $F = 1$ and later on it is adjusted according to controlling parameters. Therefore in the solution of equation (4.18) the initial value of 'F' is considered as $F_0 = 1$. Now $g_0 = g_0(F_0) = 0$.

At the end of first iteration, F will be modified as $F + \Delta F$ where F is obtained in the following way,

$$F = - g_0(F_0) / g_0'(F_0) \quad \text{--- (4.20)}$$

where, $g_0'(F)$ is the partial derivative of function $g_0(F)$ with respect to F.

The iterative process may continue till the convergence criterion is not satisfied (the desired accuracy is reached) i.e. when $|g_0(F)| < \epsilon$ where ϵ is very small quantity as for desired accuracy.

To obtain the solution of equation (4.19), the initial guess can be taken as the frequency at no load corresponding to the specified parameters at which loaded performance is to be evaluated as the change in frequency from no load to full load is very small. The rest procedure is identical as used for the solution of equation (4.18).

Using equivalent circuit of Fig. 4.1, the d.c. link current (I_d) is given as

$$I_d = PI/V_d \quad \text{--- (4.21)}$$

The motor torque (T) as

$$T = 3I_2^2 R_2 / (F S \omega_0) \quad (4.22)$$

where ω_0 is the base synchronous speed of motor

$$\text{The motor output } P_o = 3(1-S)I_2^2 R_2/S \quad (4.23)$$

and the overall system efficiency (η_s) is given by

$$\eta_s = (P_o / P_I) \times 100 \quad (4.24)$$

4.3 Digital Simulation

The equation presented for motor operation fed from LCI system at no load and loaded conditions are complex for different values of d.c. link voltage, inverter delay angle and capacitance. A general computer algorithm has been developed for no load and loaded conditions of motor and the flow chart is shown in Fig. 4.3. The listing of computer programs is given in Appendix-C.

Using the developed computer programme based on presented algorithm for no load and loaded conditions of motor, performance is simulated on a DEC-20 digital computer. The digital simulation of motor performance requires very small computational time and memory storage on digital computer.

The computed results for a motor (whose parameters are given in Appendix-B) for no load operation are presented in Fig. 4.4 for different values of d.c.

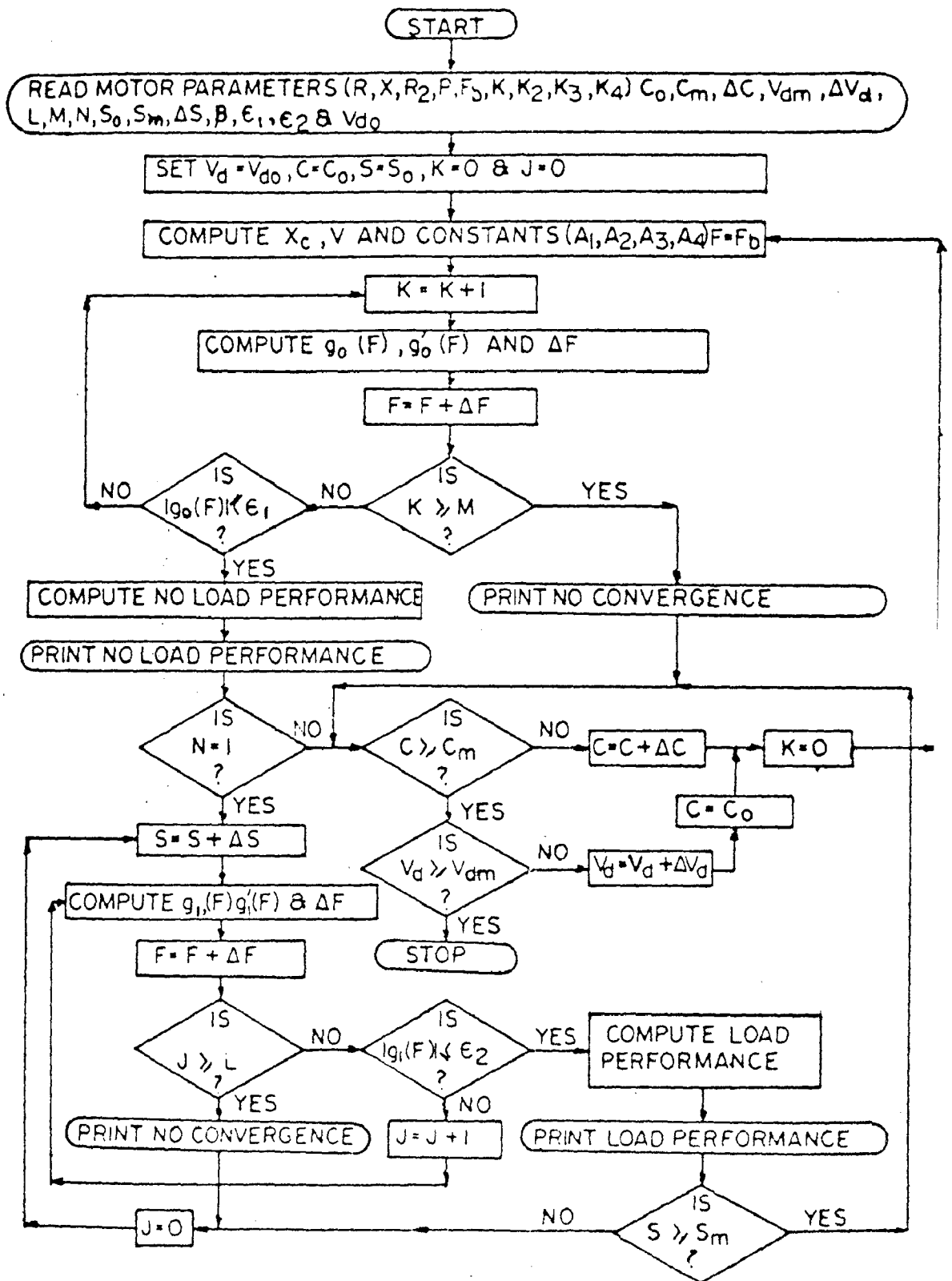


FIG. 4.3. FLOW CHART OF COMPUTER PROGRAMME.

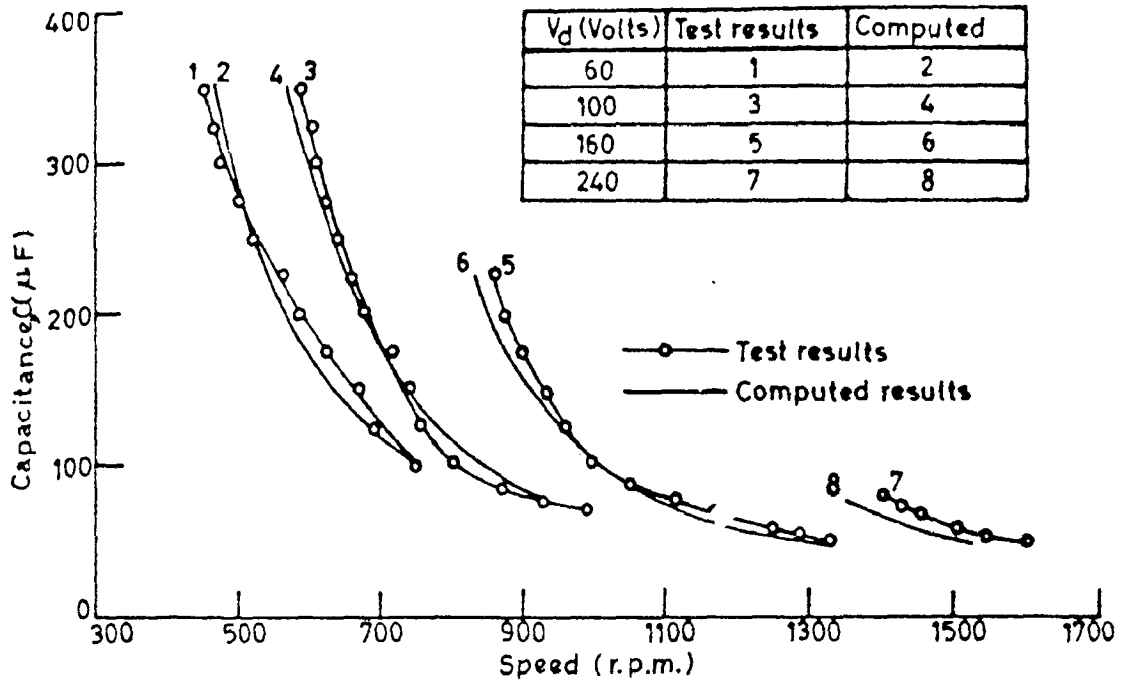


FIG. 4.4 (a) VARIATION OF CAPACITANCE WITH SPEED AT NO LOAD.

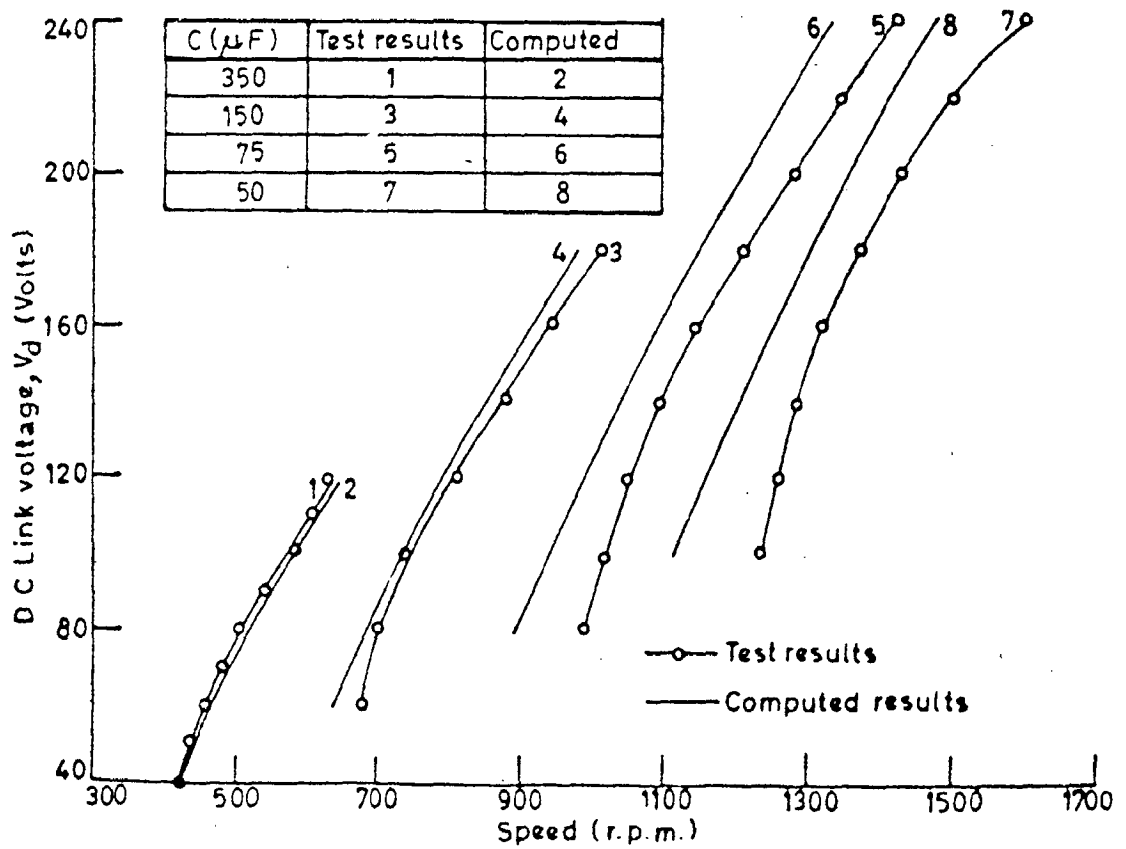


FIG. 4.4 (b) VARIATION OF D C LINK VOLTAGE WITH SPEED AT NO LOAD.

link voltage and capacitance. The motor performance at load are given in Fig. 4.5 in terms of torque speed, current, of the system.

4.4 Discussion of Results

The performance of an induction motor fed from line commutated inverter has been discussed in terms of various computed and experimental results shown in Figs. 4.4-4.5. Further, certain general observations on the basis of outcome of this attempt, has also been given mentioning the merits and attractive features of this system.

It may be observed from Fig. 4.4(a) that the value of capacitor also affects the speed of motor much at no load specially at higher speeds. It is also observed experimentally that with addition of more value of terminal capacitors speed falls down while on the other hand, speed rises by removal of the part of capacitor banks. However, it may be seen from Fig. 4.4(b), that the speed of motor is very much affected by d.c. link voltage and approximately varies linearly with d.c. link voltage. It is due to that with increase in d.c. link voltage, the terminal voltage at motor terminals and frequency are bound to increase because the system will try to maintain constant voltage to frequency ratio for stability of operation. It may also be observed from Fig. 4.4 that the computed results show the good correlation with experimental ones thus establishing the validity of model for no load operation. A little deviation in the

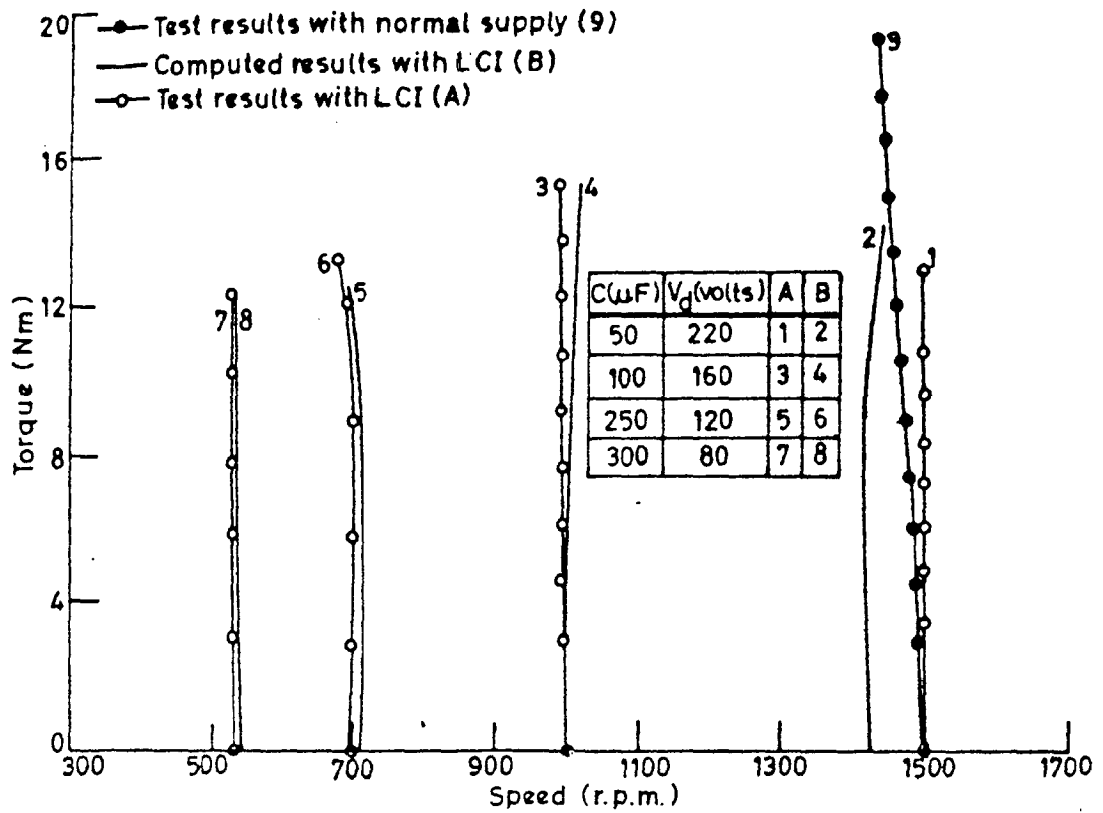


FIG. 4.5(a) TORQUE - SPEED CHARACTERISTICS OF A LCI - FED INDUCTION MOTOR.

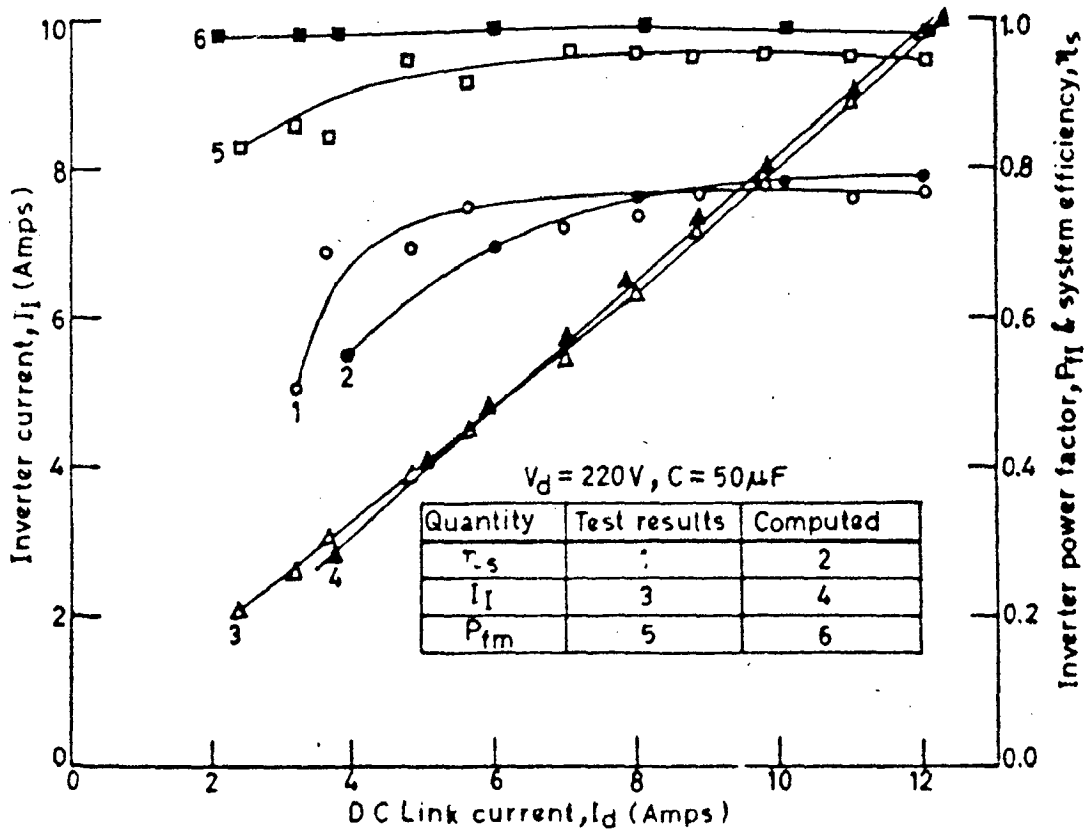


FIG. 4.5 (b) VARIATION OF INVERTER CURRENT, POWER FACTOR & SYSTEM EFFICIENCY WITH D C LINK CURRENT.

results is seen at high speeds and particularly where value of capacitor is small. It is because that the capacitor is not ideal and its effective value may be slightly different from the value considered in computation.

Fig. 4.5(a) shows the torque speed characteristics at different values of capacitance and d.c. link voltage. It is very interesting to note that the system provides that approximately constant speed on different torques. However, it may be observed from test results that there is a little fall in speed with loads and it is much lesser than that the case when motor is fed from normal 3-phase supply.

The close correlation between experimental and computed results may be observed from Fig. 4.5(a). In computed results speed rises, it is due to increased requirements of reactive power in the motor and which may be met by increasing the frequency at constant voltage and terminal capacitance. In computed results it is more due to that in computation leakage reactances are assumed constant while in practice it will not remain constant at different loads. Fig. 4.5(b) shows the overall efficiency, inverter output current and inverter power factor. From these figures it may be observed that computed results of inverter power factor have difference from test results it is due to that the effect of source impedance, overlap angle, thyristors drop and ripples in d.c. link voltage and currents are neglected in the analysis. The difference in magnitude of system efficiency and inverter current are also observed however, the

nature of these computed and test curves are identical.

4.5 Conclusions

A complete performance study computed and experimental of a variable speed cage induction motor drive fed from line commutated inverter has been studied. The developed analytical techniques for the no load and loaded operation of motor, which use equivalent circuit and Newton Raphson method were found suitable to compute the no load and on load performance in terms of speed torque, efficiency, power factor and currents for different values of d.c. link voltage and terminal capacitance. The test results shows the good correlation with computed ones. Moreover the developed analytical technique requires little computational time and small memory storage. It is also concluded that the desired range of speed control may be achieved using suitable values of terminal capacitance and d.c. link voltage.

CHAPTER - V

EXPERIMENTAL INVESTIGATIONS ON SYSTEM AS A VARIABLE FREQUENCY SOURCE

5.1 General

Variable frequency source is greatly needed in the industries to feed static resistive and inductive loads. Besides, it is also used to obtain wide speed control operation of three phase I.M. A large number of static frequency converter has been developed using thyristors and transistors. Recently, the use of LCI has been extended to convert a synchronous machine as a variable frequency source [16] to feed static resistive, inductive as well as I.M. dynamic load. This system has the drawbacks of employing a synchronous machine which not only affects the system efficiency and cost but also requires a separate d.c. source for excitation. However, these drawbacks may be overcome by using small cage induction machine with terminal capacitors for reactive power requirement of the system, but no single attempt is made on this aspect. A need is therefore felt to investigate the feasibility of line commutating inverter with small cage induction machine as a variable frequency source.

In the present chapter, an attempt has been made to employ the LCI with a small cage I.M. as a variable frequency source to feed static resistive, inductive and dynamic three phase I.M. loads. The capacitor bank at

the terminals of the motor is used to meet the requirement of lagging reactive power for the system. The performance of system (inverter as well as load) is studied using experimental data. The effects of terminal capacitors and d.c. link voltage have also been investigated to achieve wide range of frequency control. A 0.5 H.P. (details are given in Appendix-B) cage induction machine has been used in conjunction with the inverter to feed a 3 H.P. cage I.M. load and also static resistive and inductive loads.

5.2 Experimental Setup and Procedure

The block diagram of the system used in this investigation is shown in Fig. 5.1. The system consists of three phase autotransformer uncontrolled bridge rectifier, d.c. link filter choke, line commutating inverter, step up transformer, capacitor bank, small cage induction machine and static (R-L) as well as dynamic 3-phase induction motor load.

The auto transformer in combination with uncontrolled bridge rectifier gives a variable voltage d.c. supply. The d.c. filter choke smoothes out the link current ripples and maintains the current continuous in d.c. link. The naturally commutated inverter feeds the active power from the d.c. link to the load at variable frequencies. This flow of power may be controlled either by the d.c. link voltage or the delay angle of inverter. The output transformer

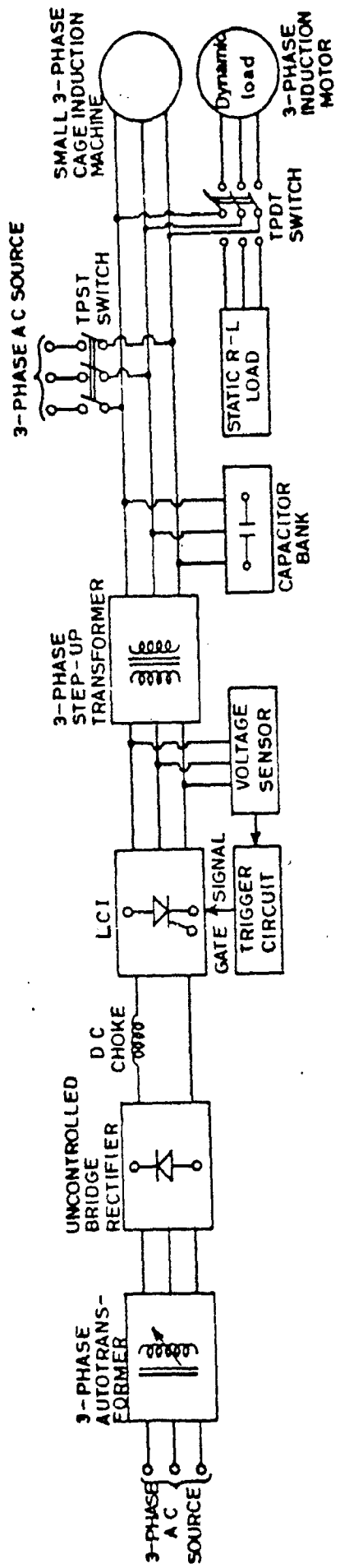
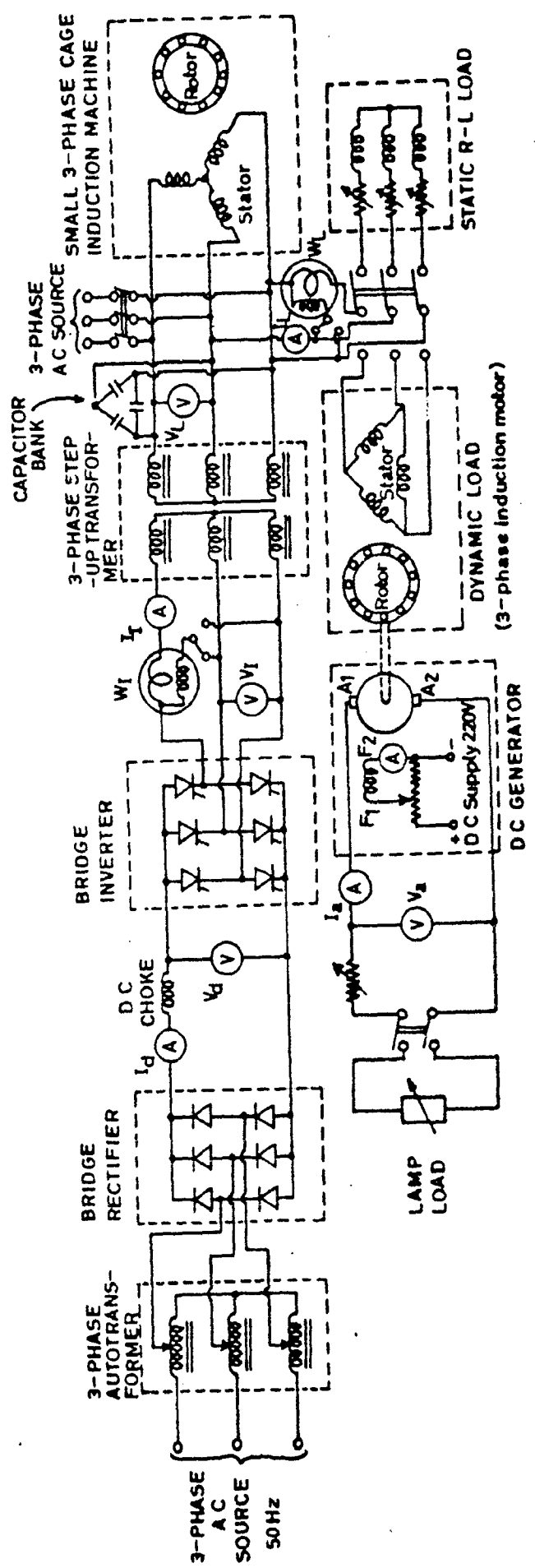


FIG.5.1 BLOCK DIAGRAM OF LCI-IM SYSTEM.



provides the isolation and stepping up the voltage of variable frequency supply. The lagging reactive power required for inverter step up transformer, small cage induction machine and load is met by connecting a capacitor bank at transformer output terminals. The output terminal voltage and frequency may be controlled over a wide range by varying the d.c. link voltage, terminal capacitor and delay angle of inverter. As the inverter is of naturally commutated nature, a small 3-phase squirrel cage induction machine is proved to give stator induced e.m.f. for natural commutation of inverter elements. This small cage induction machine operates in motoring mode and it may also be loaded up to its capacity and even then it is capable of serving the purpose of natural commutation. The wide range of speed control is obtained by varying d.c. link voltage and terminal capacitors. Using the method in section 3.2, system can be started at no load as well as at loaded conditions. Now this variable frequency and variable voltage output of LCI I.M. system is used as a variable frequency source from the machine terminals. The static loads (R and RL) have been connected in gradually increasing manner without any stability problem. In case of dynamic load (induction motor) due to its starting inrush current, it was started satisfactorily by an auto transformer and at final speed the auto transformer was disconnected from the system. Then the induction motor was loaded with the help of a separately excited d.c. generator as shown in Fig. 5.2. Various experimental data have been

obtained by instruments located at appropriate points in the circuit.

The test curves pertaining to the frequency control of the system at no load as a function of no load speed of small cage induction motor are shown in Fig. 5.3 . The various performance characteristics of the system on static load at different frequencies are given in Fig. 5.4. Performance at dynamic load (induction motor) is shown in Fig. 5.5. The oscillograms of the voltage and current waveforms for inverter and load were recorded with the help of storage oscilloscope and are shown in Figs. 5.6 - 5.7.

5.3 Discussion of Results

Based on experimental results given in Fig. 5.3 - 5.7, the following observations may be made on the performance of LCI I.M. system as a variable frequency source.

1. It is found from Fig. 5.3 that SCI I.M. system works quite satisfactorily at no load. The frequency range obtained in this scheme is from 10 Hz to 45 Hz. The frequency range may be more extended by varying d.c. link voltage, the value of terminal capacitor and the firing angle of inverter. However, with the increase in d.c. link voltage the frequency of the system increases. It is due to the fact that the increase in d.c. link voltage results in increasing inverter output voltage as well as motor terminal voltage. This increase the reactive power demand of the whole system.

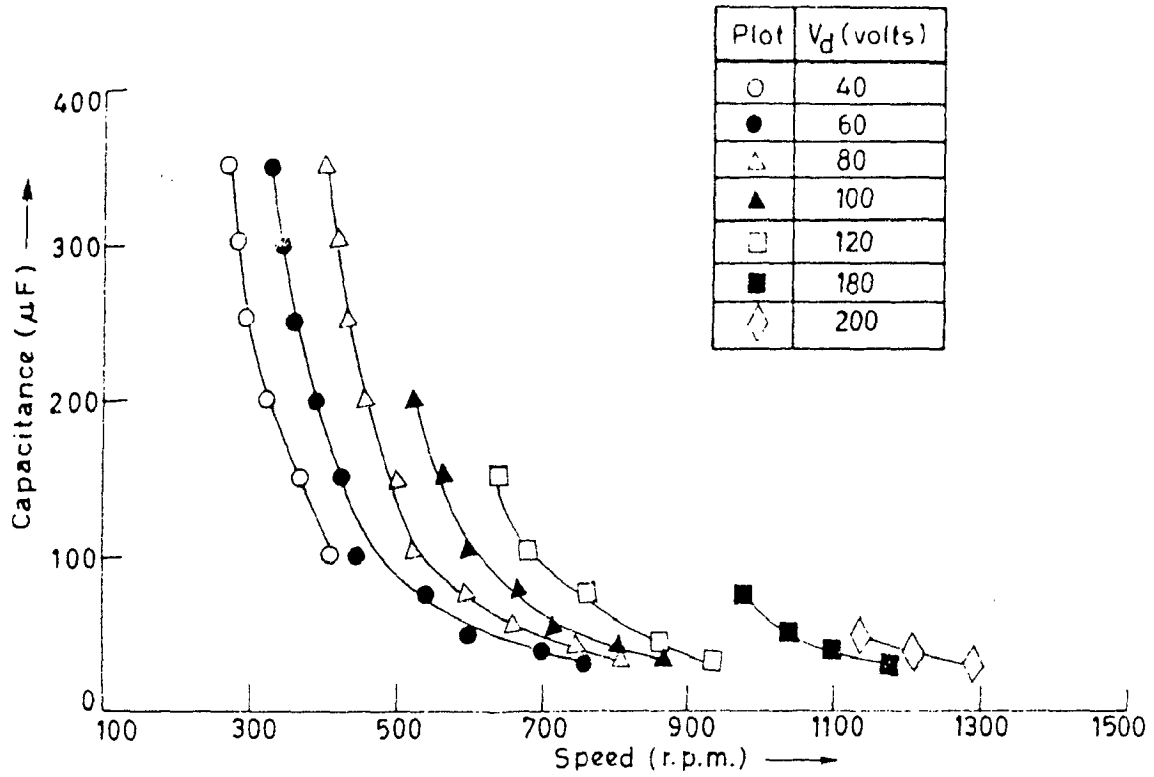


FIG. 5.3 (a) VARIATION OF CAPACITANCE WITH SPEED AT NO LOAD FOR 0.5 H.P. MACHINE.

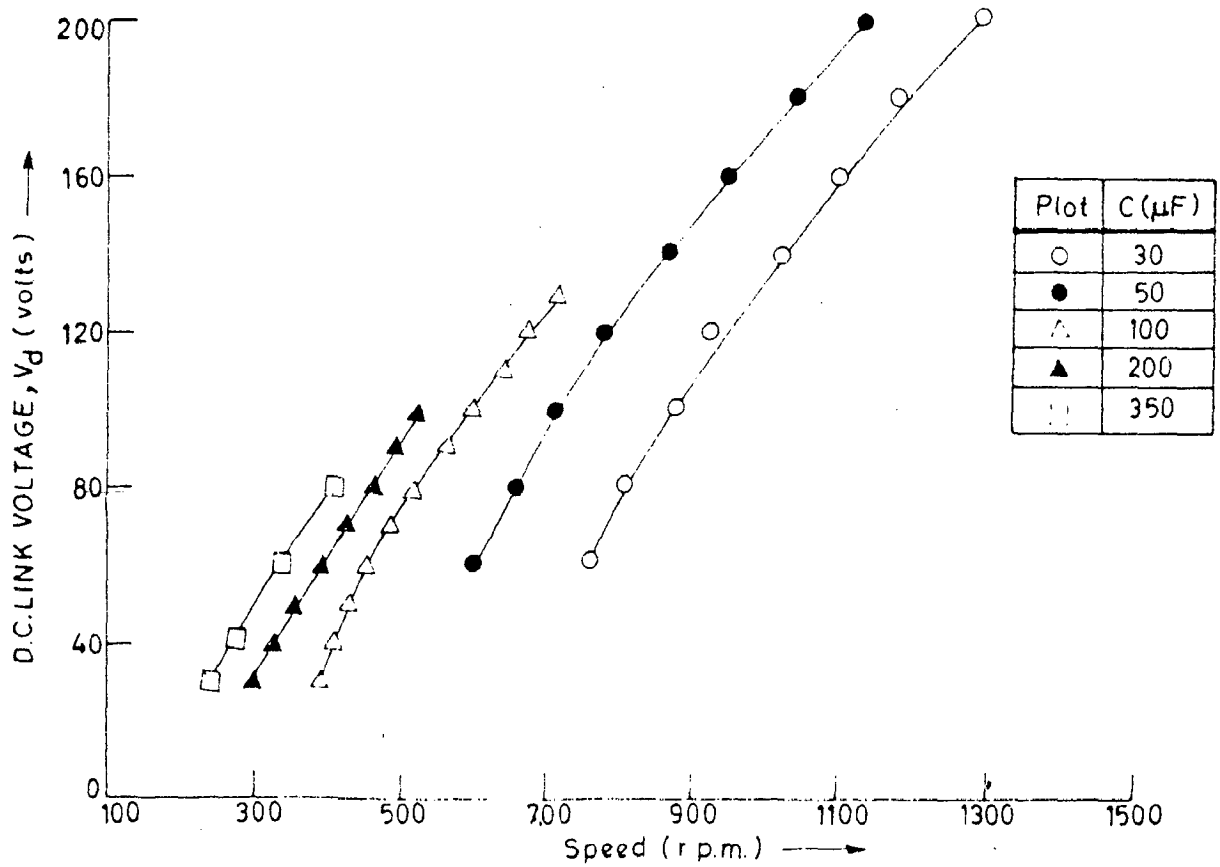
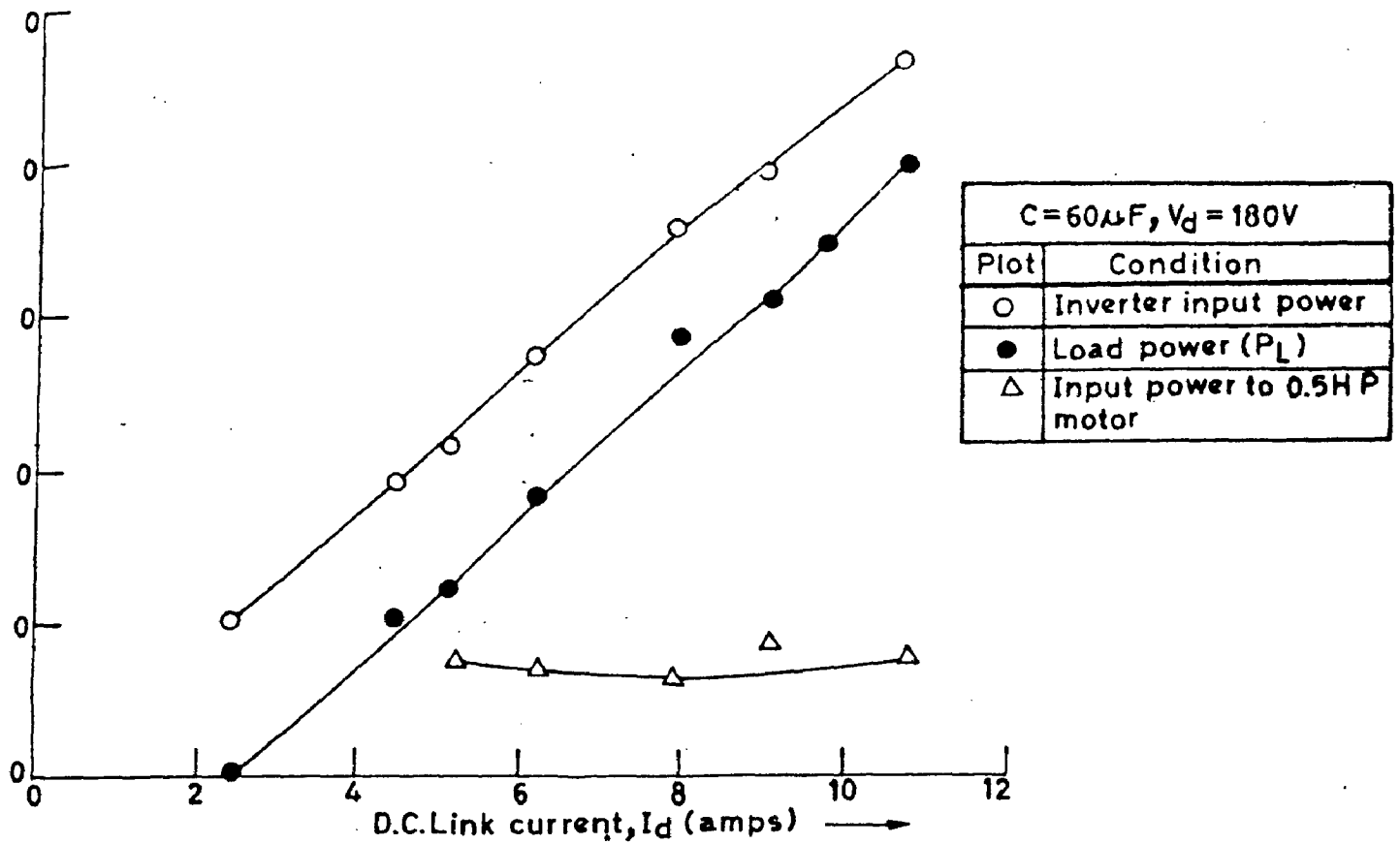
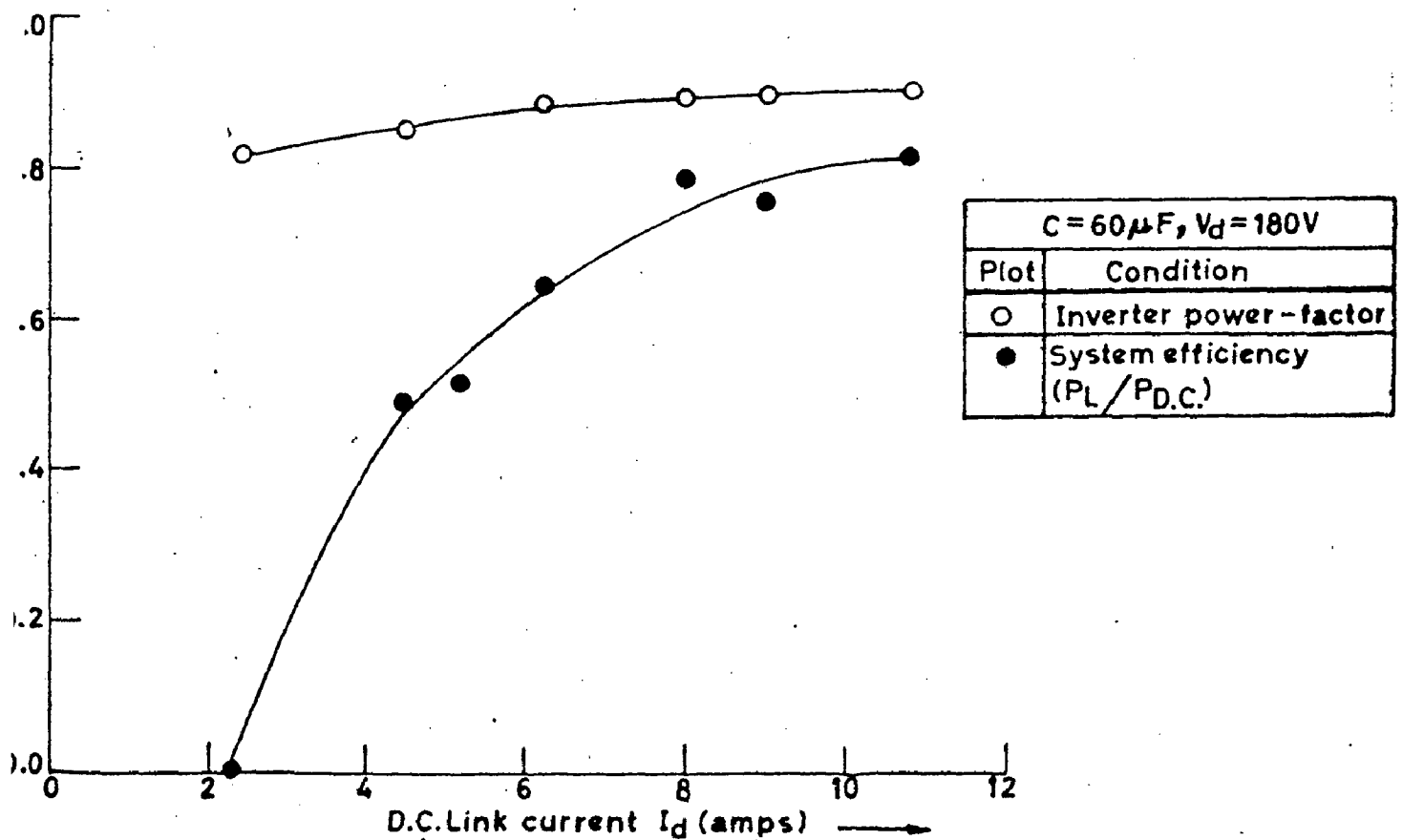


FIG. 5.3 (b) VARIATION OF D.C. LINK VOLTAGE WITH SPEED AT NO LOAD FOR 0.5 H.P. MACHINE



4(a) VARIATION OF ACTIVE POWER WITH D.C. LINK CURRENT AT RESISTIVE LOADS.



4(b) VARIATION OF EFFICIENCY AND POWER - FACTOR WITH D.C. LINK CURRENT AT RESISTIVE LOADS.

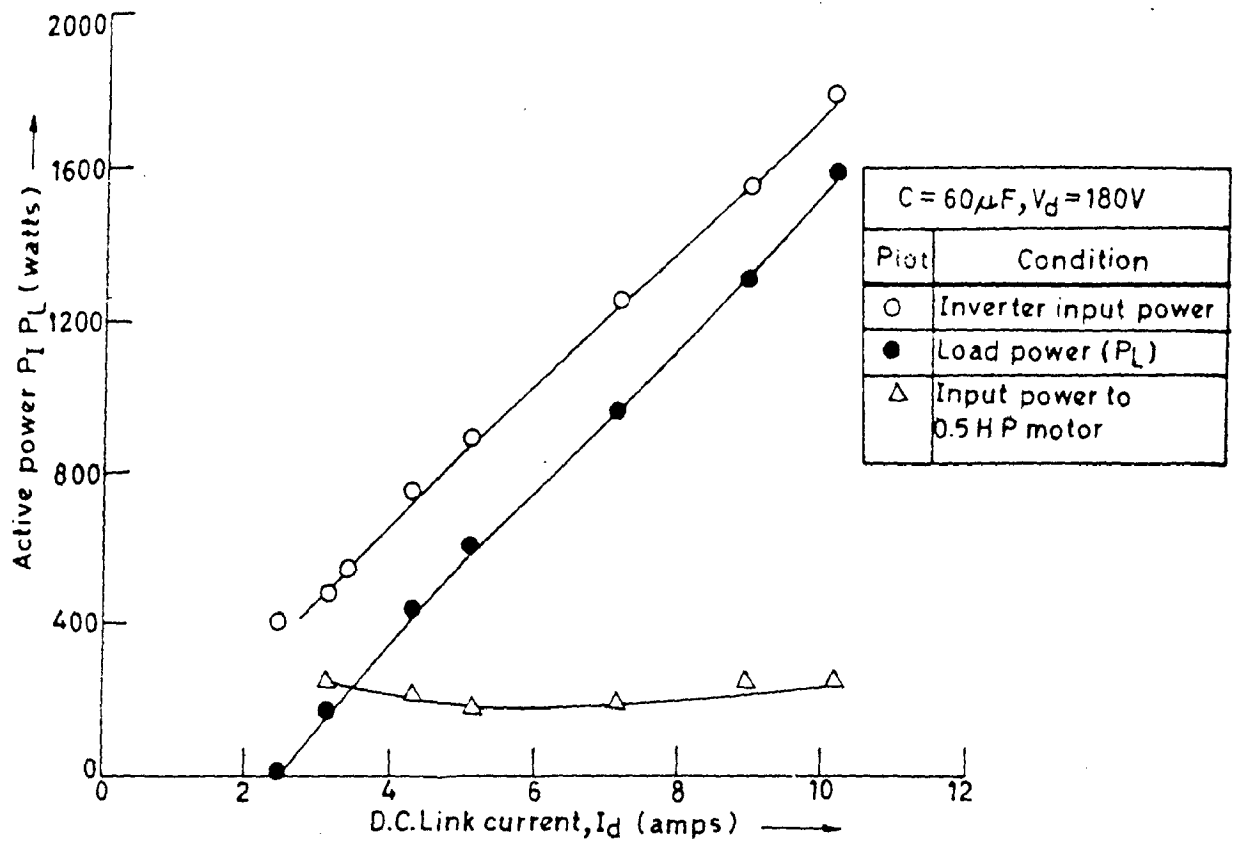


FIG. 5.4(c) VARIATION OF ACTIVE POWER WITH D.C. LINK CURRENT AT RESISTIVE - INDUCTIVE (R-L) LOAD.

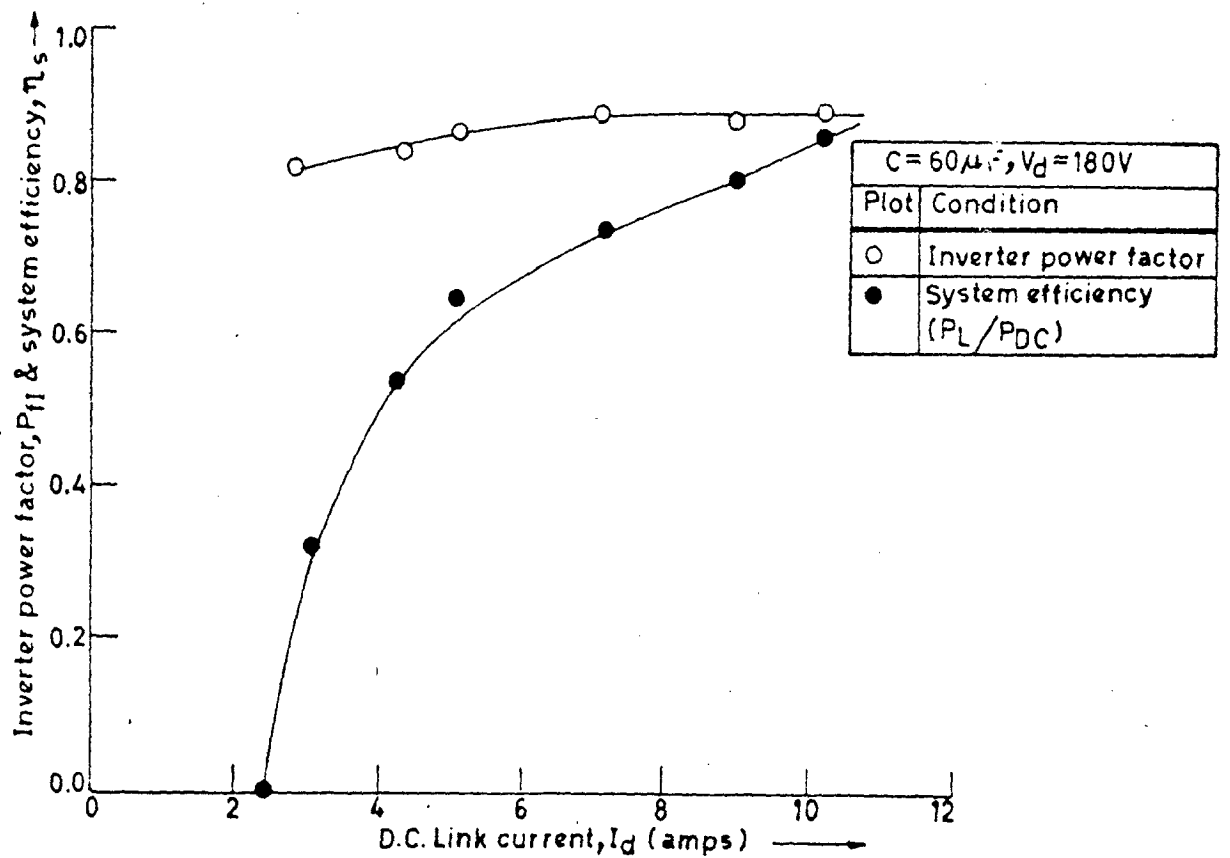


FIG. 5.4(d) VARIATION OF POWER - FACTOR AND EFFICIENCY WITH D.C. LINK CURRENT AT RESISTIVE - INDUCTIVE (R-L) LOADS.

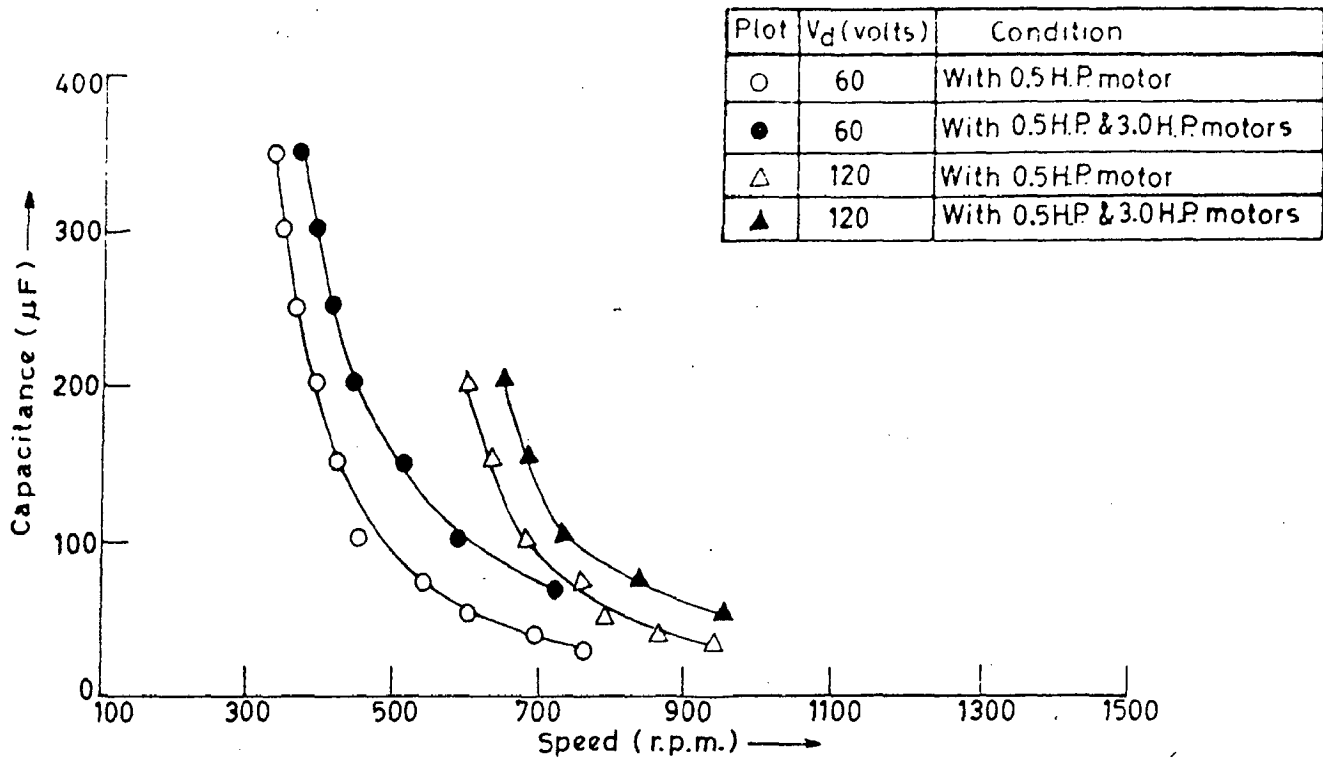


FIG. 5.5(a) VARIATION OF CAPACITANCE WITH SPEED AT NO LOAD FOR 0.5 H.P. MACHINE.

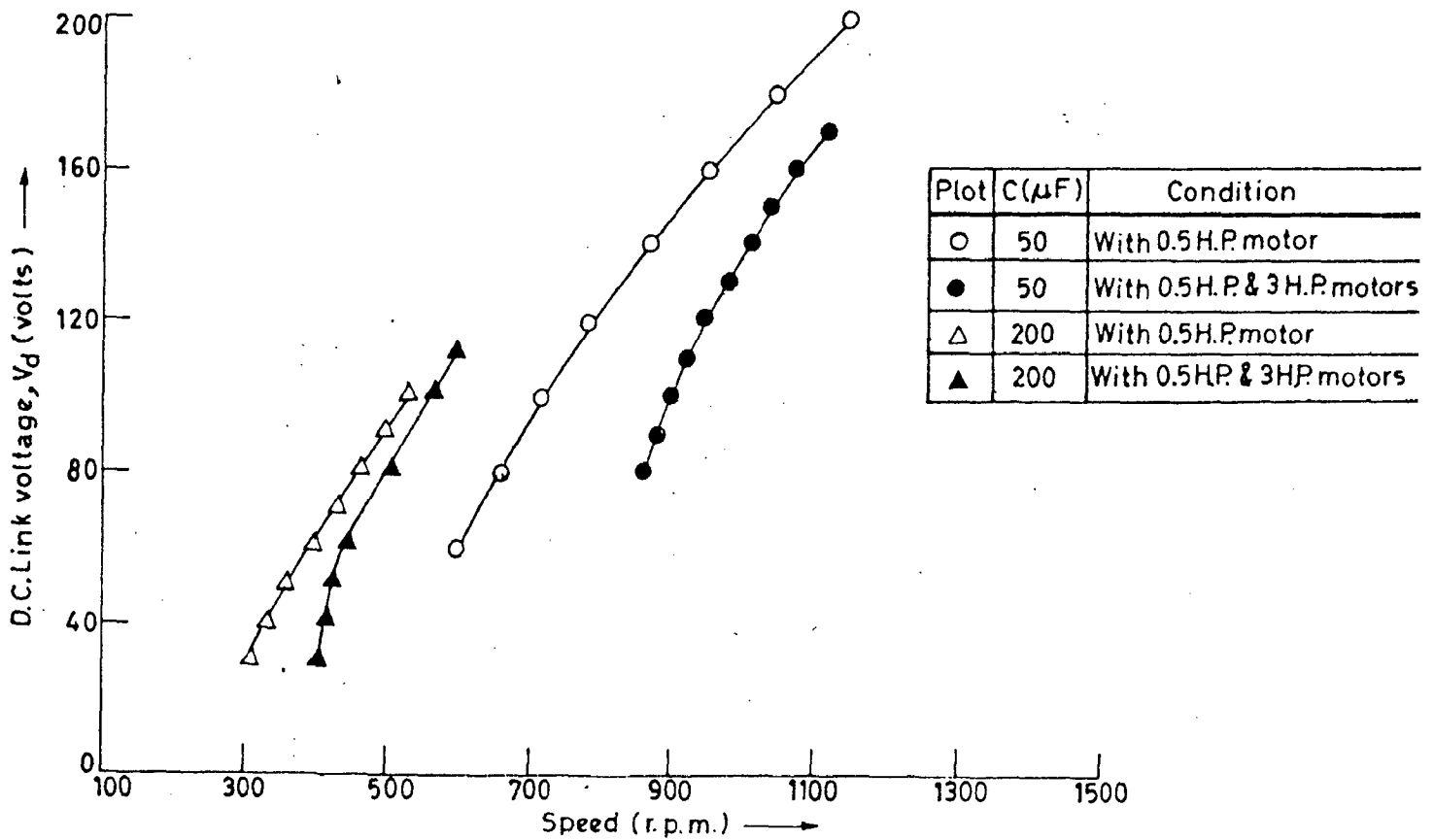


FIG. 5.5(b) VARIATION OF D.C. LINK VOLTAGE WITH SPEED AT NO LOAD FOR 0.5 H.P. MACHINE.

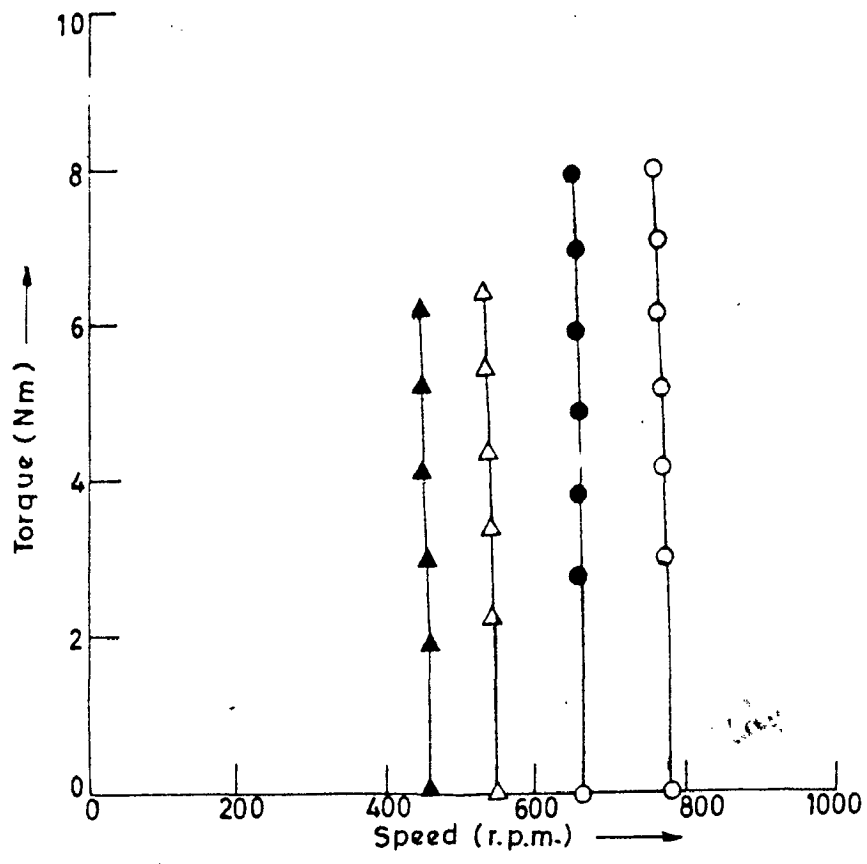


FIG. 5.5(c) TORQUE - SPEED CHARACTERISTICS OF A 3 H.P. INDUCTION MOTOR.

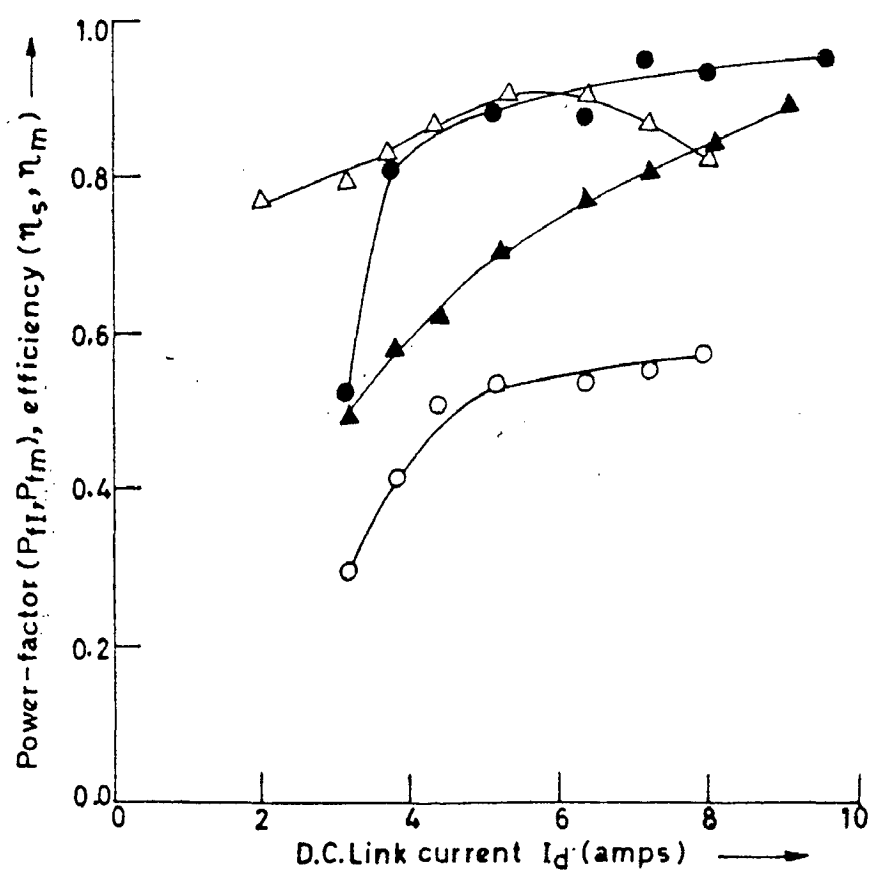


FIG. 5.5(d) VARIATION OF POWER - FACTOR AND EFFICIENCY WITH D.C. LINK CURRENT.

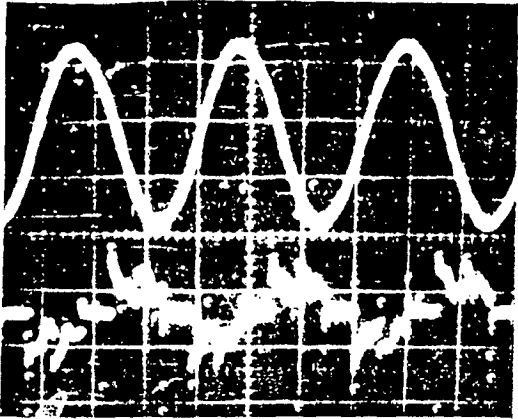


Fig. 5.6 (a)

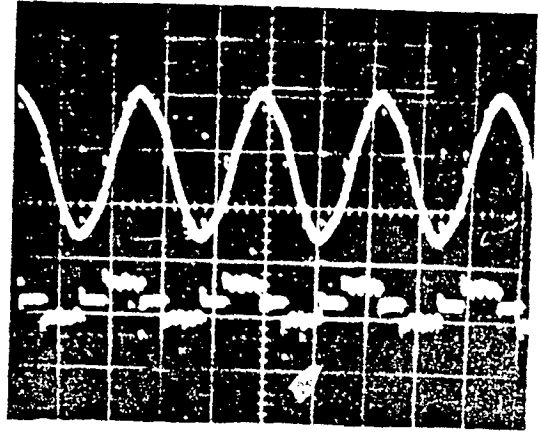


Fig. 5.6 (b)

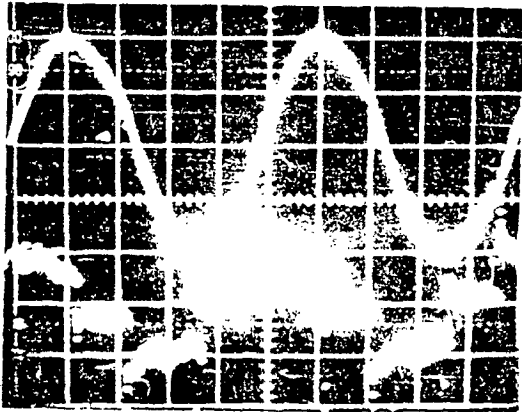


Fig. 5.6 (c)

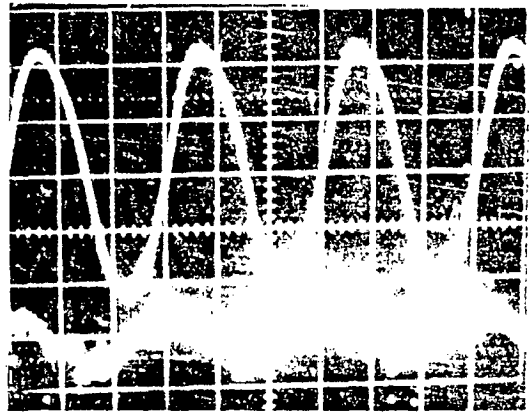


Fig. 5.6 (d)

FIG. 5.6 INVERTER VOLTAGE AND CURRENT WAVEFORMS AT (a) NO LOAD (0.5 h.p. MACHINE), (b) RESISTIVE LOAD, (c) RESISTIVE-INDUCTIVE (R-L) LOAD, (d) DYNAMIC (3.0 h.p. MOTOR) LOAD.

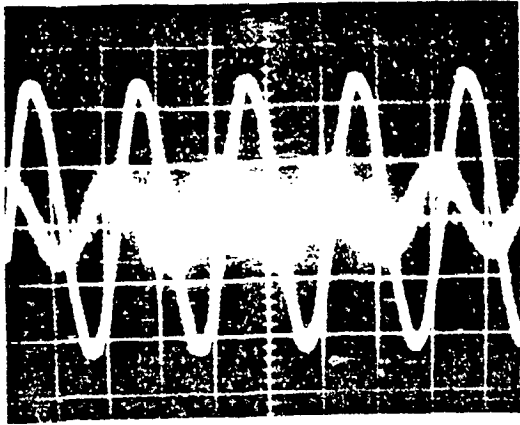


Fig. 5-7 (a)

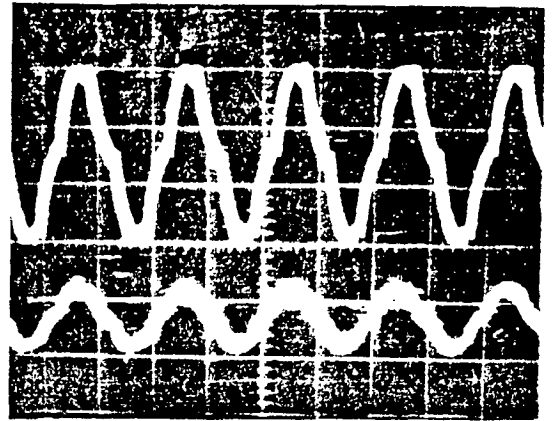


Fig. 5-7 (b)

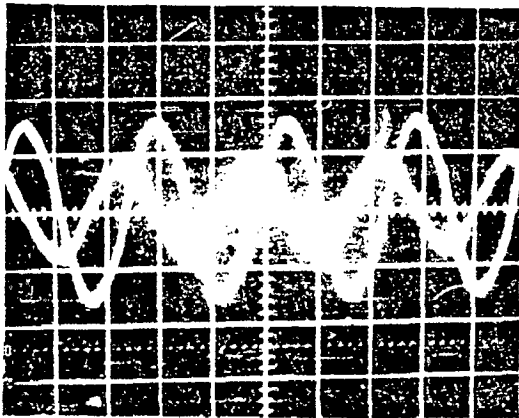


Fig. 5-7 (c)

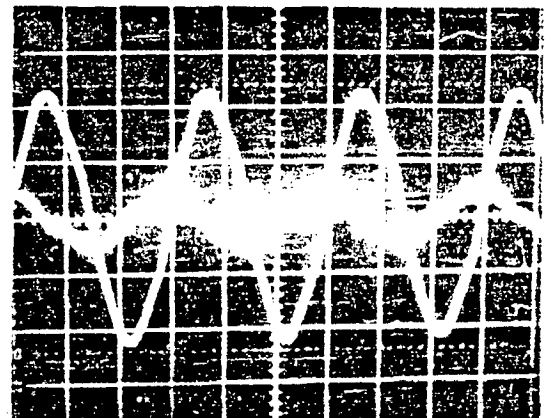


Fig. 5-7 (d)

FIG. 5-7. TERMINAL VOLTAGE AND LOAD CURRENT WAVE FORMS AT (a) NO LOAD (0.5 h.p. MACHINE), (b) RESISTIVE (R) LOAD, (c) RESISTIVE-INDUCTIVE (R-L) LOAD, (d) DYNAMIC (3.0 h.p. MOTOR) LOAD.

With the fixed value of terminal capacitor, this reactive power balance is obtained by increasing automatically the system frequency thus maintaining the ratio of terminal voltage to frequency almost constant. Similarly, it is also observed that with increasing the value of capacitance, the frequency reduces it is because that with this reactive power supplied by capacitor increases which system can not absorb, therefore, the reactive power is balanced by reducing the self adjusted frequency of the system.

2. The performance of the system at static (R and R-L) load may be observed from Fig. 5.4. It is evident from Fig. 5.4(a) that for pure resistive load, system is capable of supplying active power (P_L) many times than the rating and power input to induction machine (0.5 H.P.) used in the system. Inverter output and load power linearly varies with d.c. link current and the no load input to small cage motor is almost constant. The system efficiency (P_L/P_{DC}) rises sharply with load, it is because of constant no load losses of small induction machine (Fig. 5.4(b)). The power factor at inverter output is also almost constant and very little rise with increase in load may be seen from Fig. 5.4(b).

3. With pure inductive load, it is observed that the frequency of system rises whereas voltage slightly reduces. The increase in system frequency is due to increase in lagging reactive power requirement and which further may be fulfilled by increasing the frequency of the system. While the

terminal voltage at load reduces very slightly due to drop in transformer.

4. For resistive inductive (R - L) load again the system is capable of supplying active power (P_L) much greater than the input power and rating of small cage induction machine as it may be seen from Fig. 5.4(c). The inverter output power is also increases with increase in d.c. link current. The power factor of inverter remains almost constant. Fig. 5.4(d) shows the system efficiency, which rises with load. It is because of constancy of small machine no load losses at different system loading conditions.

5. It may be observed from Fig. 5.5 that the system is capable of supplying the dynamic load i.e. the induction motor (3 H.P.) and its speed control is achieved over a large range from 300 r.p.m. to 1400 r.p.m. by varying the d.c. link voltage and terminal capacitors. It may also be seen from Fig. 5.5(a) and Fig. 5.5(b) that by connecting the dynamic load at system output, the frequency of system rises. It is because the additional lagging reactive power requirement of load and which may be met only by increasing the frequency at fixed value of d.c. link voltage and terminal capacitor.

*result is
with varying*

6. Fig. 5.5(c) shows the torque speed characteristics of 3 H.P. cage induction motor fed from SCI I.M. system. It is found that speed of motor remains constant at different loads and speed fall is much lesser than the case when

motor is fed from normal 3-phase supply. It is due to fact that the system frequency increases with increase of load on motor as in the earlier cases of static (R-L) load.

7. Fig. 5.5(d) shows the inverter and motor (3 H.P.) power factors. The motor power factor rises with load in usual manner. However, the inverter power factor first it rises and then it decreases with load. The overall system and motor (3 H.P.) efficiencies (Fig. 5.5(d)), both rises with load and overall system efficiency is always less than the motor efficiency. It is due to additional losses in inverter, transformer and small induction machine.

8. One of the important aspect of this system with dynamic load (i.e. induction motor) is observed that the motor may be operated at any flux conditions. It means that the motor may be successfully operated in unsaturated condition. However, if only one induction machine is on the output terminals of system, it is to be operated in saturated condition for stable operation of the system.

9. The inverter output voltage and current waveforms at no load and at different types of load are shown in Fig. 5.6. The overlap notches may be clearly observed from these oscillograms. Inverter voltage waveforms are almost sinusoidal and free from harmonics. However, the inverter current waveforms are rich in harmonics specially at no load and are improved at loads. The load terminal voltage and current waveforms are shown in Fig. 5.7 voltage

waveform at load terminals are sinusoidal at no load but it is slightly distorted with different types of load.

The LCI I.M. system as the variable frequency source to feed static and dynamic load, presented in this chapter has the following positive features,

1. The system is simple, economic and more reliable due to elimination of commutating elements.
2. Converter grade thyristors may be used in the system.
3. The scheme provides the wide range of frequency and it may be further extended by selecting proper system parameters.
4. Induction motor (dynamic load) gives the constant speed characteristic at loads.
5. Induction motor may be operated at any flux condition which may be important aspect for optimum energy utilization at different loads.

5.4 Conclusions

The feasibility of line commutating inverter induction machine system as a variable frequency source to feed static (R-L) and dynamic (I.M.) load is demonstrated through experimental results. The wide range of frequency and voltage control is obtained by varying the value of terminal capacitors and d.c. link voltage. The output voltage and load currents waveforms are free from harmonic with

these novel features, it is concluded that the proposed scheme will provide the cheap, reliable and efficient source of variable frequency and voltage to feed static loads and a.c. motors for their wide range speed control in various industrial applications.

CHAPTER - VI

EXPERIMENTAL INVESTIGATIONS ON SYSTEM AS A GROUP DRIVE

6.1 General

Polyphase squirrel cage induction motors are widely used in industries due to their numerous advantages such as robust construction, simple, maintenance, free operation and above all the low cost. In modern industries, usually it is needed to operate more than one motor from the same source. In such operations, it is desired that the incoming and outgoing of any motor to the system should not affect the performance of other drives connected to the same source. A variable voltage solid state frequency converter find wide applications for the speed control of I.M.

A large number of attempts [12-20,28] have been made by its use to convert a synchronous machine either as a commutatorless d.c. machine or as a variable frequency source to feed induction motors. The later scheme, to use, LCI synchronous machine system as a variable frequency source, has the drawbacks of employing an extra synchronous machine which not only lowers the system efficiency but also increases the cost and requires a separate d.c. source for its excitation. Recently Watson [21, 22] has reported the feasibility of LCI for the variable speed operation of I.M. but it was limited to fractional horse power cage I.M.

It was confirmed from exhaustive literature survey that no single attempt is made on this type of system to feed induction motor group drive. Therefore, a need is felt to investigate the feasibility of LCI to feed not only one I.M. but a group of motors for their variable frequency operation as per desired in some applications.

In this chapter studies are made on steady state performance of the LCI fed a group of three phase induction motors experimentally at no load as well as at loaded conditions. The variable speed operation of single and group of induction motors fed from LCI is obtained by varying the d.c. link voltage and terminal capacitors. The speed torque characteristics of motor and other performance parameters such as efficiency, currents, power factors of motors and inverter have been presented for various values of terminal capacitors and d.c. link voltage. For the sake of knowledge of harmonics in voltages and currents at d.c. link inverter and motor, the various oscillograms have also been given.

6.2 Experimental Setup and Procedure

Fig. 6.1 shows the block diagram of the system considered in this work. The system consists of 3-phase auto transformer, uncontrolled diode bridge rectifier, d.c. link filter choke, LCI, its control circuitry, step up transformer, variable capacitor bank and the group of induction motors.

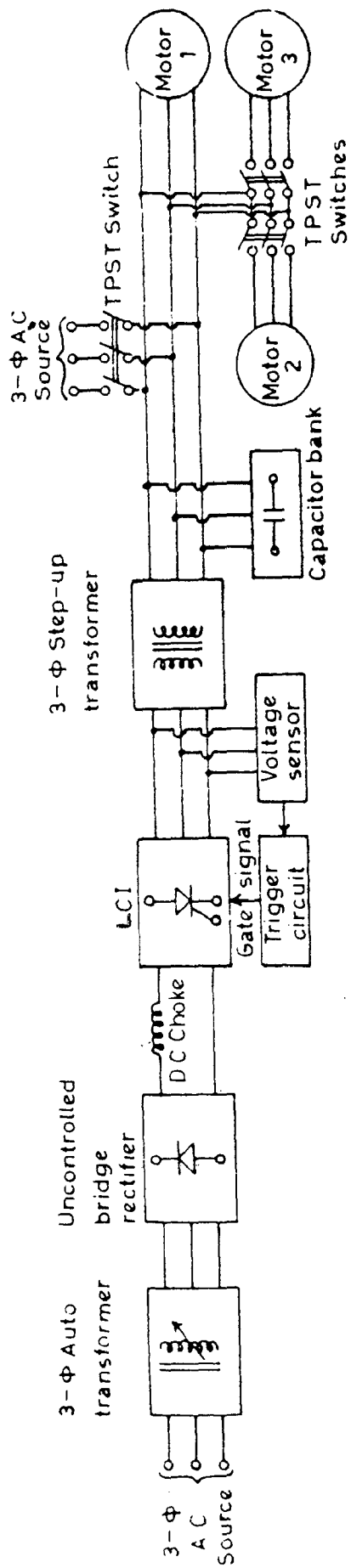
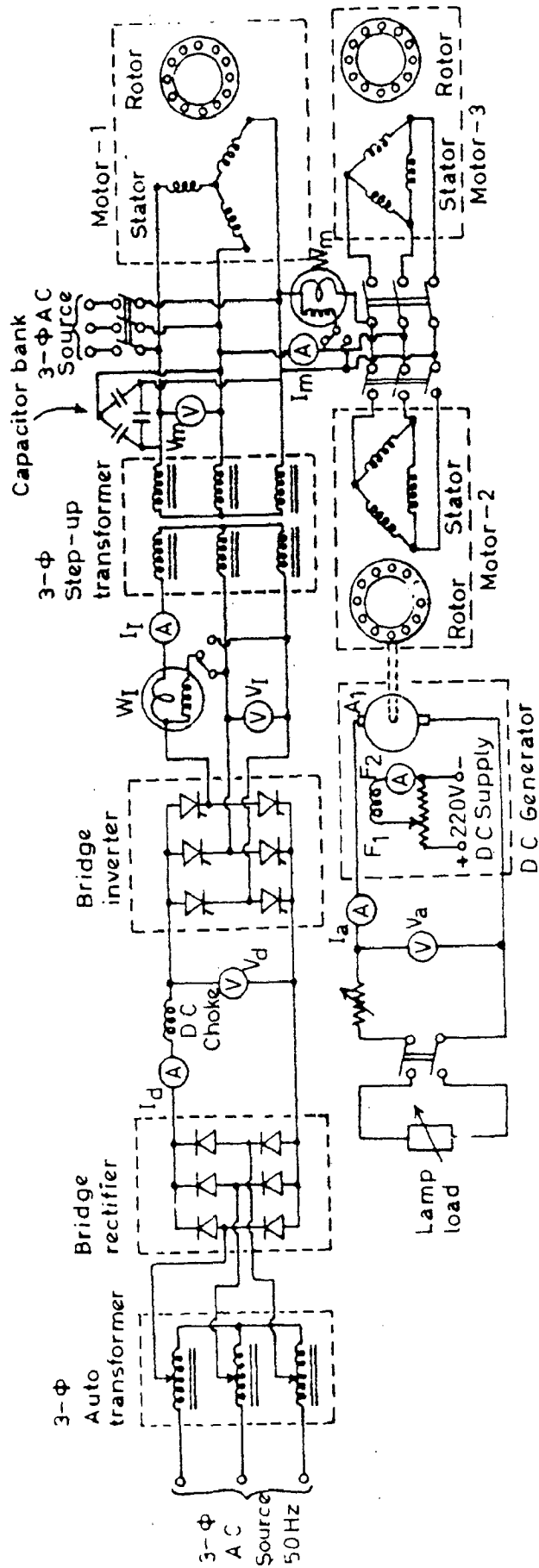


FIG. 6.1 BLOCK DIAGRAM OF LCI - FED INDUCTION MOTORS SYSTEM.



The 3-phase auto transformer alongwith uncontrolled bridge rectifier provides a variable voltage d.c. supply. The d.c. link inductor smoothes out the link current ripples and makes it continuous in d.c. link. The inverter (LCI) supplies the active power from d.c. link to motors at variable frequency. The transformer at inverter output terminals provides the isolation and stepping up the voltage for motor terminals. The lagging reactive power required for inverter, step up transformer and motors is fulfilled by connecting a variable 3-phase capacitor bank at output terminals. A detailed circuit diagram of experimental setup is shown in Fig. 6.2.

For the starting of the system atleast one I.M. out of group of motors, may be initially started by any one method of starting given in section 3.2. The I.M. was continued to run at a speed corresponding to self adjusted frequency and taking no load losses of motor from d.c. link through inverter. The output terminal voltage and self adjusted frequency are decided by the magnitudes of d.c. link voltage, the capacitor and the firing angle of inverter. Now to connect other induction motors, due to their starting inrush currents of these were started satisfactorily by an auto transformer and when these attain their final speed, the auto transformer was disconnected from the system. The I.M. was loaded with the help of coupled separately excited d.c. generator. Different combinations of three cage

induction motors of different ratings were considered to form a group drive to load the system. Various experimental data were obtained by instruments located at appropriate places in the circuit.

The test curves pertaining to variable speed operation of I.M., effect of capacitance and d.c. link voltage on the speed of motor are shown in Fig. 6.3 for different combinations of three motors at no load. The torque speed characteristics are shown in Fig. 6.4(a), 6.5(a) and 6.6(a) for combination of machines. The variation of other performance parameters such as power factor, currents and efficiency with d.c. link current are shown in Fig. 6.4(b), 6.5(b) and 6.6(b). The current and voltage oscillograms of d.c. link, inverter and motors were recorded with the help of storage oscilloscope and are shown in Fig. 6.7.

6.3 Discussion of Results

Based on experimental results obtained (Fig. 6.3 - 6.7), the following salient features on the performance of (LCI - I.M.) group drive for its variable speed operation may be noted,

1. It may be observed from Fig. 6.3(a) that in general at no load by increasing the terminal capacitor speed of I.M. decreases and by removal of part of capacitor speed rises. It may also be observed from the same figure that by connecting another I.M. at same d.c. link voltage and termi-

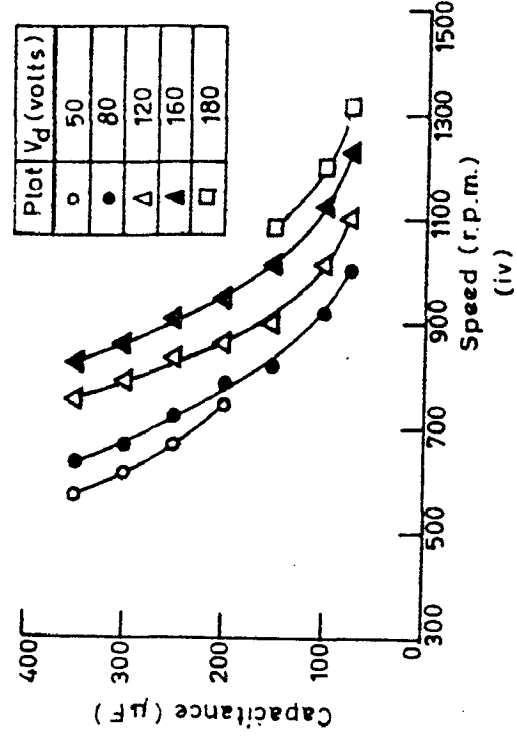
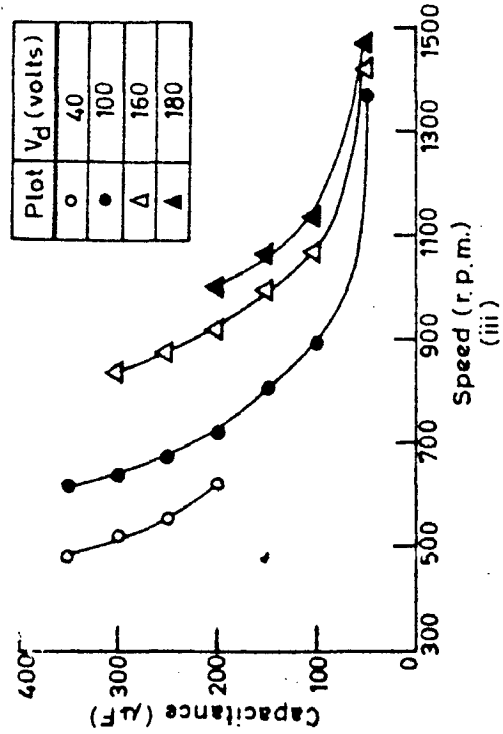
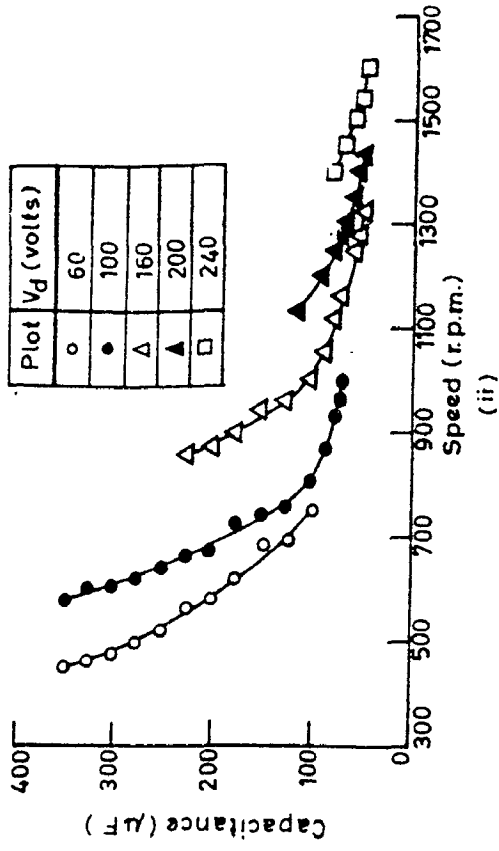
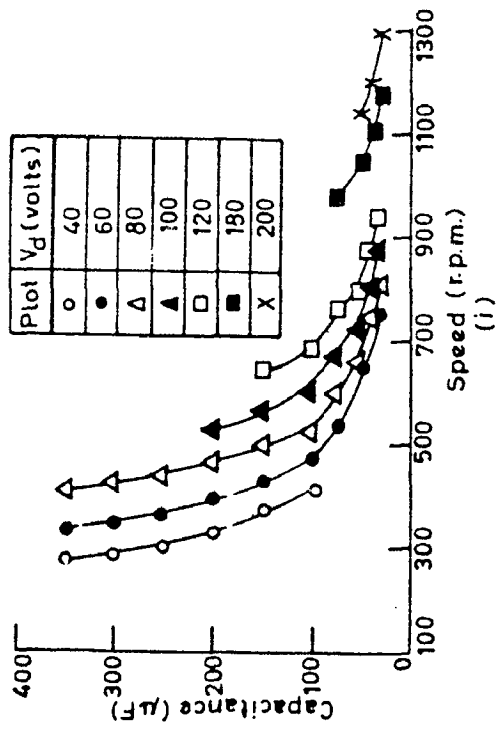


FIG. 6.3 VARIATION OF CAPACITANCE WITH SPEED AT NO LOAD FOR (i) MOTOR-1; (ii) MOTOR-2; (iii) MOTOR-1 OPERATING WITH MOTOR-2 AND (iv) MOTOR-1 OPERATING WITH MOTORS-2 & 3.

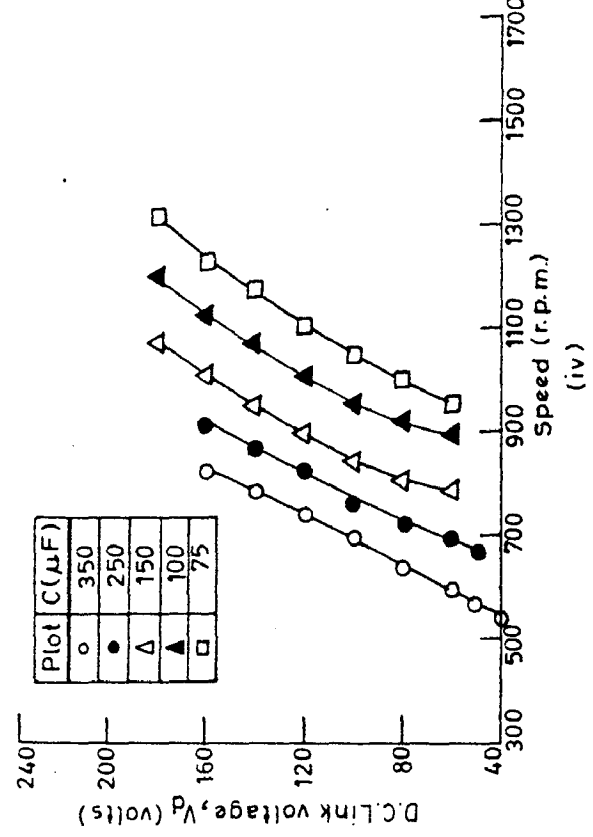
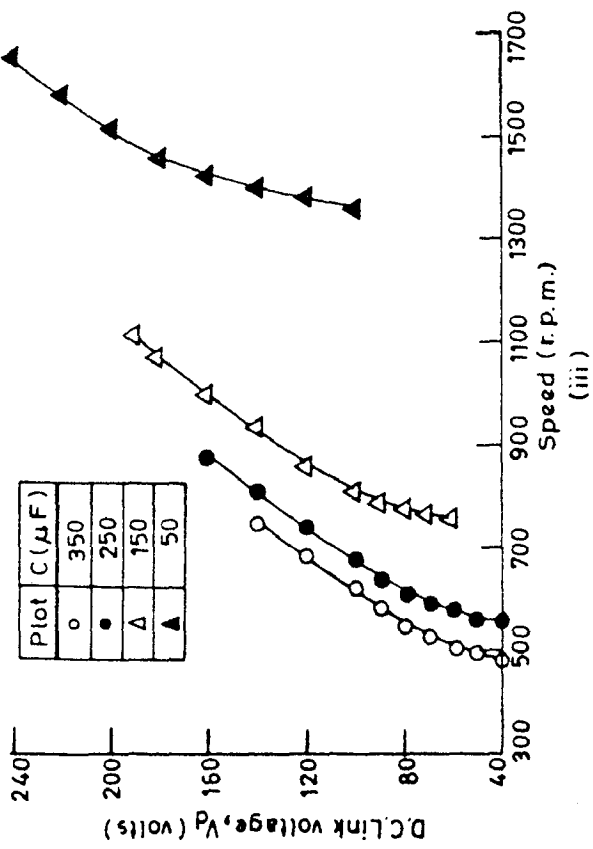
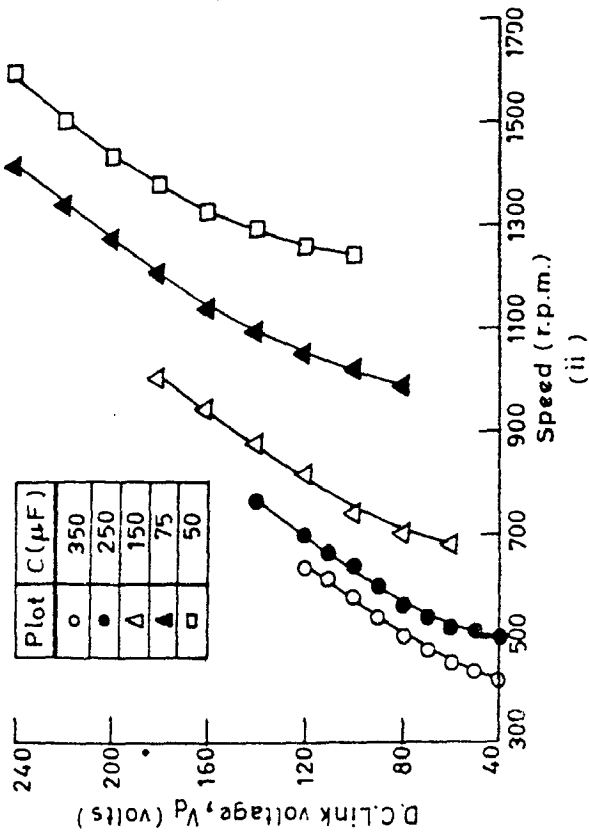
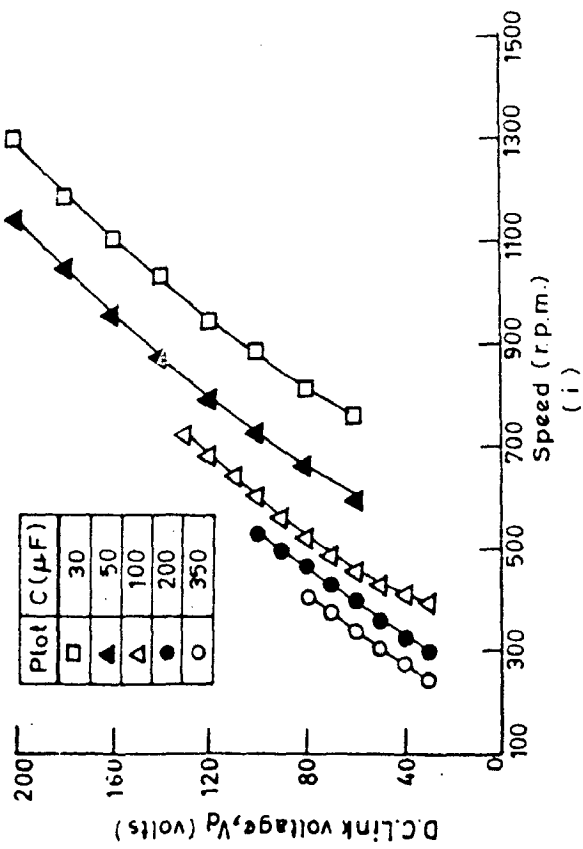


FIG 6-3 (b) VARIATION OF D.C. LINK VOLTAGE WITH SPEED AT NO LOAD FOR (i) MOTOR-1, (ii) MOTOR-2, (iii) MOTOR-1 OPERATING WITH MOTOR-2 AND (iv) MOTOR-1 OPERATING WITH MOTORS-2 & 3.

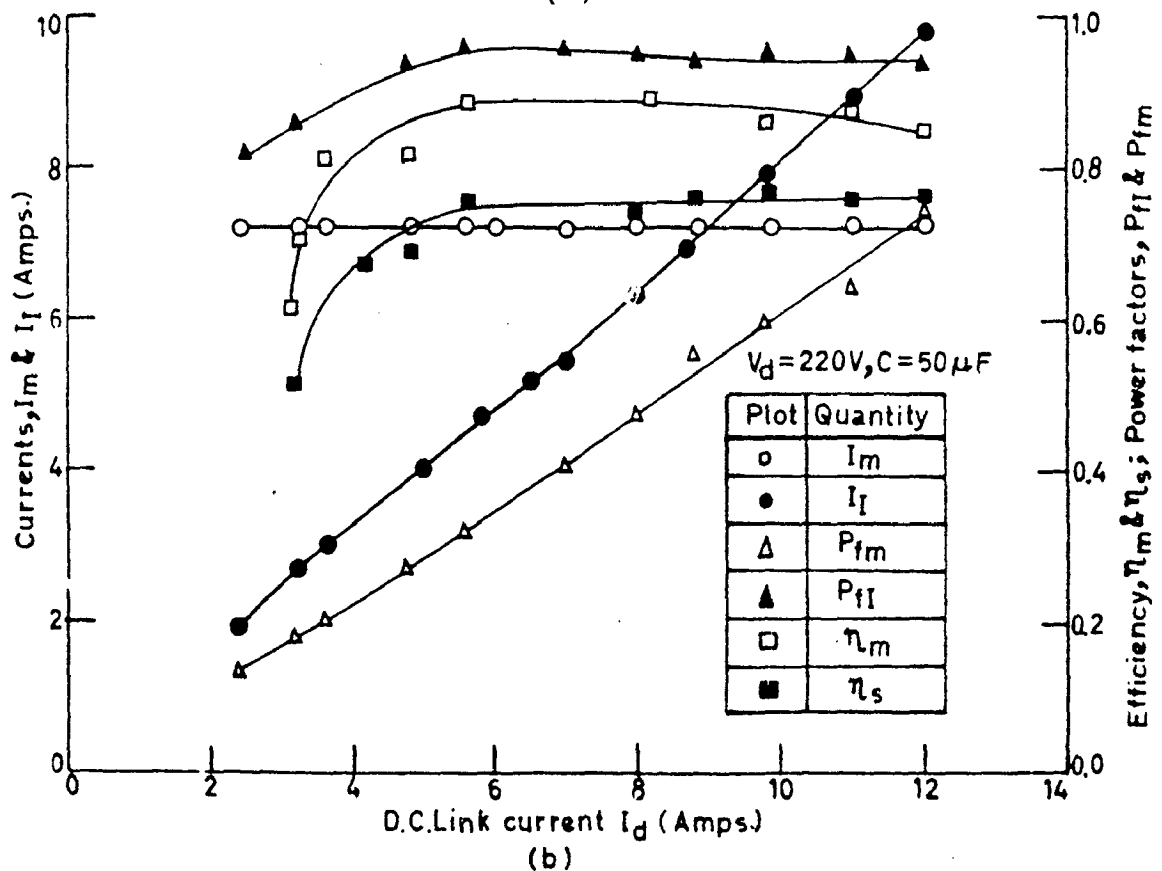
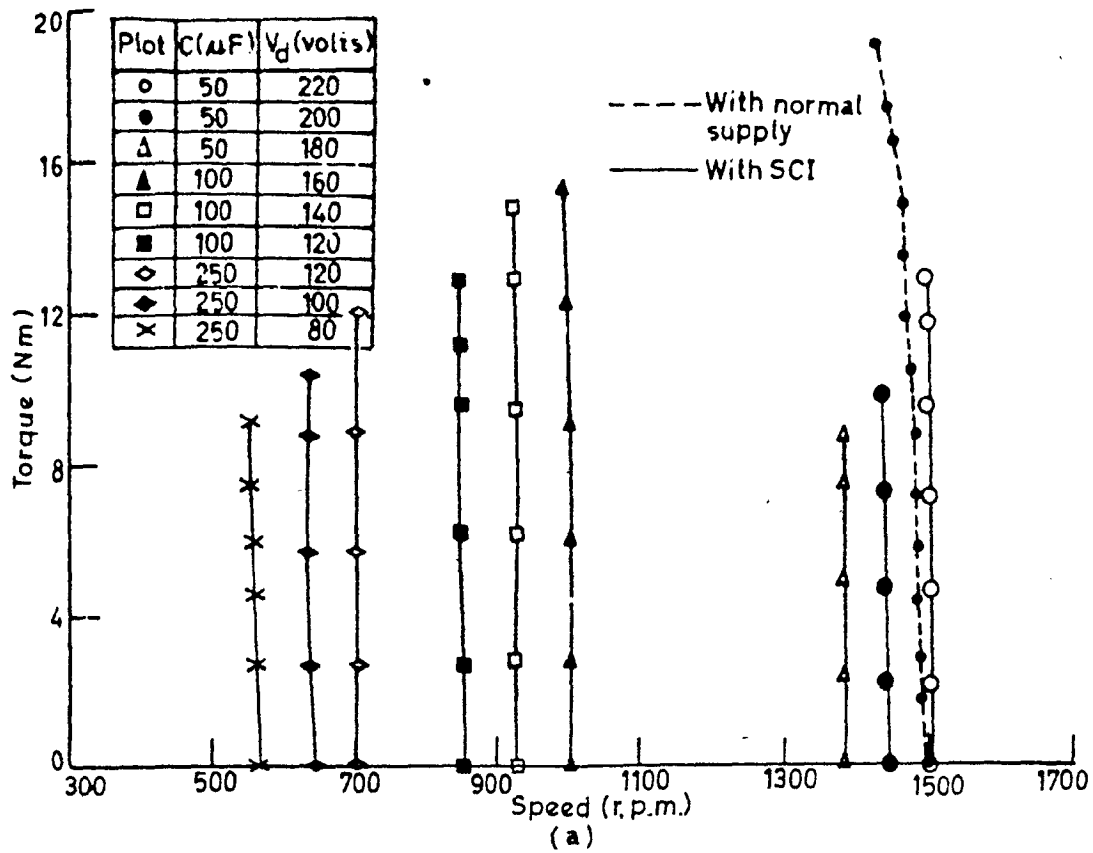


FIG. 6.4 PERFORMANCE CHARACTERISTICS OF MOTOR 2 (a) TORQUE-SPEED CHARACTERISTICS; (b) VARIATION OF MOTOR INVERTER CURRENTS, POWER FACTORS AND MOTOR & OVERALL SYSTEM EFFICIENCIES WITH D.C. LINK CURRENT.

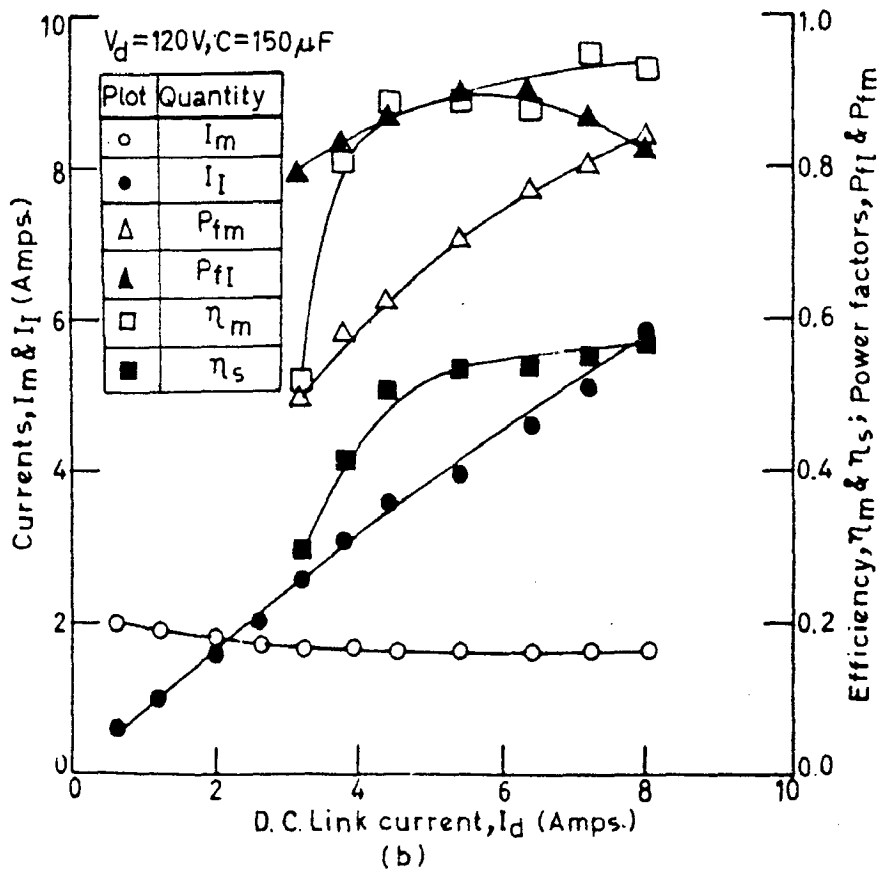
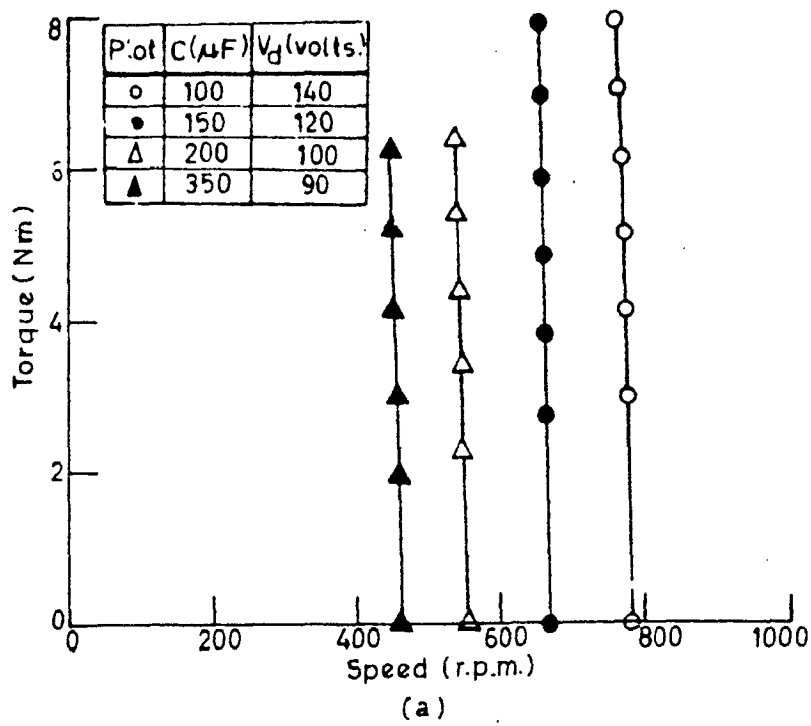


FIG. 6.5 PERFORMANCE CHARACTERISTICS OF MOTOR 3 OPERATING WITH MOTOR 1 (a) TORQUE - SPEED CHARACTERISTICS; (b) VARIATION OF MOTOR INVERTER CURRENTS, POWER FACTORS AND MOTOR & OVERALL SYSTEM EFFICIENCIES WITH D.C. LINK CURRENT.

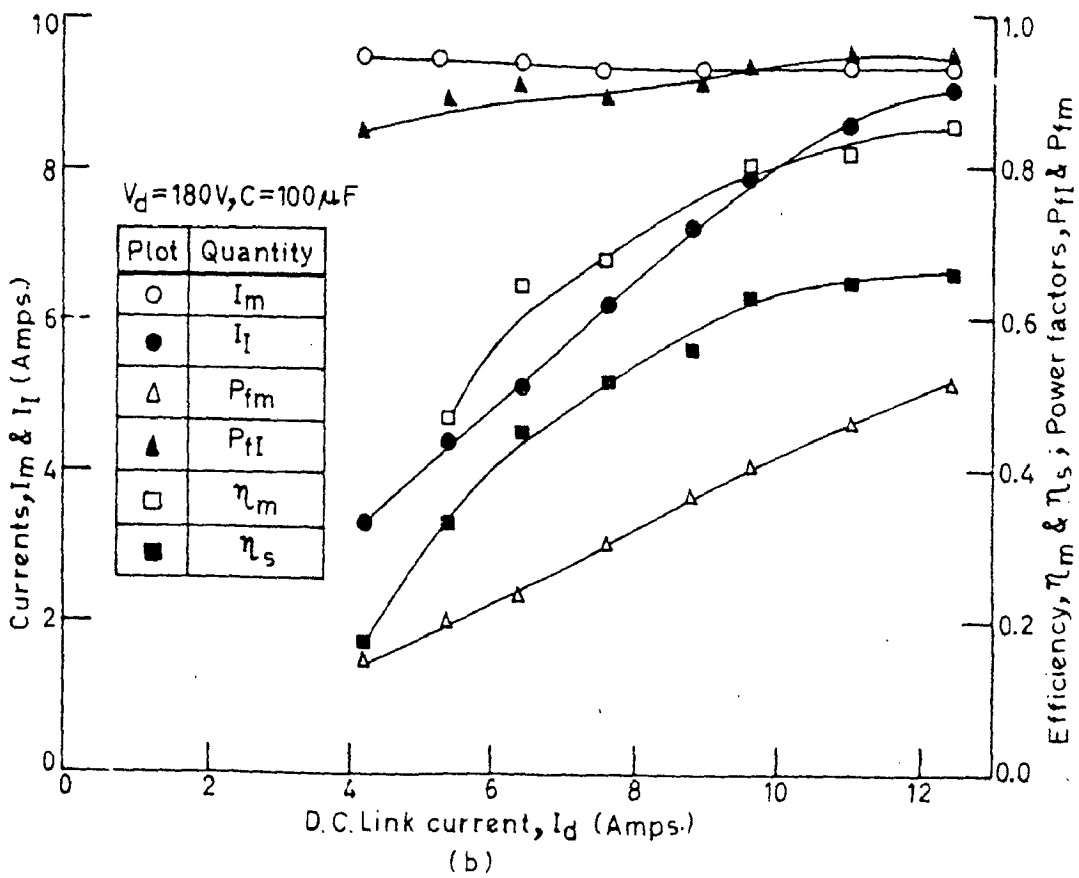
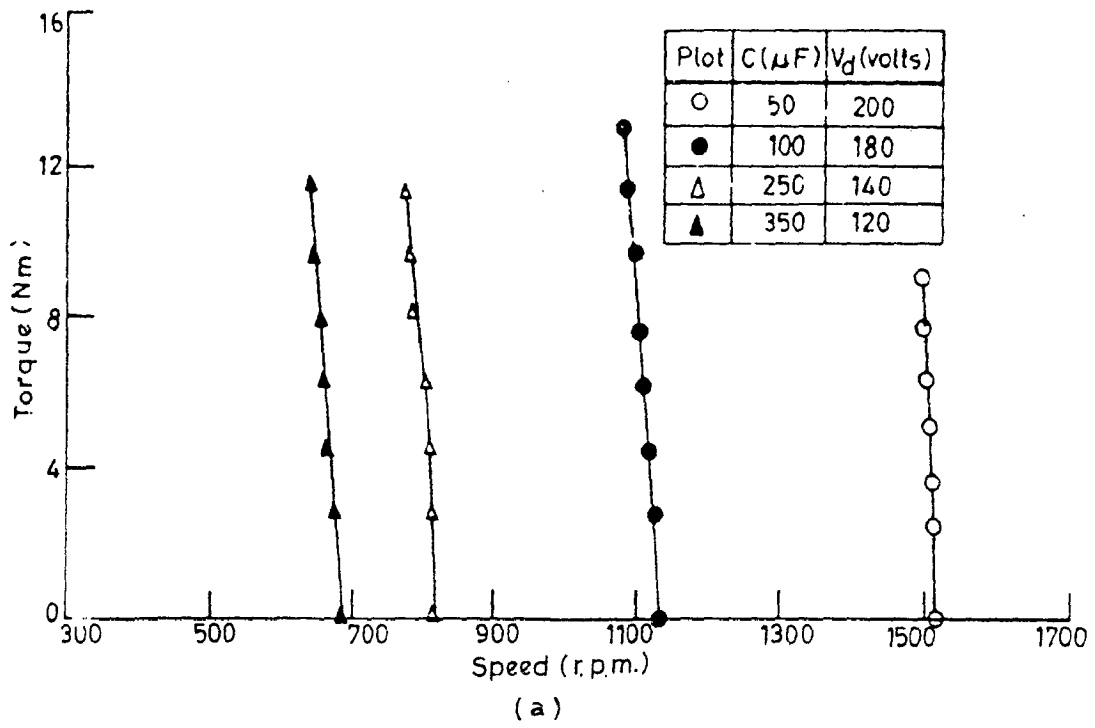


FIG.6.6 PERFORMANCE CHARACTERISTICS OF MOTOR 2 OPERATING WITH MOTOR 1 (a) TORQUE - SPEED CHARACTERISTICS ; (b) VARIATION OF MOTOR INVERTER CURRENTS, POWER FACTORS AND MOTOR & OVERALL SYSTEM EFFICIENCIES WITH D.C. LINK CURRENT.



FIG. 6.7a(i)

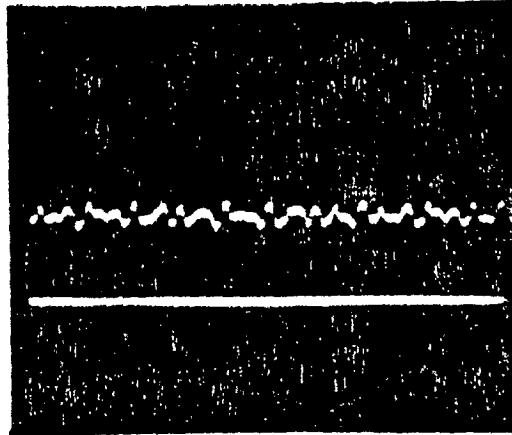


FIG. 6.7a(ii)

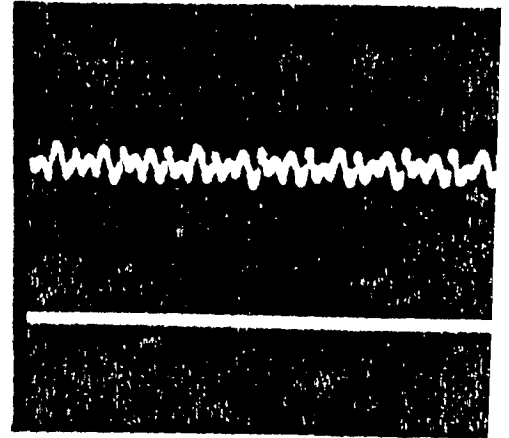


FIG. 6.7a(iii)

FIG. 6.7(a) Waveforms at d.c. link (i) D.C. link voltage, (ii) D.C. link current at no load, (iii) D.C. link current at load.

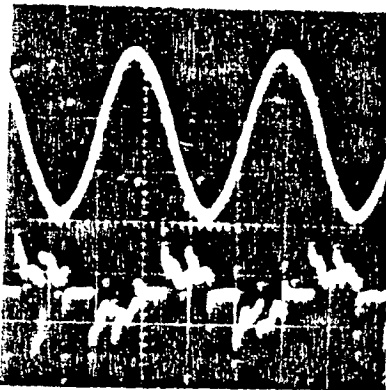


FIG. 6.7b(i)

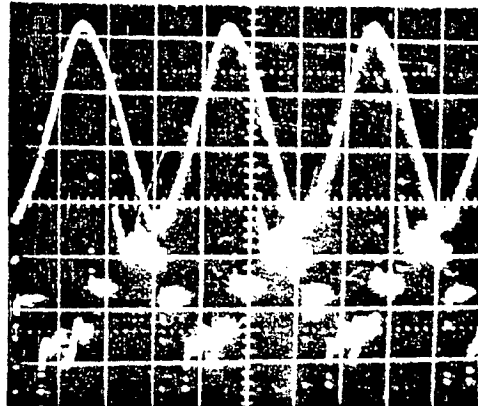


FIG. 6.7b(ii)

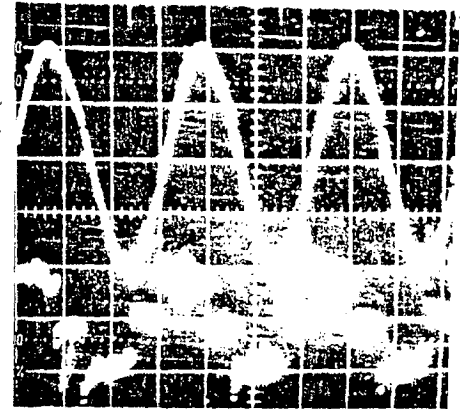


FIG. 6.7b(iii)

FIG. 6.7(b) Inverter voltage and current waveforms operating at output (i) Motor 1 (ii) Motor 2, (iii) Motors 1 with 2 and 3.

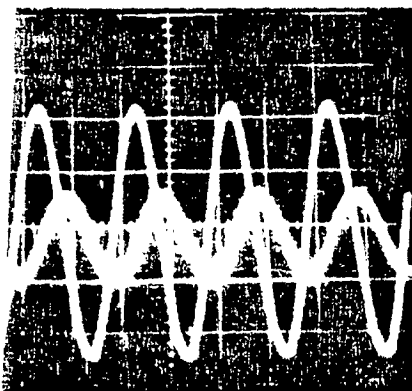


FIG. 6.7c(i)

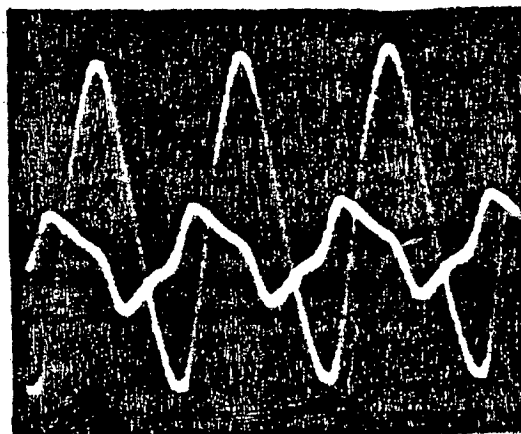


FIG. 6.7c(ii)

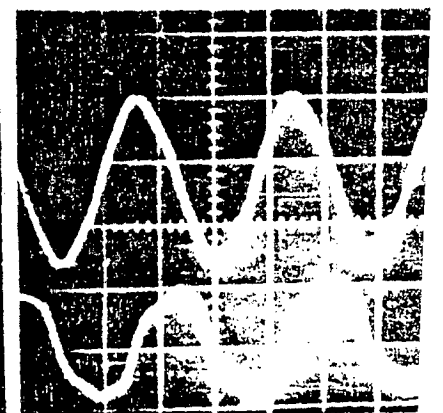


FIG. 6.7c(iii)

FIG. 6.7(c) Motor voltage and current waveforms of (i) Motor 1; (ii) Motor 2, (iii) Motor 2 operating with motors 1 and 3.

nal capacitor speed or frequency of system rises. It is because of additional requirement of lagging reactive power by the new motor and which may only be met by increasing the frequency. It is also interesting to note that frequency is much sensitive with capacitor at higher frequency range.

2. The effect of d.c. link voltage on no load speed for different combinations of motors are shown in Fig. 6.3(b). For the fixed value of capacitor, the speed or frequency of motor rises with the increase of d.c. link voltage. It is because with the rises of d.c. link voltage, the output voltage magnitude rises and the requirement of lagging power by motors is increased which is fulfilled by increasing the system frequency and try to maintain voltage to frequency ratio constant. The no load speed of motors rises linearly with the increase in d.c. link voltage. From these curves again it is confirmed that by adding the other motors on output the frequency of output rises due to additional requirement of reactive power to be met by increasing the system frequency.

3. Fig. 6.4(a), 6.5(a) and 6.6(a) show the torque speed characteristics of 3 H.P. and 4 H.P. induction motors for different group of motors. It is found that the system provides constant speed characteristics and fall in speed is even less than compared to a case when it is fed from normal 3-phase supply. It is due to the

fact that the system frequency rises slightly with the increase of load caused by extra requirement of lagging reactive power by inverter and motor and which may only be fulfilled by increasing the frequency.

4. From Figs. 6.4(b), 6.5(b) and 6.6(b) it may be observed that the power factor of LCI is almost constant in all the cases. It is because the delay angle is constant and is very near to 180° thus resulting higher power factor of LCI. However, the power factor of motor improves with increased load. With the result, LCI current rises linearly with load and motor current is almost constant because poor power factor at no load and rise in it with load as may be seen from Figs. 6.4(b), 6.5(b) and 6.6(b).

5. Figs. 6.4(b), 6.5(b) and 6.6(b) also show the variations of efficiencies of system and motor for different groups of motors. It may be observed from these curves that the efficiency of motor rises with the increase in load as in usual manner. The efficiency of overall system also rises with load but at reduced rate and is always less than the efficiency of motor due to increased losses in other elements of system such as LCI, transformer etc.

6. The oscillograms of voltage and current waveforms for d.c. link, inverter and motors are shown in Fig. 6.7. The ripples in d.c. link voltage and current due to thyristor switching are clearly visible and current waveforms improves with load. The inverter voltage and current

waveforms for different group of motors are shown in Fig. 6.7(b). The inverter output voltage is almost sinusoidal and free from harmonics. However, the small notches related to overlap during commutation process may be observed from waveforms. The current waveforms seems to be rich in harmonic under different conditions.

7. The voltage and current waveforms at motor terminals are shown in Fig. 6.7(c). The voltage waveforms are sinusoidal and free from harmonics but the motor currents are rich in harmonics due to operation in saturation condition. However, the current waveforms for the 3 H.P. motor is observed sinusoidal because it is operated in unsaturated conditions.

6.4 Conclusions

The line commutated inverter system for wide range speed control of group of induction motors works satisfactorily at no load as well as at loaded conditions. The system provides the simple, economic and reliable variable frequency source for groups of cage induction motors due to elimination of commutating elements and converter grades thyristors may be used because of their natural commutation. Further, scheme provides attractive features such as it gives the constant speed of I.M. and it may be operated for any flux conditions. With this it is anticipated that

a cheap, reliable and efficient method of speed control of group drives consisting of a number of induction motors would be available and will find good applications in various industries.

CHAPTER - VII

CONCLUSIONS AND SUGGESTIONS FOR FURTHER WORK

7.1 General

The main objectives of this investigation were to fabricate the whole scheme in a laboratory and also to obtain the performance of motor practically under varied conditions of operations and to verify the results analytically obtained. The results of the investigation reported in preceding chapters shown that these objectives have been realized. This investigation will hopefully open up a number of possible developments in future on the LCI fed I.M.

7.2 Main Conclusions

The main conclusions of this investigation are summarised as follows;

- (i) The system modules i.e. power circuits and firing circuit have been developed. The recorded waveforms at the different points of firing circuit are observed identical to the theoretical ones. The cosine wave crossing technique results the LCI as a linear amplifier.
- (ii) From the experimental investigation on LCI system, it is observed that the system is stable

at no load as well as loaded conditions. It is concluded that a desired range of speed control with specified loading may be achieved using appropriate values of terminal capacitor and d.c. link voltage. An interesting feature of the system is observed that the motor speed remains constant irrespective of load and results its operation at constant flux condition over a wide speed range.

- (iii) The computed results under loaded as well as no load condition of motor shows the good correlation with test results, thus establishing the validity of developed analytical model. Moreover the developed analytical technique based on equivalent circuit approach and Newton - Raphson method requires small computational time and marginal memory storage.
- (iv) The LCI - I.M. system provides the stable operation as a variable frequency source for feeding static (resistive inductive) and dynamic (I.M.) loads. The wide range of output frequency and voltage may be obtained by varying the value of terminal capacitor and d.c. link voltage.
- (v) From the experimental results on LCI system, it is concluded that the system is capable for feeding simultaneously to group of induction motors satisfactorily.
- (vi) The oscillograms of voltage and current at load terminals contain less amount of harmonics and are close to sinusoidal. However, the voltage and current waveforms at LCI output contain the much amount of harmonics.

The system provides the cheap, reliable, efficient source of variable frequency and efficient method of speed control of single as well as group drives and will find good applications in various industries.

7.3 Suggestions for Further Work

Although the basic objectives of this dissertation has been brought to a successful conclusion, certain problems have arisen during the course of investigation which would require further investigation. These problems are listed here for further investigations,

- (i) Since as such LCI - I.M. system is not self start for desired frequency, hence it is an important need to develop cheap starting method for the system to start initially at required frequency.
- (ii) The analytical model may be developed based on exact equivalent circuit and in time domain by considering the harmonics presents in the system. Further the model must be developed in generalized form to study the steady state and dynamic behaviour of the system.
- (iii) For the reliable operation of LCI system a variable leading reactive power source is required to feed for the lagging reactive power of inverter and load. Therefore, a cheap and efficient lagging reactive power source may be developed.

- (iv) The entire work was in open loop form, however, for fast response better stability, the close loop control may be devised for LCI system.
- (v) In the present system, the analog control scheme was used, which may be improved by digital control scheme for more accuracy and flexibility using the cheap available digital I.Cs including microprocessors.

BIBLIOGRAPHY

1. Steven C. Peak and Allan B. Plunkett, 'Transistorized PWM inverter induction motor drive system', IEEE Trans. on Industry Applications, Vol. IA-19, No. 3, May/June 1983, pp 379 - 387.
2. P. Bowler and B. Nair, 'Transistorized inverters for the control of small induction motor', Proc. of IEEE Con. Electrical variable speed drive, No. 93, pp 232-233. *year 9*
3. J.M.D. Murphy, 'Thyristor control of A.C. Motors', Oxford Pergamon Press, 1973.
4. T.A. Lipo, 'The analysis of induction motor with voltage control by symmetrical triggered thyristors', IEEE Trans. on Power Apparatus and system, Vol. PAS-90, No. 2, March/April 1971.
5. B.R. Pelly, 'Thyristor phase controlled converters and cycloconverters', New York, Willy Interscience 1971.
6. T.A. Lipo and P.C. Krause, 'Stability analysis of a rectifier inverter induction motor drive', IEEE Trans. on Power Apparatus and system, Vol. PAS-88, No. 1, Jan. 1969, pp 55 - 66.

7. D.W. Novotny, 'Steady state performance of inverter fed induction machines by means of the domain complex variables', IEEE Trans. on Power Apparatus and system, Vol. PAS - 95, No. 3, May/June 1976, pp 927 - 935.
8. S.M. Sriraghavan, B.E. Pradhan and G.N. Revanhas, 'Multi stage pulse width modulated inverter system for generating stepped voltage waveforms', Proc. IEE Vol. 125, No. 6 June 1978, pp529 - 530.
9. N. Sawaki and N. Sato, 'Steady state and stability analysis of induction motor driven by CSI', IEEE Trans. on Industry Applications, Vol. IA-13, No. 3, May/June 1977, pp 244 - 253.
10. T.A. Lipo and E.P. Cornell, 'State variable steady state analysis of a controlled current induction motor drive', IEEE Trans. on Industry Applications, Vol. IA-11, No. 6, Nov/Dec. 1975, pp 704 - 712.
11. A. Nabae, K. Otsuka, H. Uchino and R. Kurosawa, 'An approach to flux control of induction motor operated with variable frequency power supply', IEEE Trans. on Industry Applications, Vol. IA-16, No. 3, May/June 1980., pp 342 - 349.
12. A.C. Williamson, N.A.H. Iase and A.R.A.M. Makky, 'Variable speed inverter fed synchronous motor employing natural commutation', Preceeding IEE

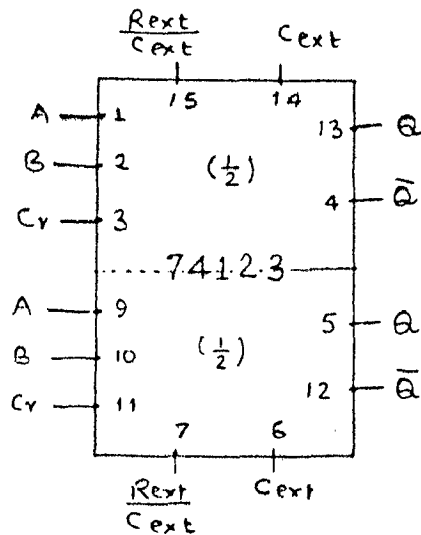
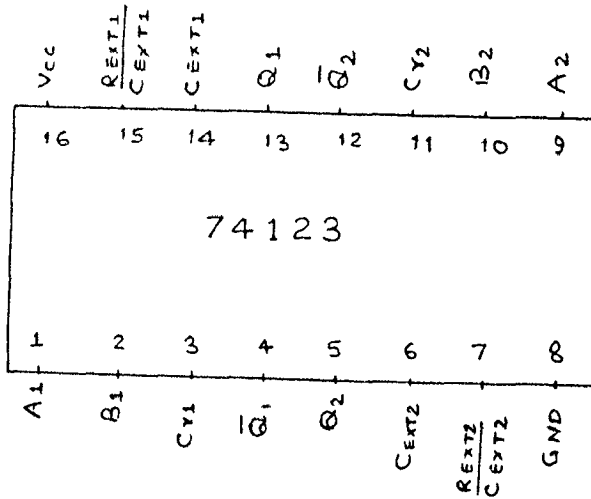
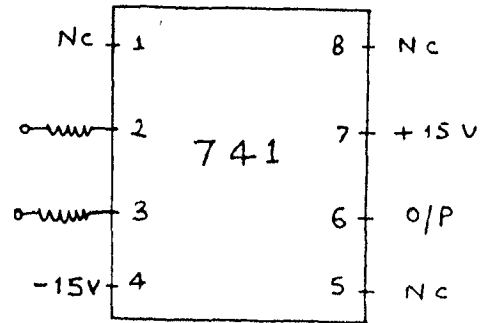
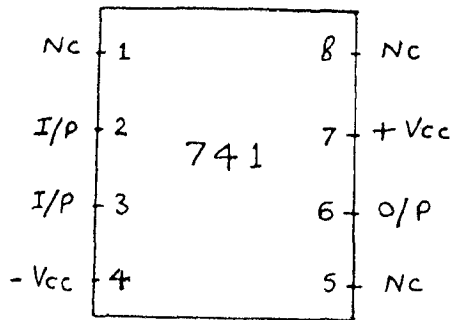
- Vol. 125, No. 2, March 1978, pp 113 - 119.
13. S. Tadakuma, Y. Tamura and S. Taraka, 'Driving characteristics of commutatorless motor controlled by induced voltage detector', *Elect. Engg. in Japan*, Vol. 98, No. 1, 1978, pp 37 - 49.
 14. J. Rosa, 'Utilization and rating of machine commutated inverter synchronous motor drives', *IEEE Trans. on Industry Applications*, Vol. 14 - 15, No. 2, March/April 1979, pp 155 - 164.
 15. F. Brockhurst, 'Performance equation for d.c. commutatorless motor using salient pole synchronous type motor', *IEEE Trans. on Industry Applications*, Vol. IA-16, No. 3, May/June 1980, pp 362 - 370.
 16. Y. Takeda, S. Morimoto and T. Hirasu, 'Generalised analysis for steady state characteristics of d.c. commutatorless motors', *IEE proceedings*, Vol. 130, Pt. 13, No. 6, Nov. 1983, pp 373 - 380.
 17. M.V.S.S. Rangandhari, B.P. Singh, R. Anbarsu and R. Arockiasamy, 'Experimental investigations on line commutated inverter synchronous machine as a variable frequency source', *Electric machines and Power systems*, Vol. 9, No. 1, Jan. 1984, pp 13 - 21.

18. M.V.S.S. Rangandhachari, B.P. Singh, R. Anbarsu and R. Arockiasamay, 'Experimental investigations on steady state performance of commutatorless machine induction motor system', Journal of Institution of Engineers (India), Vol. 64, Pt. EL-3, December, 1983, pp 159 - 163.
19. T. Tasuchrya, H. Sesajima and K. Tastuguchi, 'Basic characteristics of series commutatorless motors', Electrical Engineering in Japan, Vol. 89, No. 9, 1969, pp 71.
20. Ajay Kumar, R. Anbarsu and B.P. Singh, 'Steady State performance of series commutatorless d.c. motor', Journal of Institution of Engineers (India), Vol. 65, Pt. EL-6, June 1985, pp 185 - 188.
21. D.B. Watson, 'Induction motor drive from self commutated inverter', Proc. IEE Vol. 128, Pt. B, No. 1, Jan. 1981, pp 79 - 80.
22. D.B. Watson, 'Performance of induction motor drive from self commutating inverter', Proc. IEE, Vol. 129, Pt. B, No. 5, Sept. 1982, pp 245 - 250.
23. F.W. Gutzwiller, 'Silicon controlled rectifier manual', New York, General Electric Company, 1967.
24. B. Ilango, R. Krishan, R. Subramanian and Sadasivam, 'Firing circuit for three phase thyristor bridge

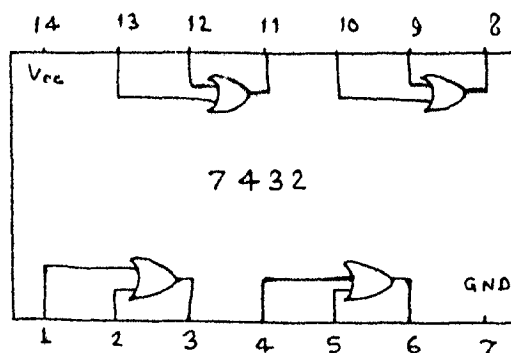
- rectifier', IEEE Trans. Industry Electronics Control Instrum., Vol. 25, 1978, pp 45 - 49.
25. T. Krishan and B. Ramaswami, 'A fast response d.c. motor control', IEEE Trans. on Industry Application, Vol. 10, 1974, pp 643 - 651.
 26. R. Simord and V. Rajgopalan, 'Economic equidistant pulse firing scheme for thyristorized d.c. drives', IEEE Trans. on Industry Electron. Control Instrum. Vol. 22, 1975, pp 425 - 429.
 27. R. Arockiasamy and S. Doraipandy, 'A novel trigger scheme for thyristor operating under variable frequency anode supply', IEEE Trans. Ind. Electron. Control Instrum., Vol. 22, 1975, pp 83 - 85.
 28. R. Venkataraman and B. Ramaswami, 'Thyristor converter fed synchronous motor drive', Electric Machines, and Electromechanics, Vol. 6, No. 5, Sept./Oct. 1981, pp 433 - 449.
 29. M. Ramamoorthy, 'An introduction to thyristors and their applications', New Delhi, Affiliated East, West Press Pvt. Ltd., 1977.
 30. S.B. Dewan, A Stranghen, 'Power semi conductor circuits', New York, Willey Interscience, 1975.
 31. Malvin J. Maron, 'Numerical analysis a practical approach', Machrillan Publishing Company Inc., New York, 1982.

APPENDIX - A

PIN DETAILS AND CONNECTION DIAGRAMS OF
DIFFERENT I.C. CHIPS



C _v	I/P		O/P	
	A	B	Q	\bar{Q}
0	x	x	0	1
x	1	x	0	1
x	x	0	0	1
1	0	↓	⌋	⌋
1	↓	1	⌋	⌋
↑	0	1	⌋	⌋



APPENDIX - B

DETAILS AND PARAMETERS OF MACHINES USED

1. Details of Machine Used

- (a) (i) Induction Motor 1: 0.5 H.P., 220V, 2.1 A,
Star connected, 4 pole, 50 Hz, cage rotor.
- (ii) D.C. Machine coupled to I.M. 1: 0.5 H.P.,
125V, 1300 r.p.m.
- (b) (i) Induction Motor 2: 4 H.P., 240V, 10.2A, delta
connected, 4 pole, 50 Hz semicage rotor.
- (ii) D.C. Machine coupled in I.M. 2 : 3 H.P., 200/
240V, 1500 r.p.m.
- (c) (i) Induction Motor 3: 3 H.P., 400V, 4.5A, delta
connected, 4 pole, 50 Hz, cage rotor.
- (ii) D.C. Machine coupled to I.M. 3: 4 H.P., 220V,
1500 r.p.m.

2. Parameters of Machine b(i)

R (Total resistance of circuit per phase referred
to stator excluding rotor resistance) = 4.62 ohms.

X (Total leakage reactance of circuit per phase
referred to stator) = 10.57 ohms

R_2 (Rotor resistance per phase referred to stator)
= 2.35 ohms

Parameters
of M/C 9

```

00100 C      NO LOAD PERFORMANCE OF I.M.FED FROM LCI SYSTEM
00200      PRINT 11
00300 11     FORMAT (25X,'NO LOAD PERFORMANCE OF I.M.FED
00400      1 FROM SCI SYSTEM')
00500      VB=240.
00600      AIB=10.3/SQRT(3.)
00700      ZB=VB/AIB
00800      FB=50.
00900      B=15.
01000      PI=22./7.
01100      DO 10 IVD=80,240,20
01200      DO 10 IC=45,70,25
01300      VD=IVD
01400      C=IC
01500      XC=10.**6/(2.*PI*C*FB)/ZB
01600      VP=2.*PI*VD/(3.*COSD(B)*SQRT(2.))/1.2
01700      V=VP/VB
01800      F=1.
01900      K=0
02000 22     VPF=V/F
02100      K=K+1
02200      IF(VPF.GT.1.5) GO TO 15
02300      AK1=4.875;AK2=3.125;AK3=2.42;AK4=7.14
02400      GO TO 17
02500 15     AK1=4.95;AK2=2.5;AK3=-2.79;AK4=17.54
02600      GO TO 17
02700 17     A1=AK1*AK3
02800      A2=(AK1*AK4-AK2*AK3)*V-(SIND(B)/COSD(B))
02900      1*XC*AK1
03000      A3=- (AK2*AK4*V**2+XC*AK3-XC*AK2*V*SIND(B)/
03100      2COSD(B))
03200      A4=-XC*AK4*V
03300      FW=A1*F**3.+A2*F**2.+A3*F+A4
03400      FWD=3.*A1*F**2.+2.*A2*F+A3
03500      DF=-FW/FWD
03600      F=F+DF
03700      IF (K.GT.50) GO TO 20

```

```
03800      IF (ABS(FW).LT..0001) GO TO 20
03900      GO TO 22
04000 20    F1=F*FB
04100      W=2.*PI*F1
04200      AN=30.*F1
04300      XM=AK1-AK2*VPF
04400      ROP=AK3+AK4*VPF
04500      PRINT *,C,VD,F1,AN,VP,F,W,B
04600      PRINT*,K,V,VPF,XM,ROP,FWD,FW
04700 10    CONTINUE
04800      STOP
04900      END
```

```

00100 C      APPROX:ANALYSIS OF SELF COMMUTATING INVERTER FED IM
00200      PRINT 22
00300 22     FORMAT (25X,'APPROX:ANALYS OF SELF COM INV FED IM')
00400      OPEN(UNIT=1,DEVICE='DSK',FILE='B.DAT')
00500      READ(1,*)R1,R2,XL,P,B
00600      PRINT44,R1,R2,XL,P,B
00700 44     FORMAT (2X,'R1=',F5.2,2X,'R2=',F5.2,2X,'XL=',
00800      1F5.2,2X,'P=',F4.1,2X,'VD=',F5.1,2X,'C=',F5.1,2X,
00900      2'B=',F5.1)
01000      VB=240.0
01100      AIB=10.3/SQRT(3.0)
01200      FB=50.0
01300      PIE=22./7.0
01400      DD 10 IC=250,250
01500      DD 10 IVD=120,120
01600      F=0.43
01700      DD 10 IS=5,100,5
01800      C=IC
01900      VD=IVD
02000      S=IS*.001
02100      V=2.0*VD*PIE/(3.0*1.2*COSD(B)*SQRT(2.0))
02200      AK=(-2.69*COSD(B))/(C*VD)*10.0**6
02300      W0=AK+SQRT(AK*AK+(((SIND(B)/COSD(B))/1.72)+6.1)/C*10.0**6)
02400      ZB=VB/AIB
02500      R1P=R1/ZB
02600      R2P=R2/ZB
02700      XLP=XL/ZB
02800      XCP=10.0**6/(2.0*PIE*FB*C*ZB)
02900      VP=V/VB
03000      J=0
03100 15     VPF=VP/F
03200      IF (VPF.GT.1.0) GO TO 16
03300      IF (VPF.GT.0.5) GO TO 17
03400      XMP=4.875-3.125*VPF
03500      ROP=7.14*VPF+2.42
03600      GO TO 18
03700 16     XMP=4.95-2.5*VPF

```



```

03800      ROP=15.0
03900      GO TO 18
04000 17    XMP=4.95-2.5*VPF
04100      ROP=17.54*VPF-2.79
04200 18    CONTINUE
04300      A=(XLP**2*XMP/XCP)
04400      D=(XLP**2*XMP*SIND(B))/(ROP*COSD(B))
04500      E=((XMP*(R1P+R2P/S)**2/XCP)-XLP**2-XLP*XMP)
04600      G=XMP*SIND(B)/(ROP*COSD(B))*(R1P+R2P/S)**2+XMP
04700      I*(R1P+R2P/S)*(SIND(B)/COSD(B))
04800      H=(R1P+R2P/S)**2
04900      FW=A**4-D**3+E**2-G**2-H
05000      F0=W0/(2.0*PIE)
05100      FWD=4*A**3-3*D**2+2**E**2-G**2
05200      DF=-FW/FWD
05300      F=F+DF
05400      IF(ABS(FW).LE.0.0001) GO TO 20
05500      J=J+1
05600      IF (J.GT.800) GO TO 20
05700      GO TO 15
05800 20    PRINT45,F,DF,FW,FWD,W0,F0,IS,J,C
05900 45    FORMAT (2X,'F=',F8.4,2X,'DF=',F15.11,2X,'FW=',F15.
06000      211,2X,'FWD=',F15.11,2X,'W0=',F8.4,2X,'F0=',
06100      3F8.4,2X,'IS=',I4,2X,'J=',I5,2X,'C=',F6.1)
06200      F1=F*FB
06300      W=2*PIE*F1
06400      AL=XL/(2*PIE*FB)
06500      R0=ROP*ZB
06600      XM=XMP*ZB
06700      AI2=V/(SQRT((R1+R2/S)**2+(W*AL)**2))
06800      AI1=V/(R0*COSD(B))+(AI2/COSD(B))*(R1+R2/S)
06900      I/(SQRT((R1+R2/S)**2+(W*AL)**2))
07000      P0=3.0*(1.0-S)*AI2*AI2*R2/S
07100      PI=V*AI1*COSD(B)*3
07200      PFI=COSD(B)
07300      AID=PI/VD
07400      EFIE=P0/PI

```

```
7500 RE=R1*XM/(XL/2.0+XM)
7600 AII=AI1*1.7321
7700 XE=XI/2.0*XM/(XL/2.0+XM)
7800 XC=(XI/2.0+XE)
7900 VE=V*XM/(XI/2.0+XM)
8000 AN=F1*120*(1.0-S)/P
8100 AKT=3*P*VE**2/(4*PIE*F1)
8200 SMT=R2/SQRT(RE**2+XC**2)
8300 TEM=AKT/(2.0*(RE+SQRT(RE**2+XC**2)))
8400 T=3*P/(4*PIE*F1)*AI2*AI2*R2/S
8500 PRINT 46,AI2,AII,AID,R0,XM,V,SMT,TEM,PFI
8600 46 FORMAT(2X,'AI2=',F8.4,2X,'AI1=',F8.4,2X,'AID=',F8.4,
8700 42X,'R0=',F9.3,2X,'XM=',F8.3,2X,'V=',F8.3,2X,'SMT=',
8800 5F9.5,2X,'TEM=',F8.3,2X,'PFI=',F8.6)
8900 PRINT25,S,EFIE,F1,AN,T,P0,PI,VPF,VD
9000 25 FORMAT(1X,'S=',F7.4,2X,'EFIE=',F7.3,2X,'FREQ=',F7.3,
9100 12X,'AN=',F7.2,2X,'T=',F7.3,2X,'P0=',F10.2,2X,
9200 2'PI=',F10.2,2X,'VPF=',F6.3,2X,'VD=',F6.2)
9300 10 CONTINUE
9400 STOP
9500 END
```